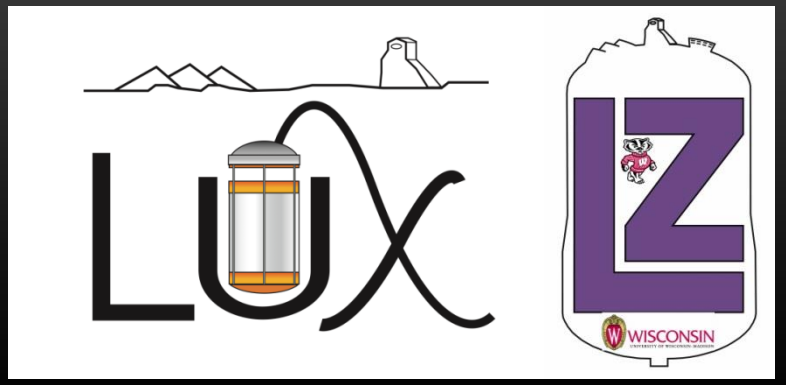

LUX AND LZ

DESIGN, CALIBRATION, AND WIMP SEARCH

Shaun Alsum

Preliminary Examination

August 30, 2016

WISCONSIN

UNIVERSITY OF WISCONSIN–MADISON

PROJECTS

- The Large Underground Xenon (LUX) experiment
  - A dark matter direct detection experiment
- LZ - LUX-Zeplin
  - It's like LUX, but bigger…
  - My focus: The LZ system test.
    - It's like LZ, but smaller…

Members of the LUX collaboration present at the Albany meeting. Oct, 2015

Members of the LZ collaboration present at the Livermore meeting. Jan, 2016

OVERVIEW

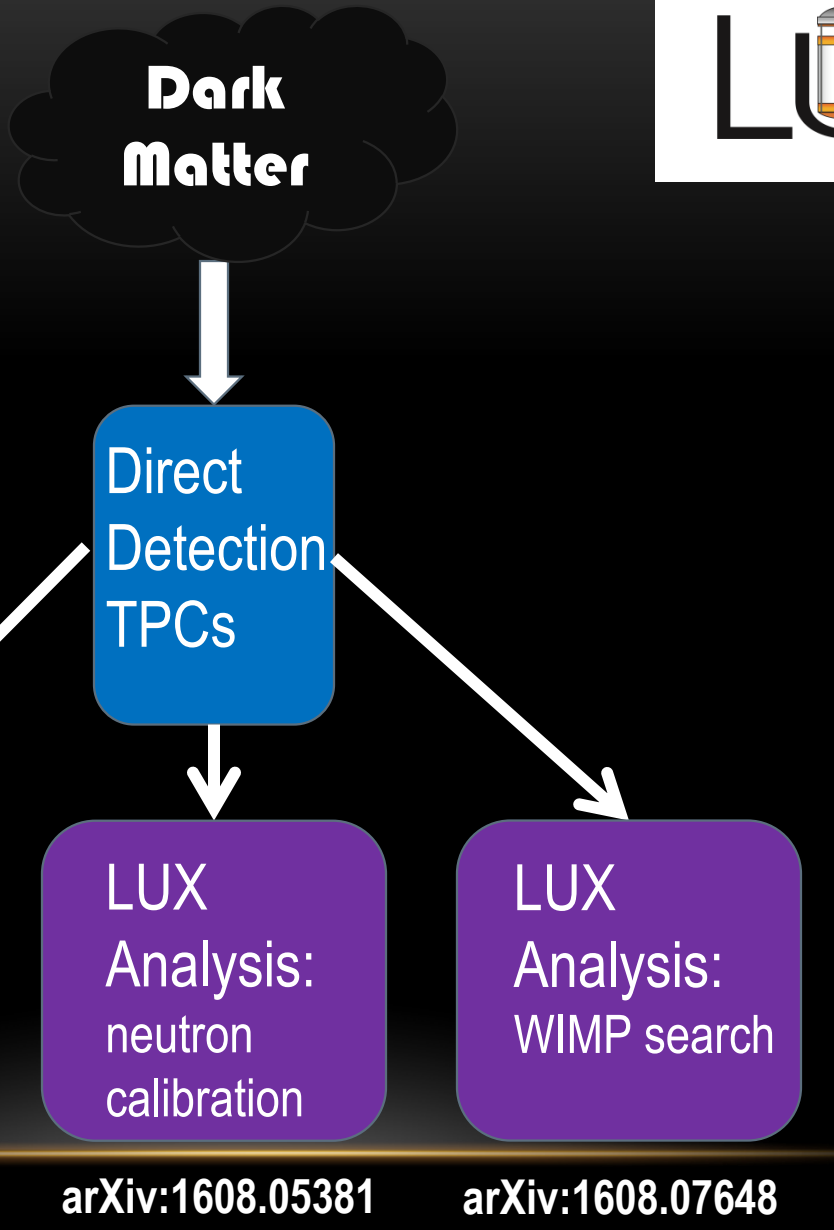
Dark Matter
Direct Detection TPCs
System Test Hardware: Phase II circulation
LUX Analysis: neutron calibration
LUX Analysis: WIMP search
arXiv:1608.05381
arXiv:1608.07648

DARK MATTER

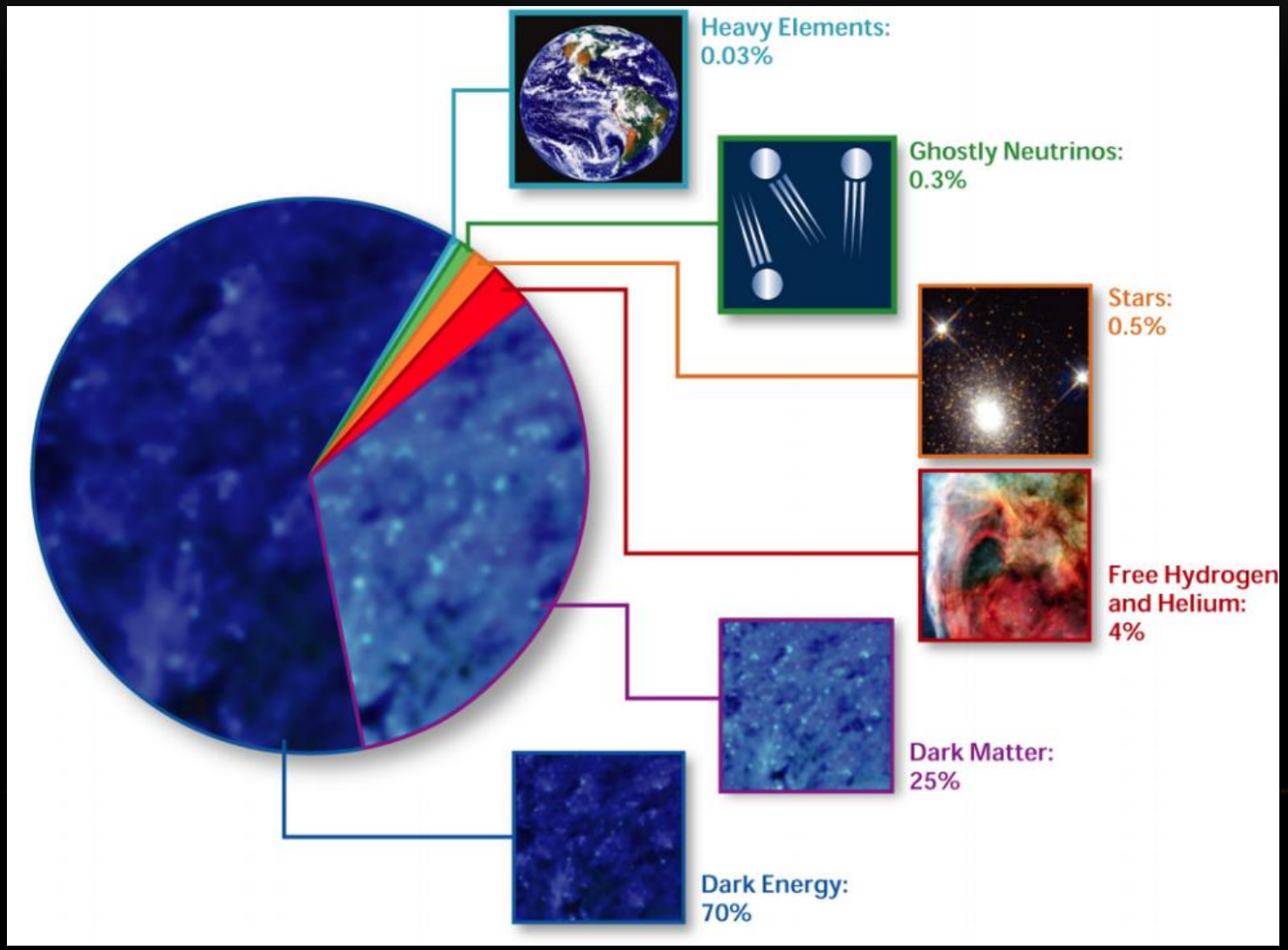
Heavy Elements:
0.03%
Ghostly Neutrinos:
0.3%
Stars:
0.5%
Free Hydrogen
and Helium:
4%
Dark Matter:
25%
Dark Energy:
70%

DARK MATTER – EVIDENCE: BBN AND CMB

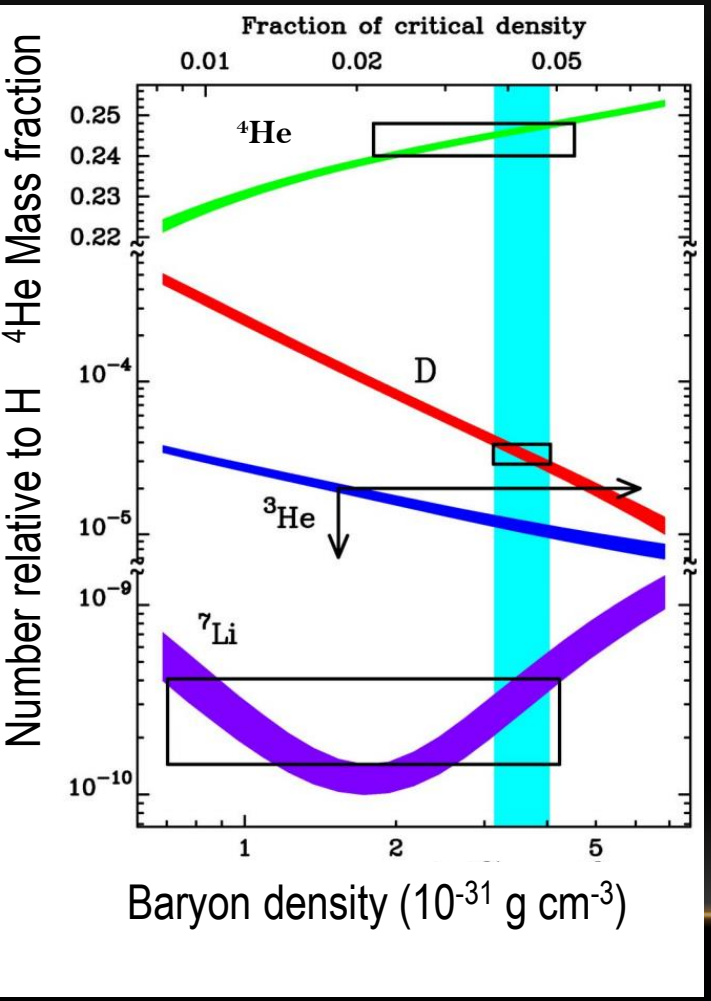

Review of Big Bang Nucleosynthesis and Primordial Abundances arXiv:astro-ph/0001318

- Matter density of the universe is measured at

$$\rho_m = .34 \times 10^{-30} \frac{g}{cm^3} \rightarrow \Omega_m = 0.30$$

- Relative density of light elements is sensitive to baryon density, measurements indicate

$$\rho_b \approx 0.05 \times 10^{-30} \frac{g}{cm^3} \rightarrow \Omega_b \approx 0.044$$

- Shape of the CMB power spectrum also sensitive to the ratio of cold (non baryonic) dark matter

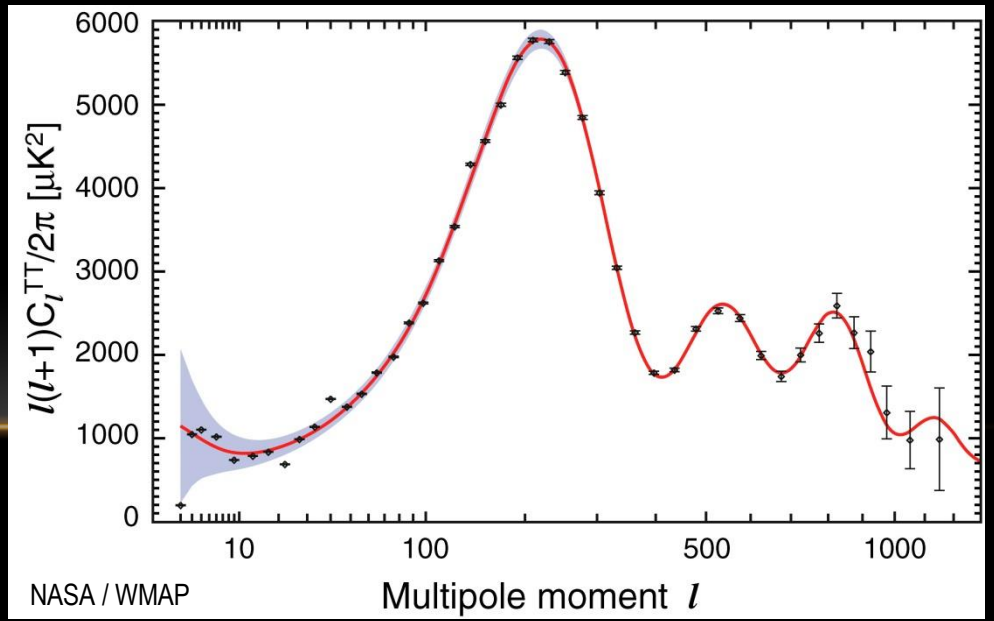

DARK MATTER – EVIDENCE: ROTATION CURVES

- Galactic rotation curves plateau or increase as one passes beyond the edge of the visible matter.

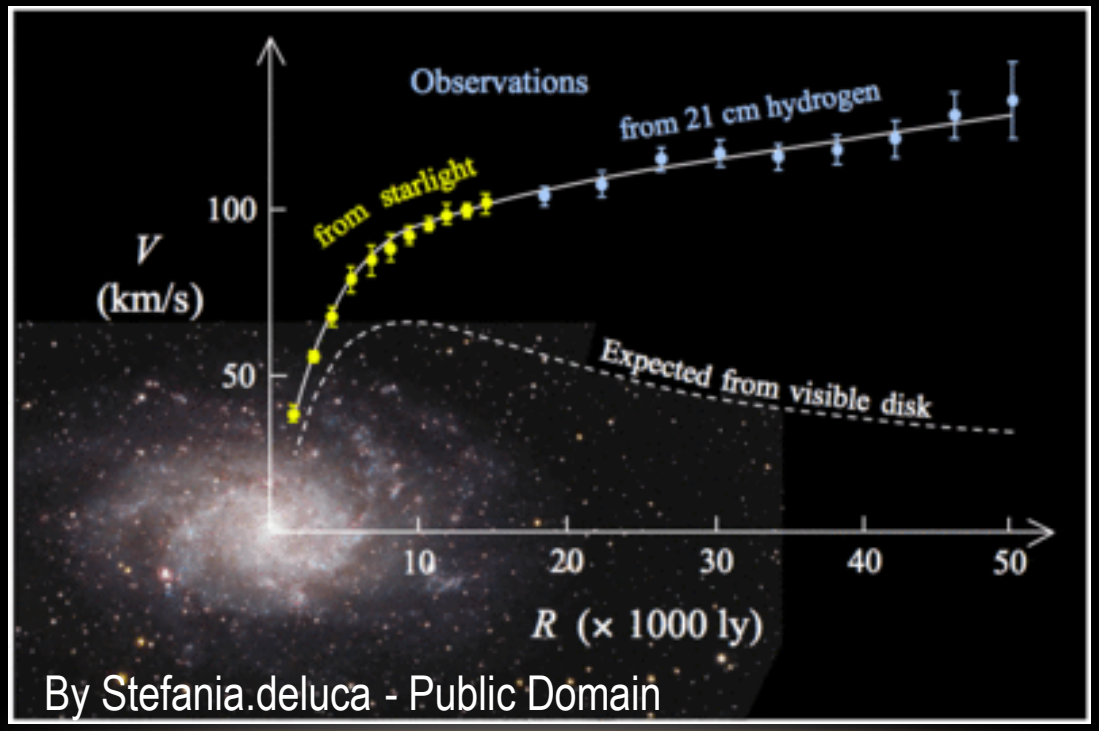

Observed and Predicted rotation curves of the galaxy M33.

DARK MATTER – WIMP FREEZE OUT

- Assume a DM particle (X) in thermal equilibrium in early universe

$$X + X \leftrightarrow SM + SM \quad (1)$$

- Expansion occurs, no longer enough energy for SM particles to annihilate to X

$$X + X \rightarrow SM + SM \quad (2)$$

- Expansion continues, dilute enough that X no longer find each other (3)

- $\Omega_X h^2 \approx \frac{3\times10^{-27}\,\frac{cm^3}{s}}{\langle\sigma v\rangle}$
- $\langle\sigma v\rangle \approx 3 \times 10^{-26}\frac{cm^3}{s}$
- $v = O(c)$ so $\sigma = O(10^{-34}\ cm^2)$

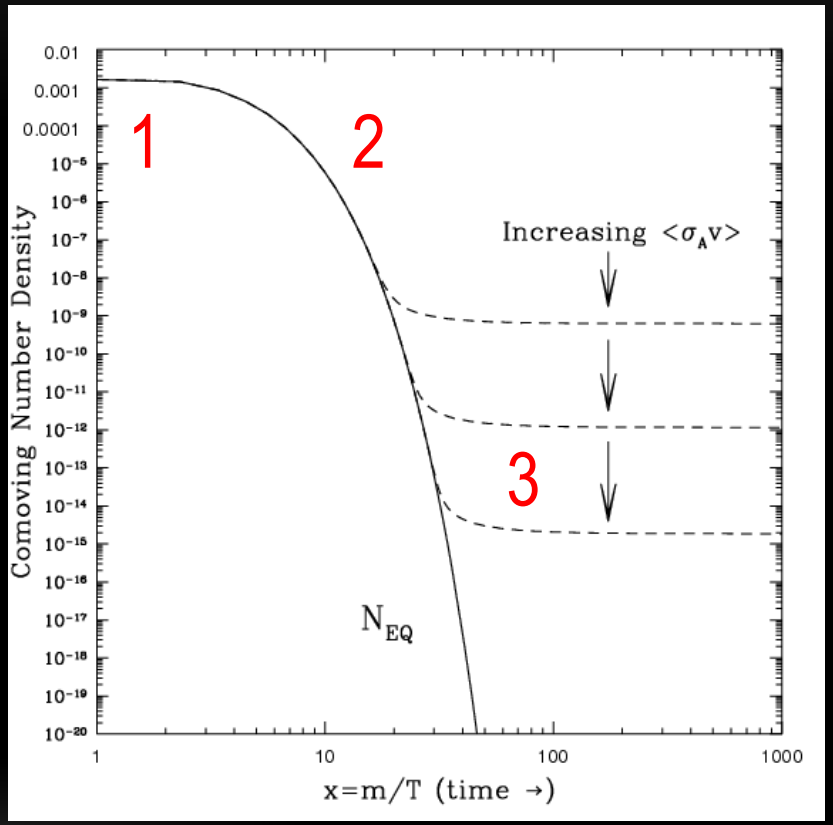

TASI 2008 Lectures on Dark Matter, Dan Hooper:

DARK MATTER - DETECTION METHODS

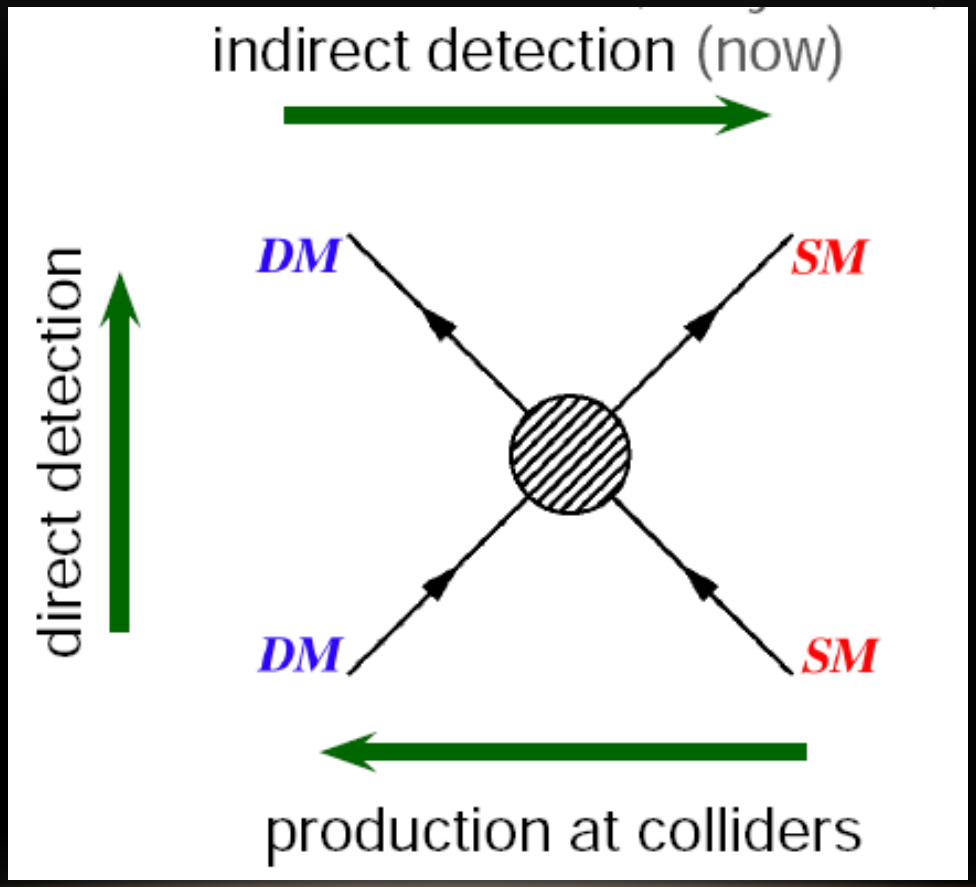

Max-Planck-Institut für Kernphysik
Particle & Astroparticle Physics

DARK MATTER - DETECTION METHODS

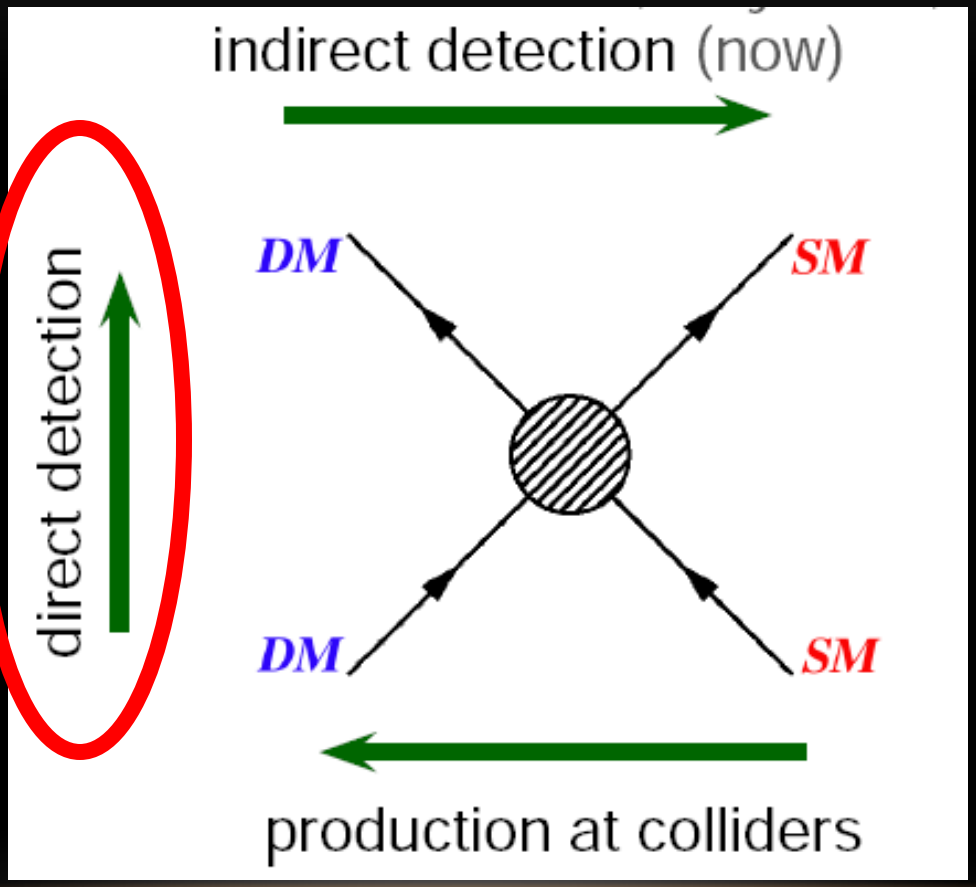

Max-Planck-Institut für Kernphysik
Particle & Astroparticle Physics

DARK MATTER – DIRECT DETECTION

- Has to be DM to hit
  - Milky way has flat rotation curve, requires DM
  - Local density predicted as $\rho_0 \approx 0.3 \frac{GeV}{cm^3}$
- Has to hit us hard enough
  - Local DM has average speed $\bar{v} \approx 270 \frac{km}{s}$ with no preferred tangential direction, due to weak self-interaction
  - The solar system moves with a tangential velocity $v = 230 \frac{km}{s}$
  - Results in $\frac{dR}{dE_R} \propto e^{-\frac{E_r}{E_0}}$ for $E_r > E_{threshold}$
    - $E_0 = \frac{1}{2} m_x v_{earth}^2 \approx 2.94 \times 10^{-7} c^2 * m_x$

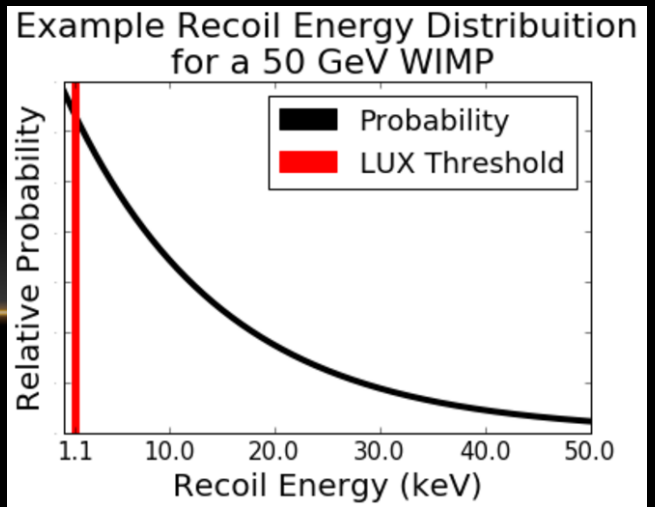

DIRECT DETECTION - SHIELDING

- Escape Cosmic radiation by going 4850 ft underground
- Muon flux reduced by factor of 3.7×10^6

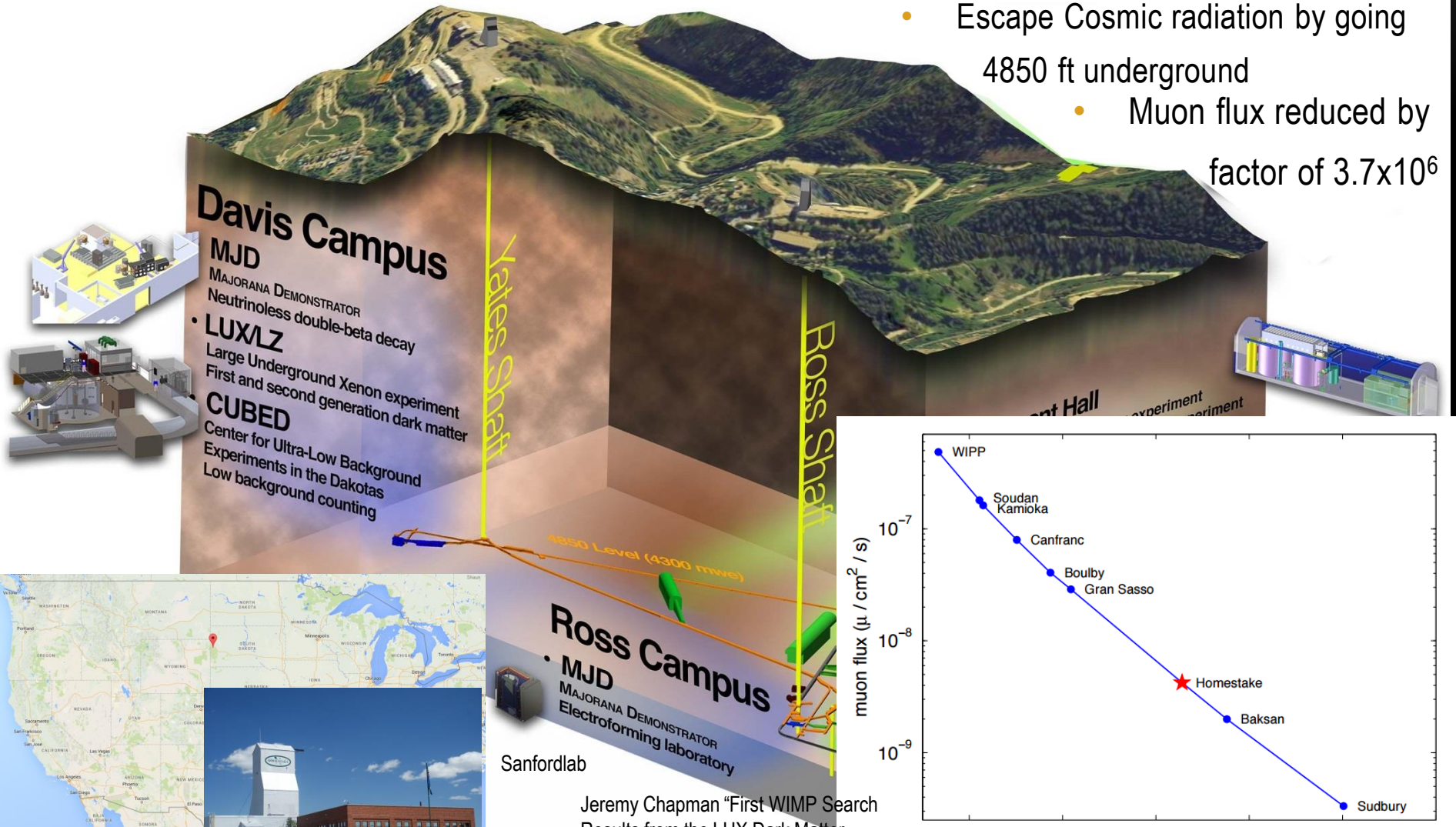

Sanfordlab

Jeremy Chapman "First WIMP Search Results from the LUX Dark Matter Experiment"

DIRECT DETECTION - SHIELDING

- Water tank shields from muon-induced spallation and radioactivity from heavy metals in cavern walls
- Time Projection Chamber (TPC) addresses radiation in detector materials themselves
  - Uses target material as its own shield

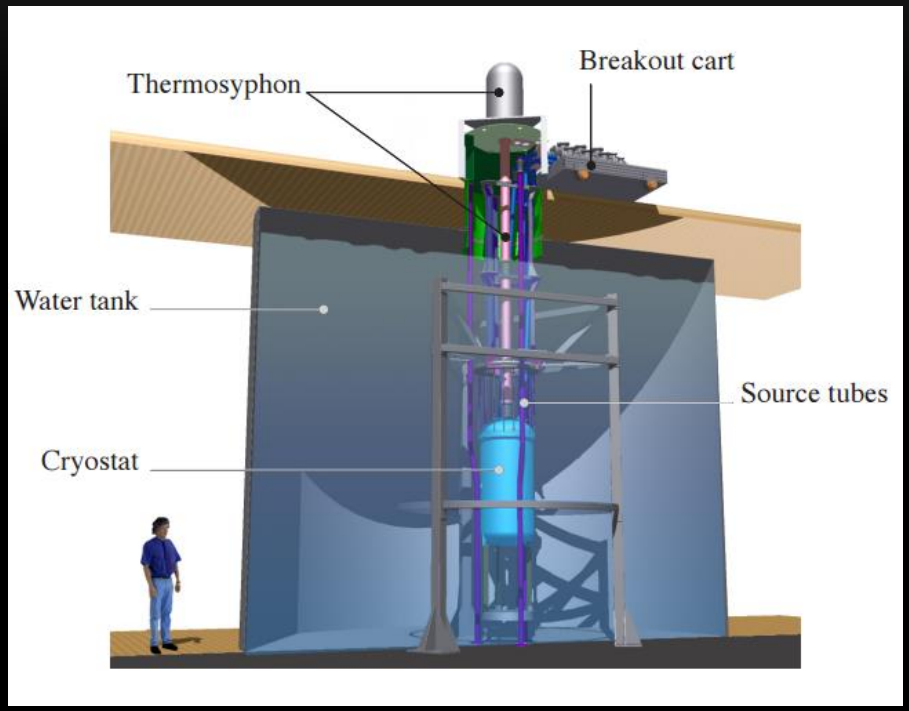

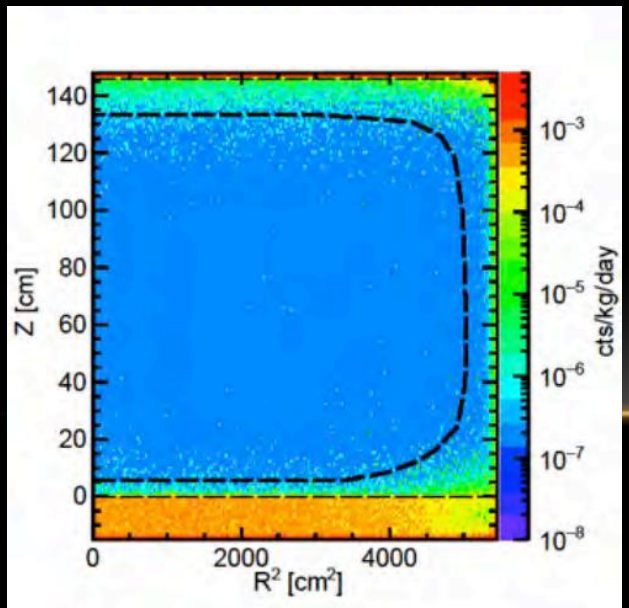

TPCS – THE BASICS

- Cylindrical container with PMTs at the top and bottom
- Contains liquid scintillator target with gas layer
- Applied electric field to drift free electrons
- Particle interaction creates two signals:
  - Scintillation (S1) measured by PMTs
  - Charge (S2) caused by extraction of freed electrons measured by PMTs via electroluminescence
- XY position measured by S2 Pattern
- Z position measured by time delay between S1 and S2

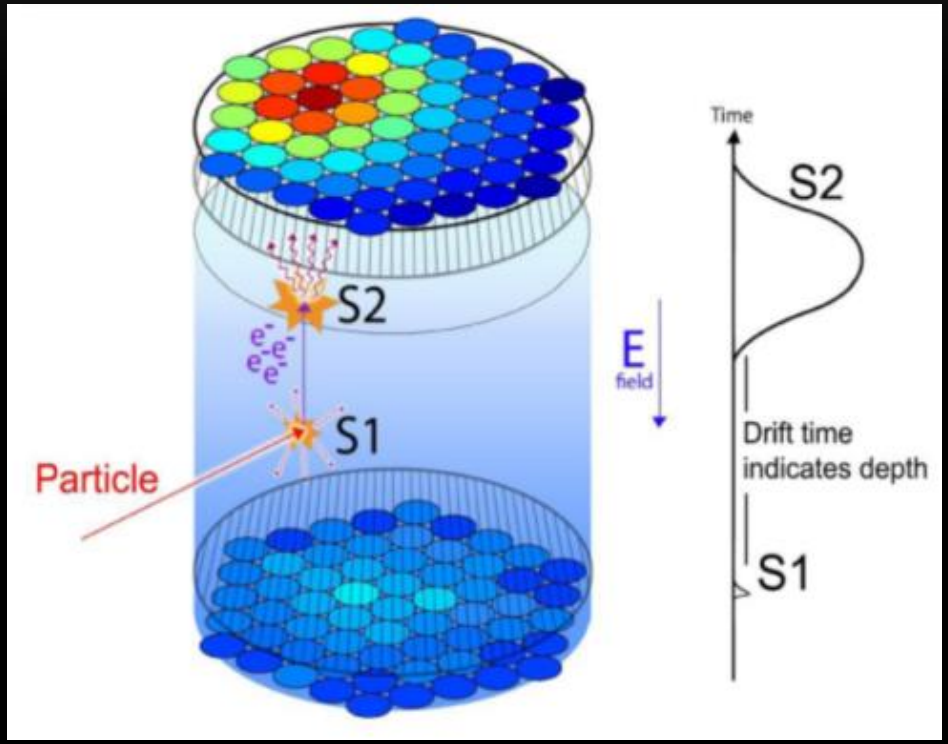

TPCS - LUX/LZ SPECIFIC DESIGN

- Xe target mass: scintillates at 178nm
- 5 grids:
  - Bottom: ground. Protects PMTs
  - Cathode: bottom of drift field
  - Gate: top of drift, bottom of extraction region
  - Anode: top of extraction region
  - Top: Protects PMTs
- Field shaping rings keep field uniform and vertical
- PTFE (Teflon) walls, liquid Xe-PTFE interface ~100% reflective at 178nm

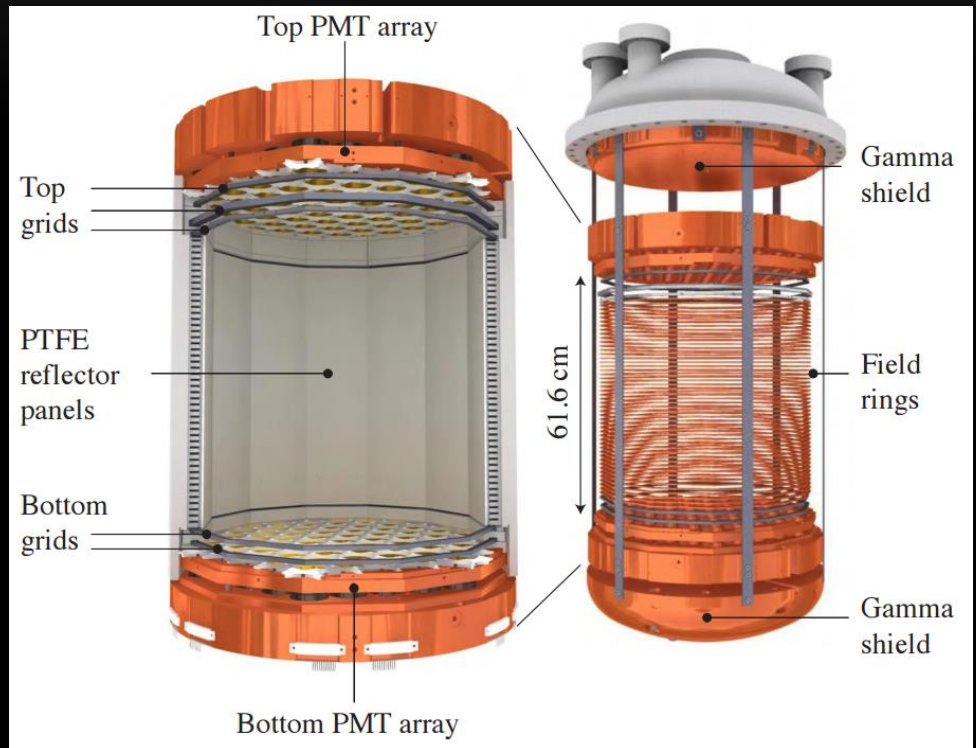

Figure 7: Rendering of the LUX TPC, supported from the top flange of the inner cryostat.

TPCS - PURITY

- Non-noble impurities capture drifting electrons
- Outgassing from plastics introduces impurities
- Purification needed
- Large support system
  - LUX purifies via circulation through a getter
  - Requires vaporization and recondensation

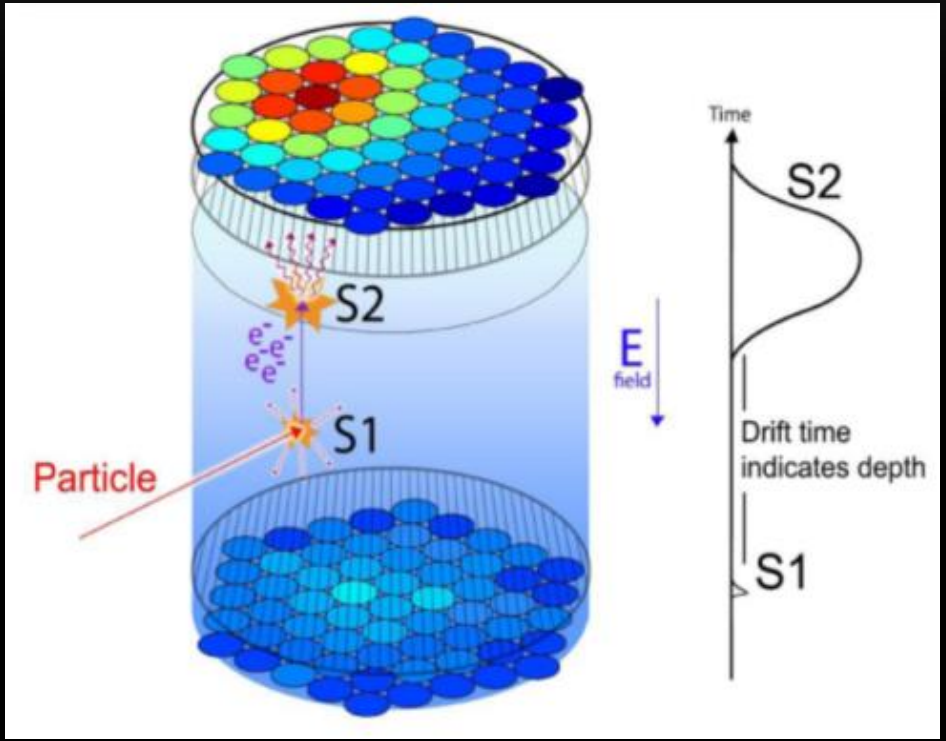

This is LUX

370 kg of Xenon

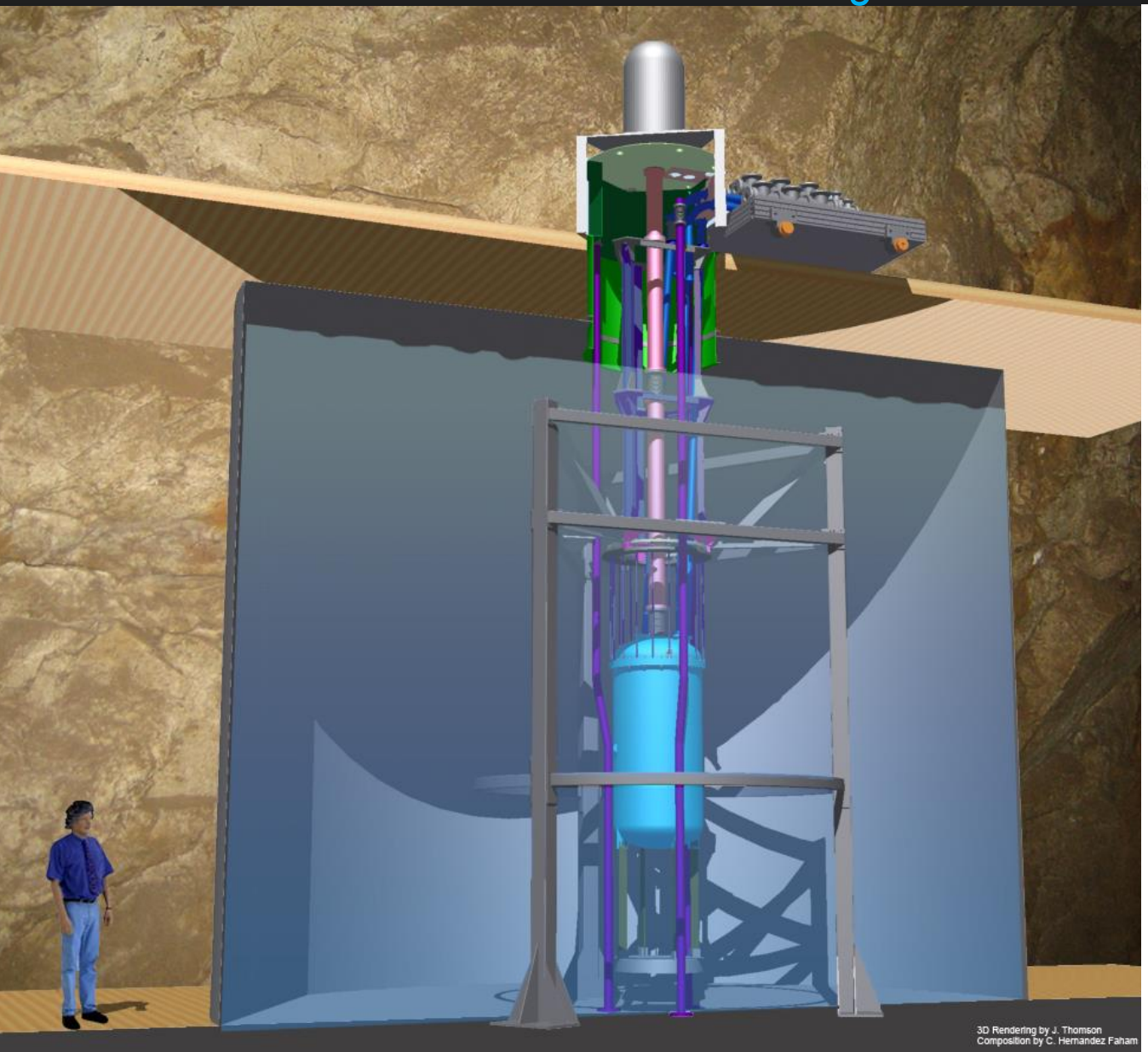

And this is LZ

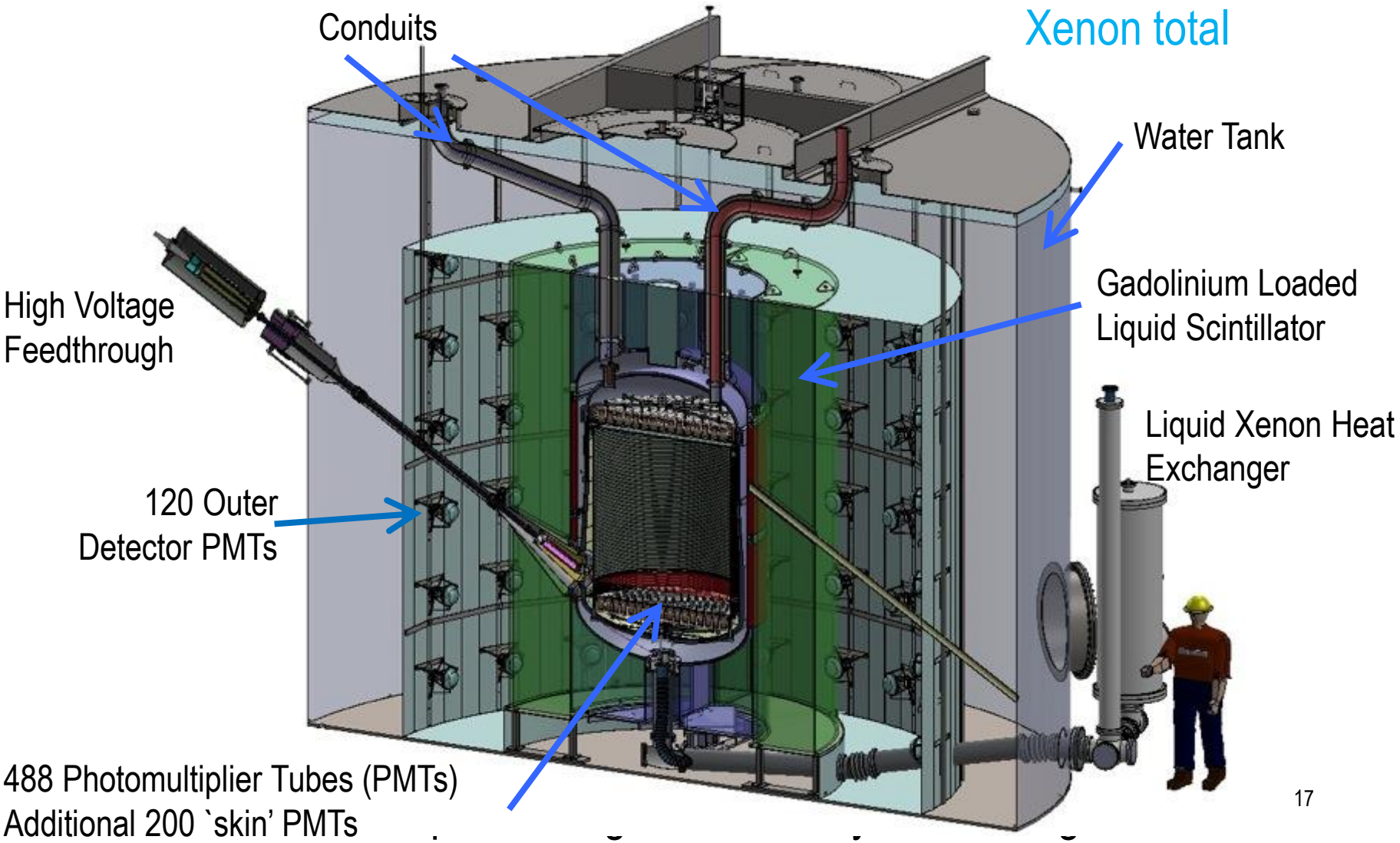

THE SYSTEM TEST

- Prototype to test design changes
- Built by me, those from SLAC, and a few others

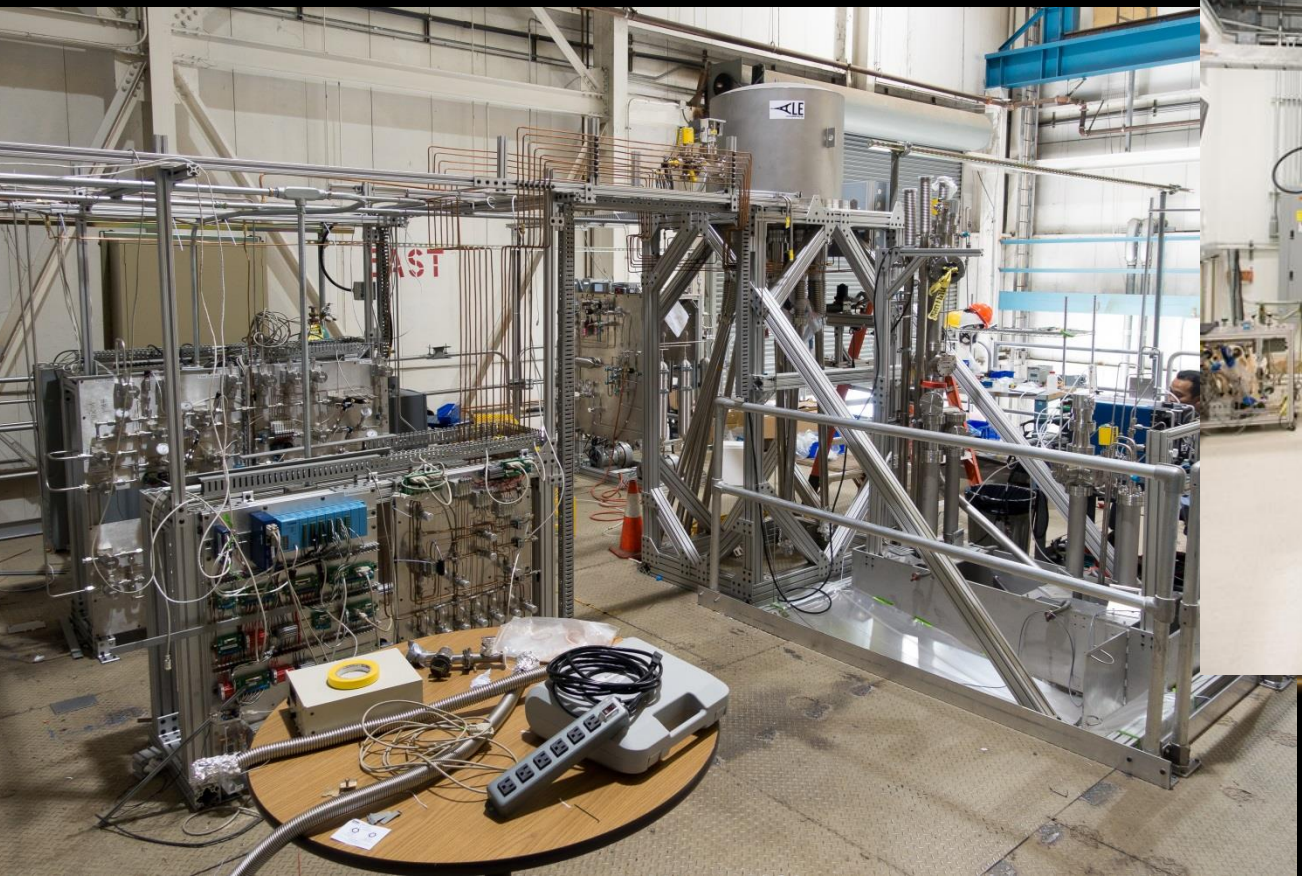

CIRCULATION

- Key elements tested in new configuration, at higher flow
- Designed to mimic LZ design as much as possible

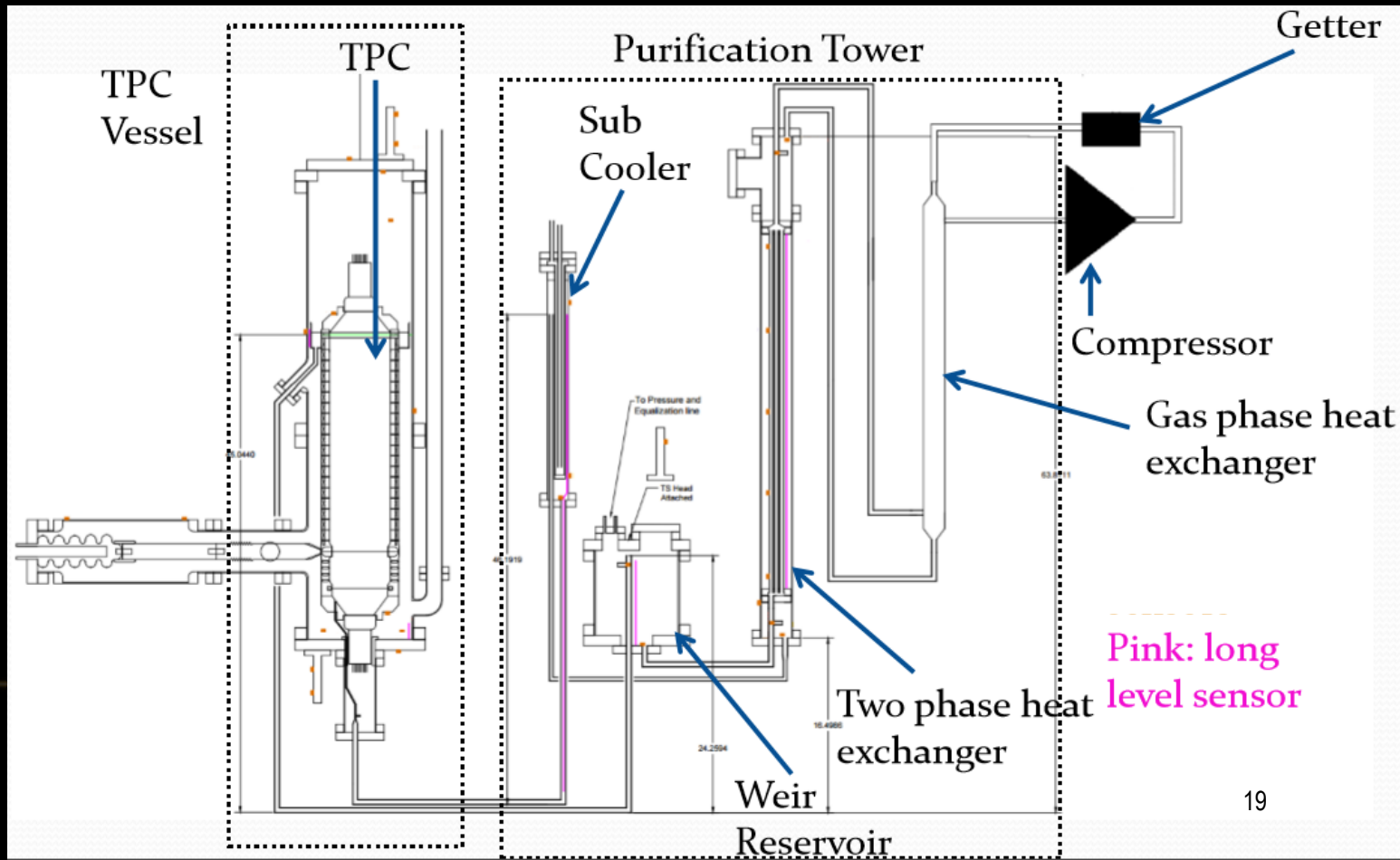

A simplified schematic of the system test gas system.

SYSTEM TEST - PHASE I TPC: FIELDS

- System Test split into phases
- Phase I designed to test electric fields
- ~1/2 LZ height, much smaller radius

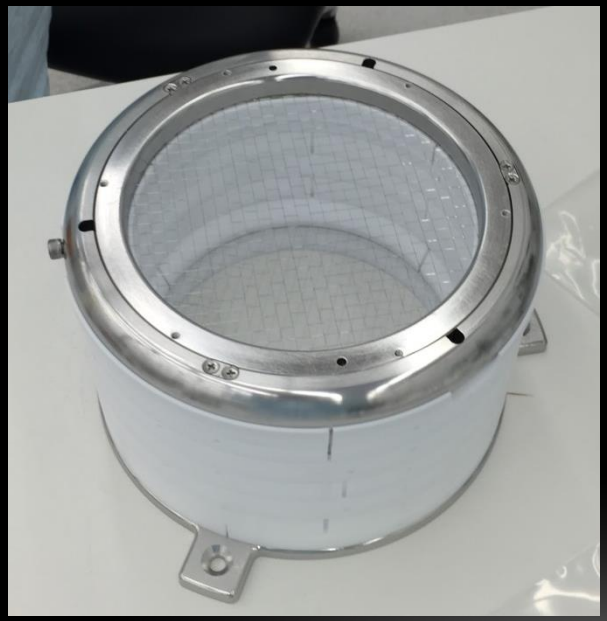

Reverse Field Region of the TPC with the Cathode Grid mounted

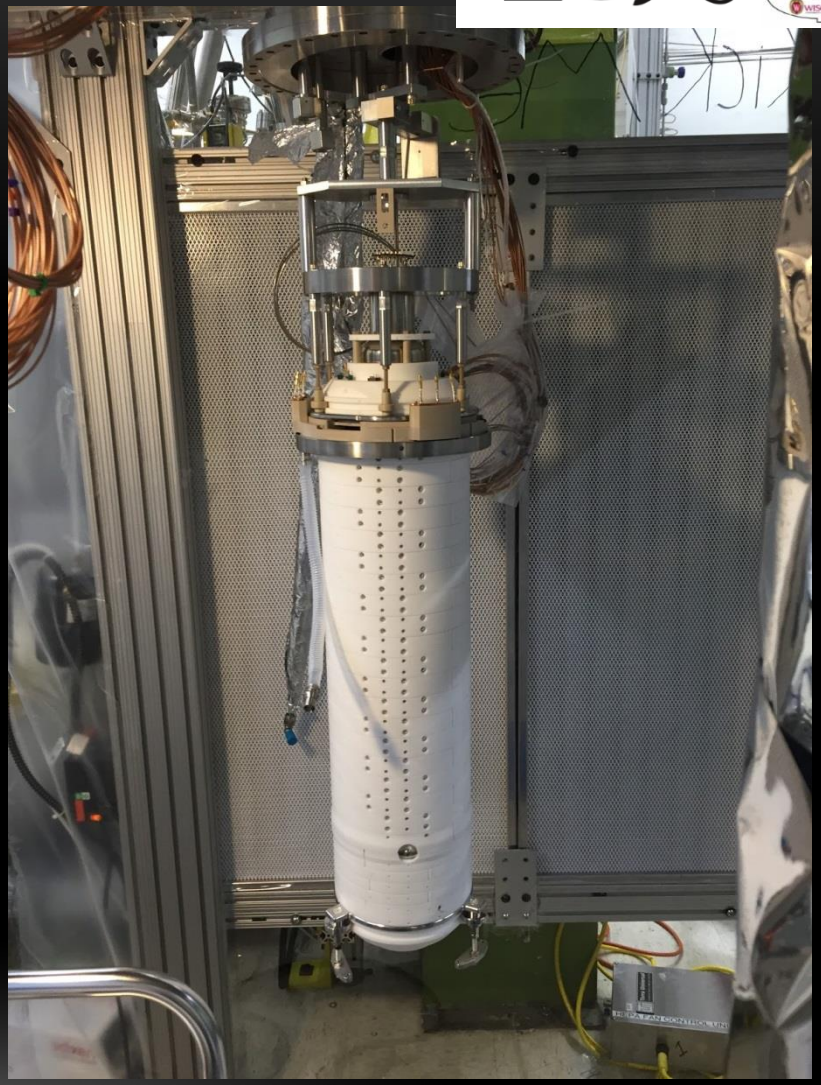

Full TPC without cryostats hung in place

SYSTEM TEST - PHASE II

- Full diameter, but short
- Designed to test full-sized grids
  - Possible spontaneous emission
  - Final LZ grids to ensure quality
- Also requires circulation
  - **Phase II Circulation will be my design project**

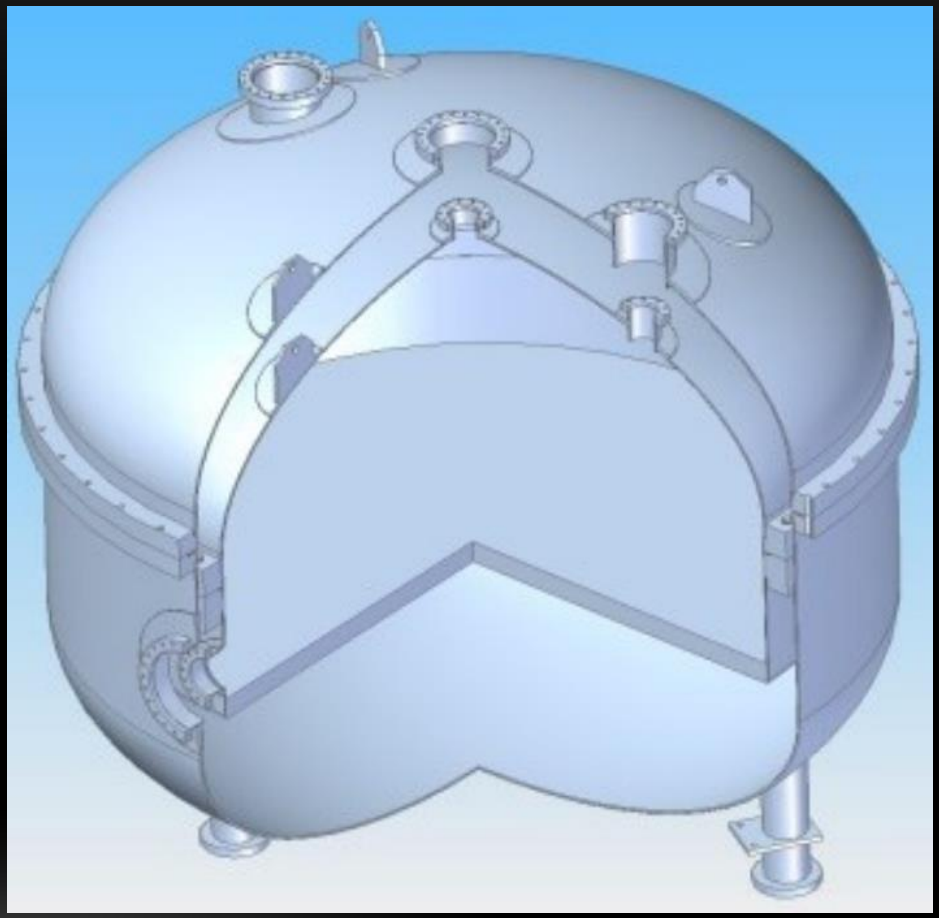

The outer and inner cryostats for the Phase II system test. 1868 width units

SYSTEM TEST – PHASE II DESIGN PROJECT

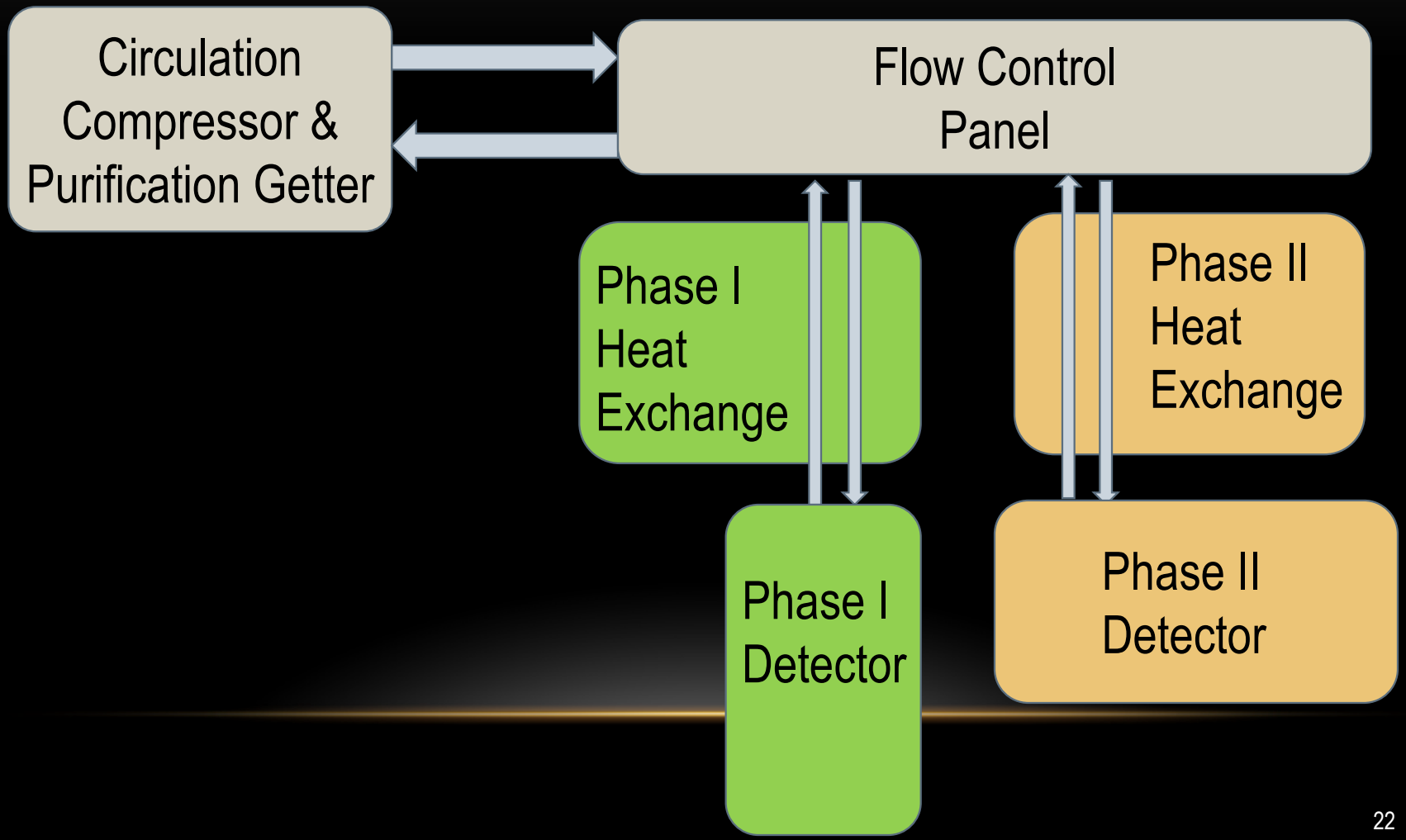

SYSTEM TEST – PHASE II DESIGN PROJECT

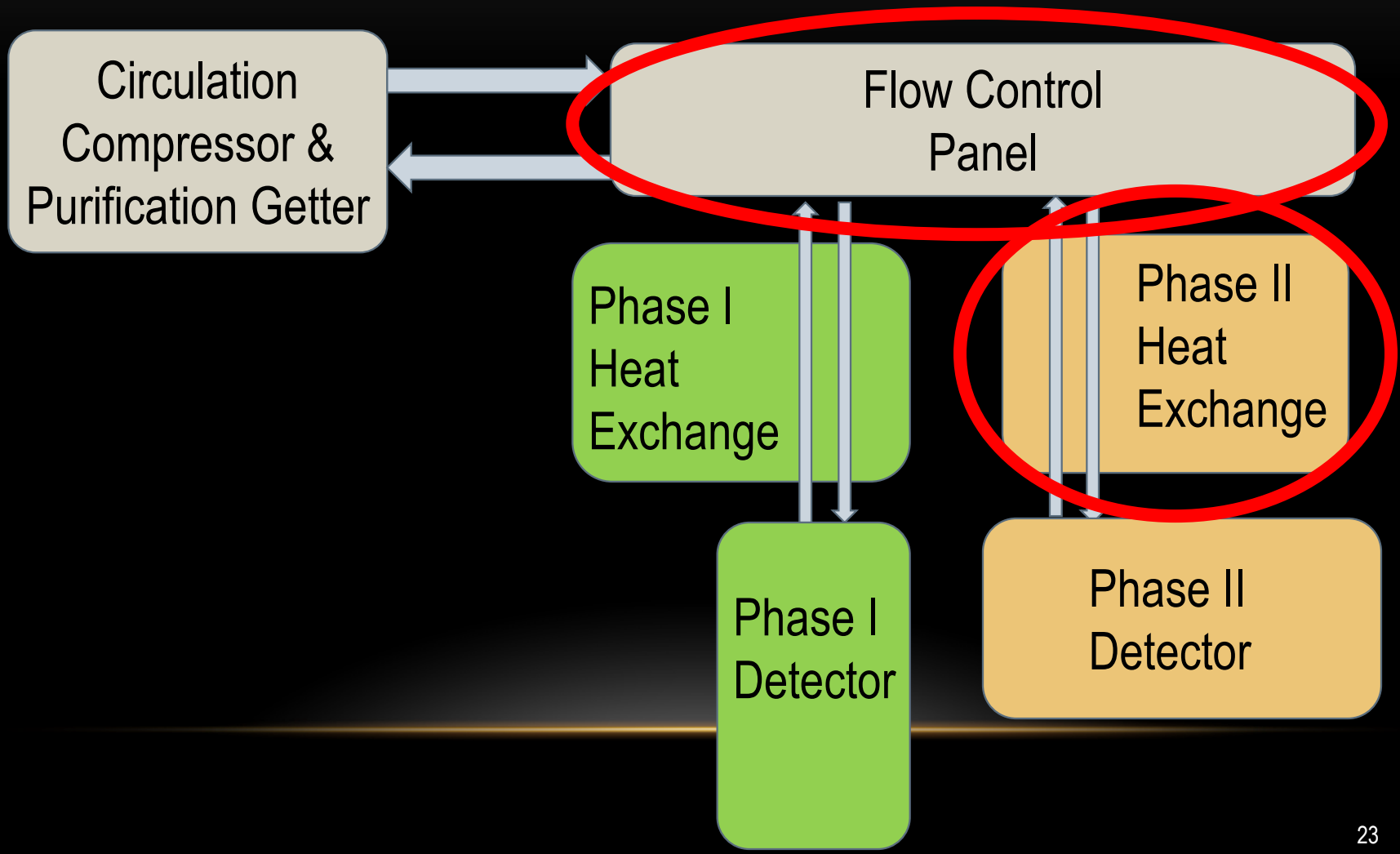

TPCS – SCINTILLATION AND IONIZATION

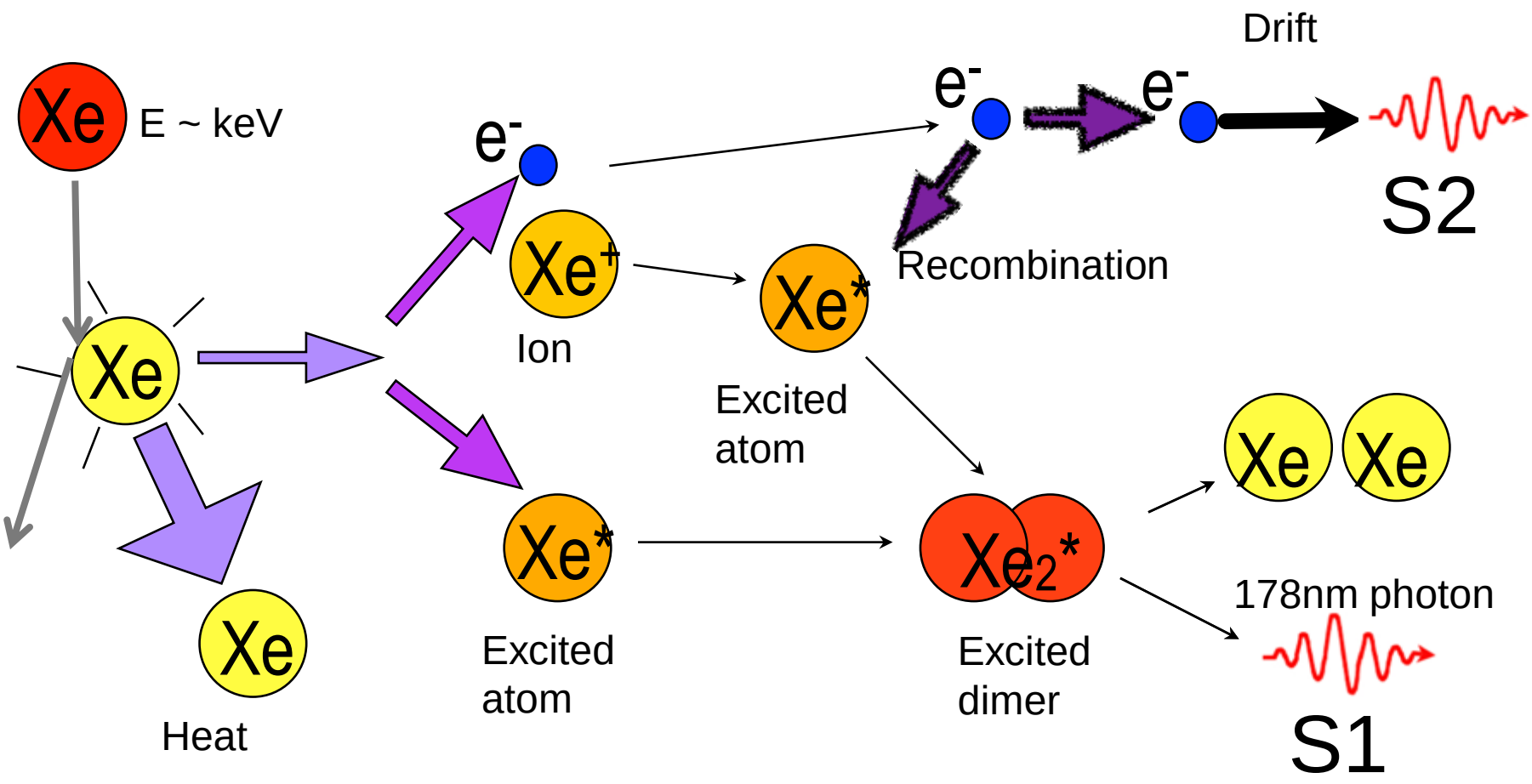

Figure: Gibson/Shutt

LUX CALIBRATION - ER & NR

- Events are separated into two categories:
  - Electron Recoil (ER): charged particles, photons
  - Nuclear Recoil (NR): neutral particles (like WIMPS)
- An event's S2/S1 ratio can distinguish between ER and NR

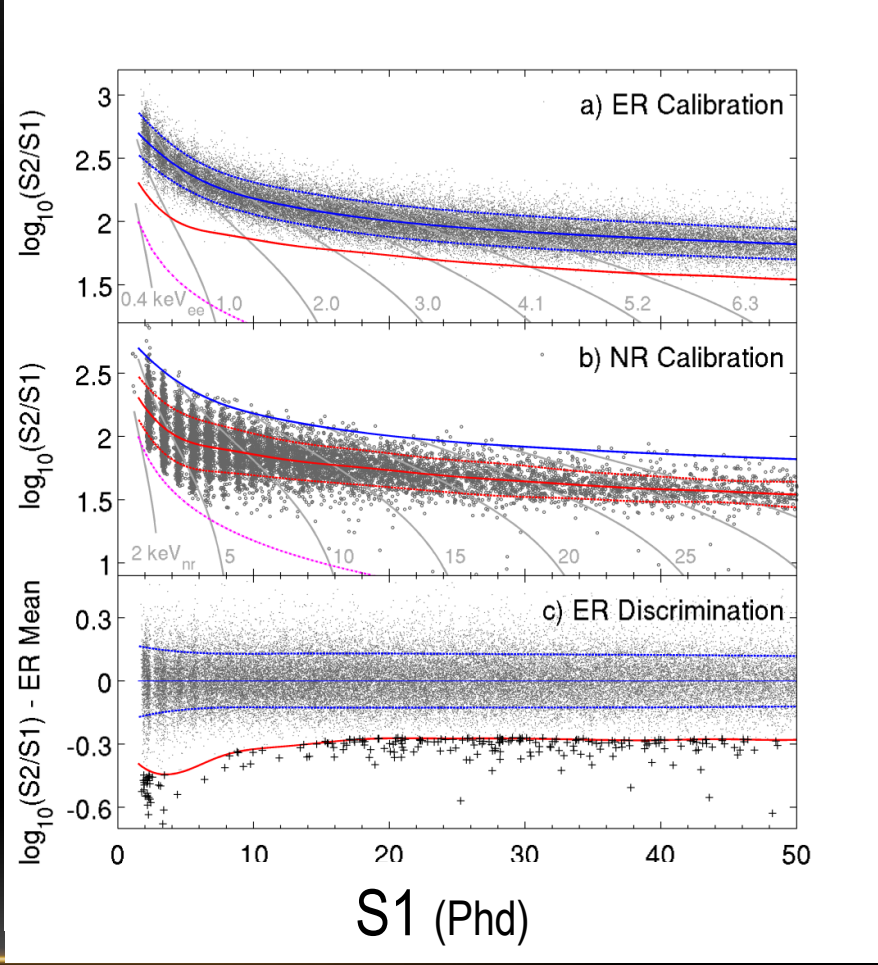

LUX CALIBRATION – NR OVERVIEW

- Calibrated via monoenergetic (2.45 MeV) neutrons from DD fusion
- Signal model (WIMPs cause NR) requires size of signal (S1 or S2) at different energies.
  - $S_1 = E_{nr} L_y(E_{nr}) g_1$
  - $S_2 = E_{nr} Q_y(E_{nr}) g_2$
    - E_{nr}: nuclear recoil energy
    - L_y (Q_y): light (charge) yield, number of photons (electrons) produced per unit energy
- Want to determine L_y, Q_y

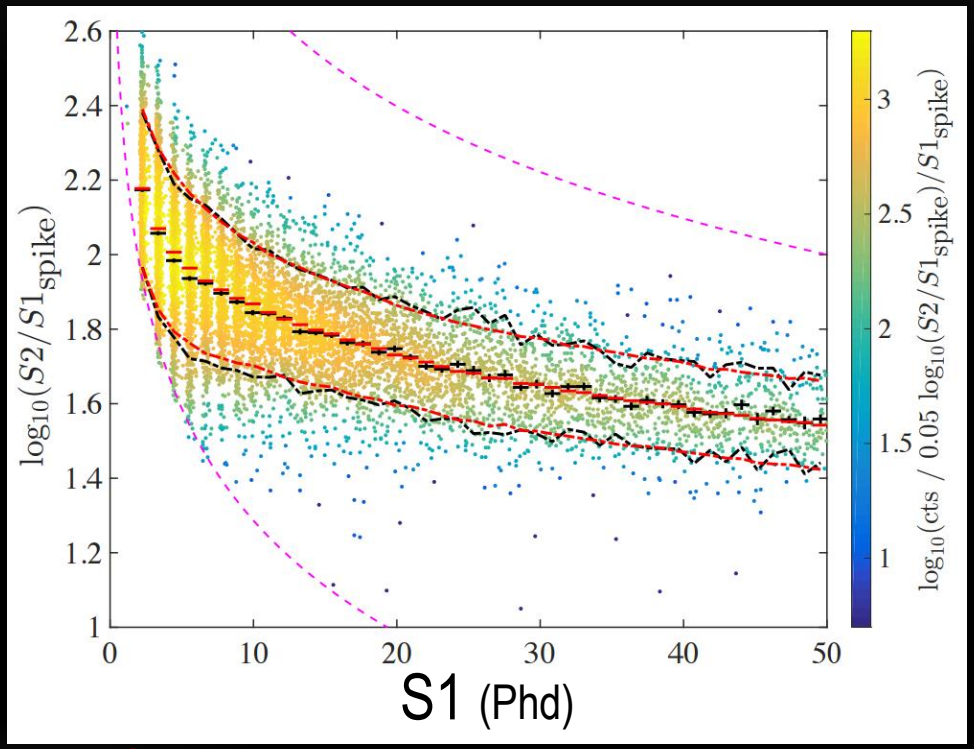

Red: Simulation

Black: Data

LUX CALIBRATION - THE NEUTRON GENERATOR

- Adelphi DD-108M neutron generator
- Produces neutrons in 4π
- Surrounding insulation blocks neutrons except towards water tank

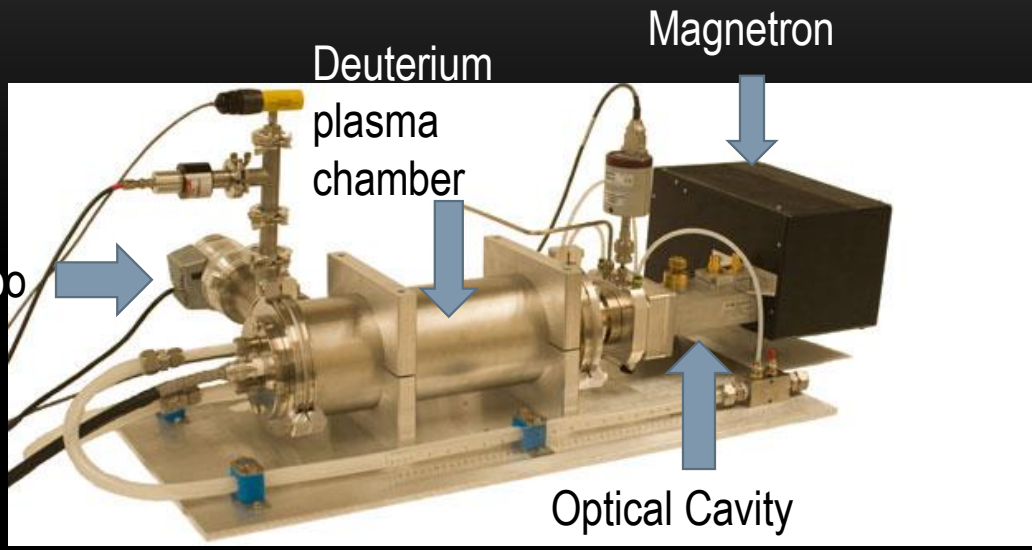

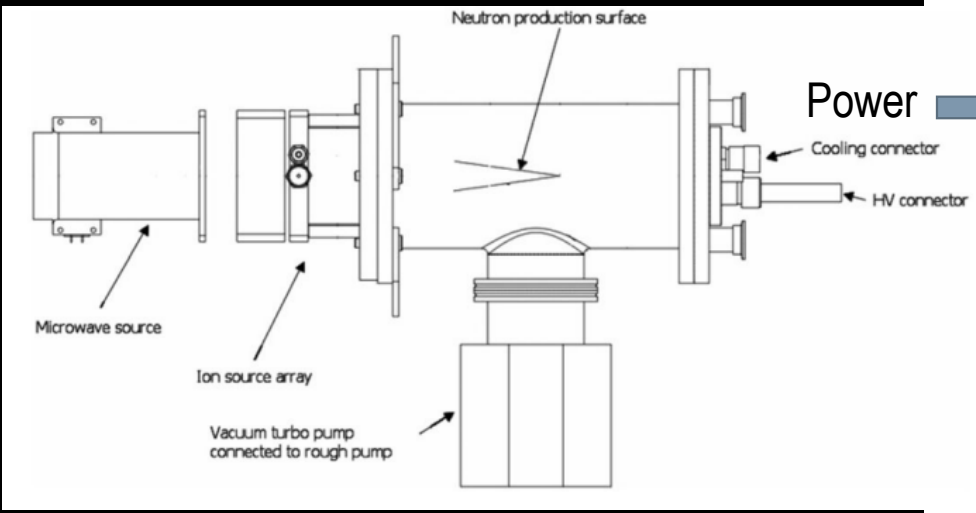

Diagram from "Development of a transportable neutron activation analysis system to quantify manganese in bone in vivo: feasibility and methodology" Liu et al.

LUX CALIBRATION – THE FUSION PROCESS

- The titanium target wedge is biased to at least 80 kV.

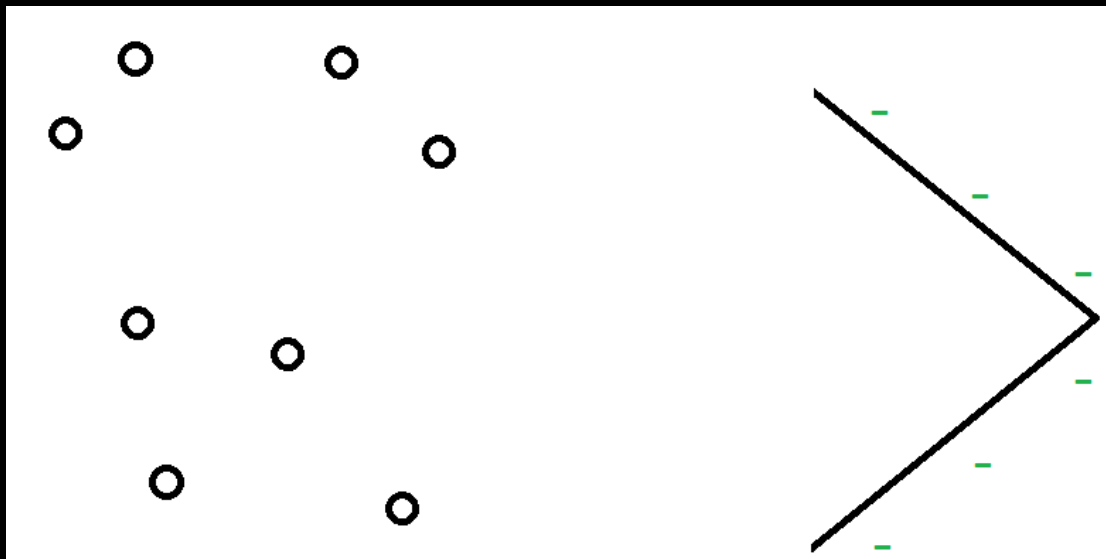

LUX CALIBRATION – THE FUSION PROCESS

- The titanium target wedge is biased to at least 80 kV.
- When the magnetron pulses the Deuterium gas becomes ionized.

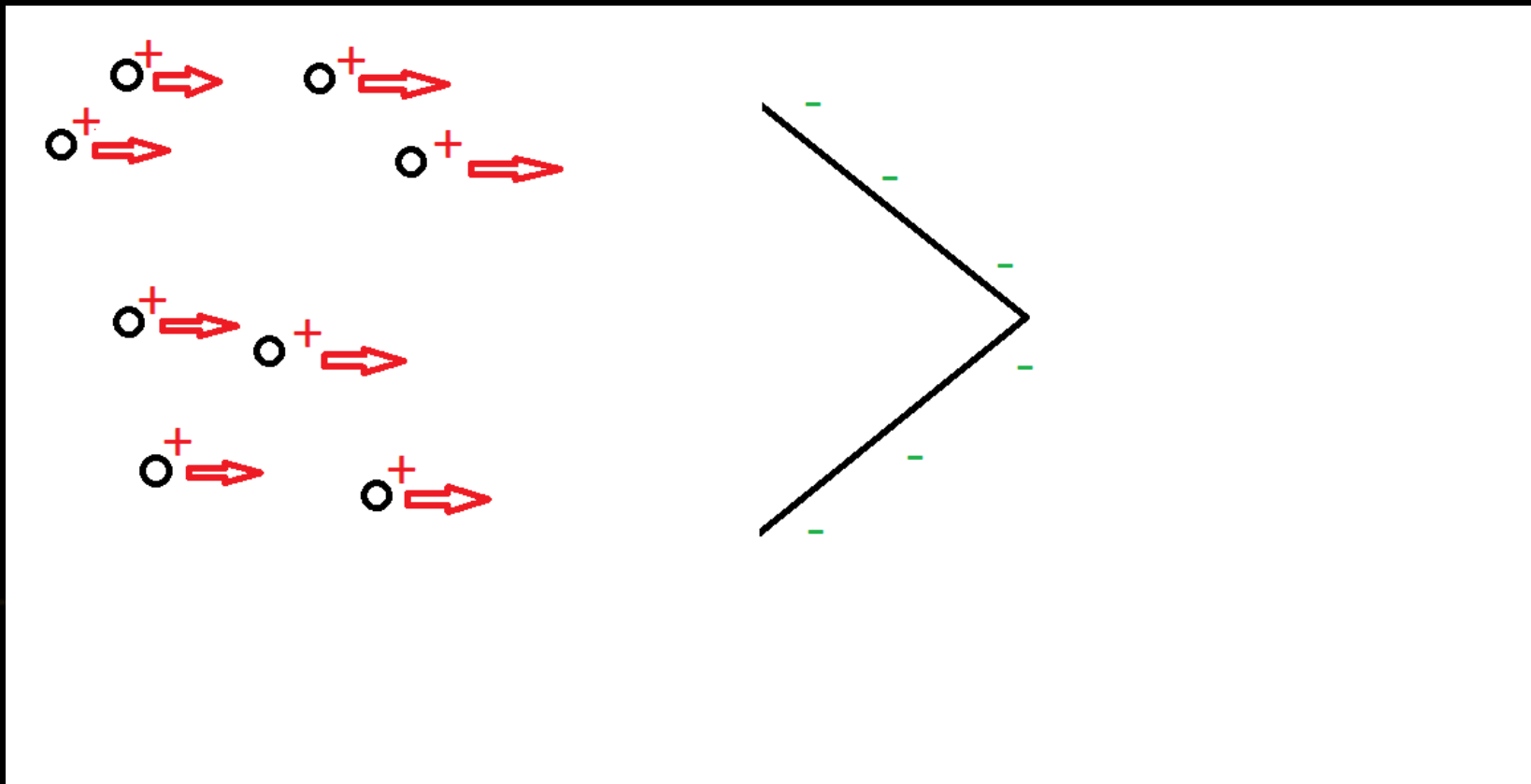

LUX CALIBRATION – THE FUSION PROCESS

- The titanium target wedge is biased to at least 80 kV.
- When the magnetron pulses the Deuterium gas becomes ionized.
- The first bunch of Deuterium that strikes the target binds to the surface to form Titanium Hydrate.

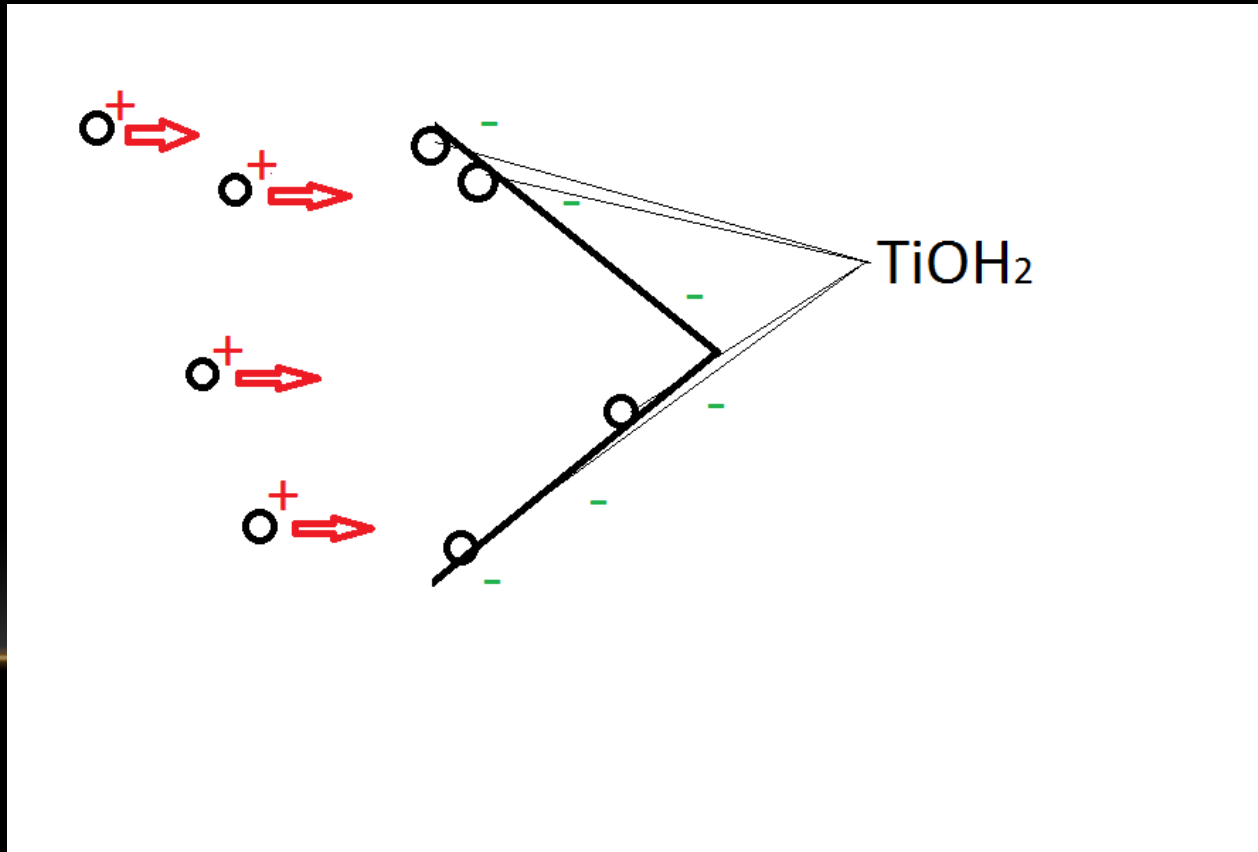

LUX CALIBRATION – THE FUSION PROCESS

- The titanium target wedge is biased to at least 80 kV.
- When the magnetron pulses the Deuterium gas becomes ionized.
- The first bunch of Deuterium that strikes the target binds to the surface to form Titanium Hydrate.
- When another Deuterium strikes a bound one they can fuse to produce Helium 3 and a 2.45 MeV neutron.

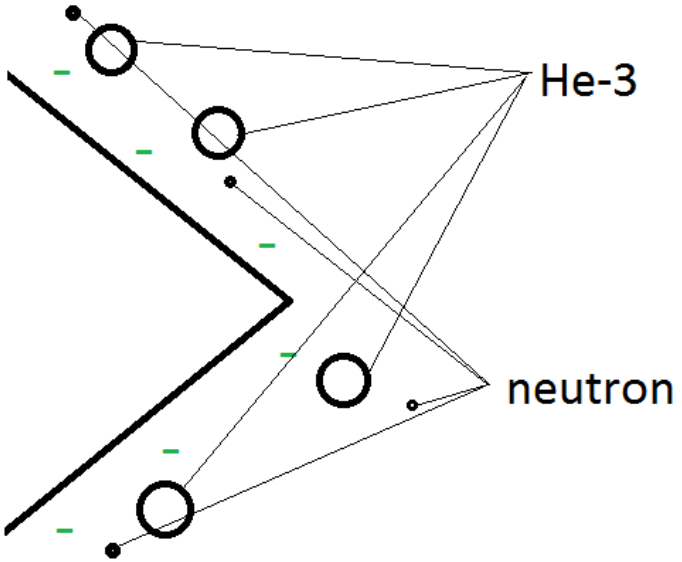

LUX CALIBRATION – NEUTRON ENERGY

- 2 possible fusion processes for D-D.
  - D + D -> Tritium + Proton
  - D + D -> ^{3}He + n (the one we care about)
- $2m_{D_2} - (m_{^3He} + m_n)$ gives a Q-value of 3.268 MeV
- The max 80 keV from acceleration is insignificant, so $p_{^3He} = p_n$. Since this is non-relativistic (3.268 MeV << m_n or m_{He}), the neutron gets ¾ of the energy (m_{He} ~ 3 m_n). 2.45 MeV

Reaction Probability

	Slam Energy (KeV)			
Reaction:	10	100	1250	1750
D & D -> T + p	49.73%	52.86%	50.79%*	52.75%*
D & D -> He3 + n	50.27%	47.14%	49.20%*	47.24%*

* estimated from Reference [24]

http://www.thepolywellblog.com/

24. "The Physics of Inertial Fusion: Beam Plasma Interaction, Hydrodynamics, Hot Dense Matter", Stefano Atzeni Et al. 2004

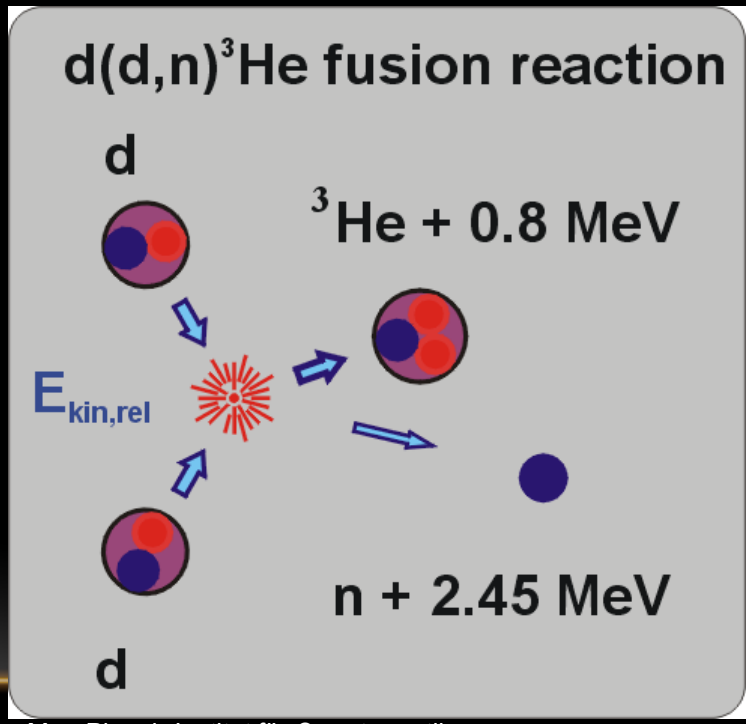

Max-Planck-Institut für Quantenoptik

http://www2.mpq.mpg.de/lpg/research/neutrons/neutrons.html

LUX CALIBRATION - DD CALIBRATION SETUP

- Neutrons created externally, collimated via tube through water tank
- Start by only considering events with two scatters
- Energy of first scatter determined exactly (within error from position reconstruction) by $E_r = E_n \frac{4m_n m_{Xe}}{(m_n+m_{Xe})^2} \frac{1-\cos(\theta_{CM})}{2}$

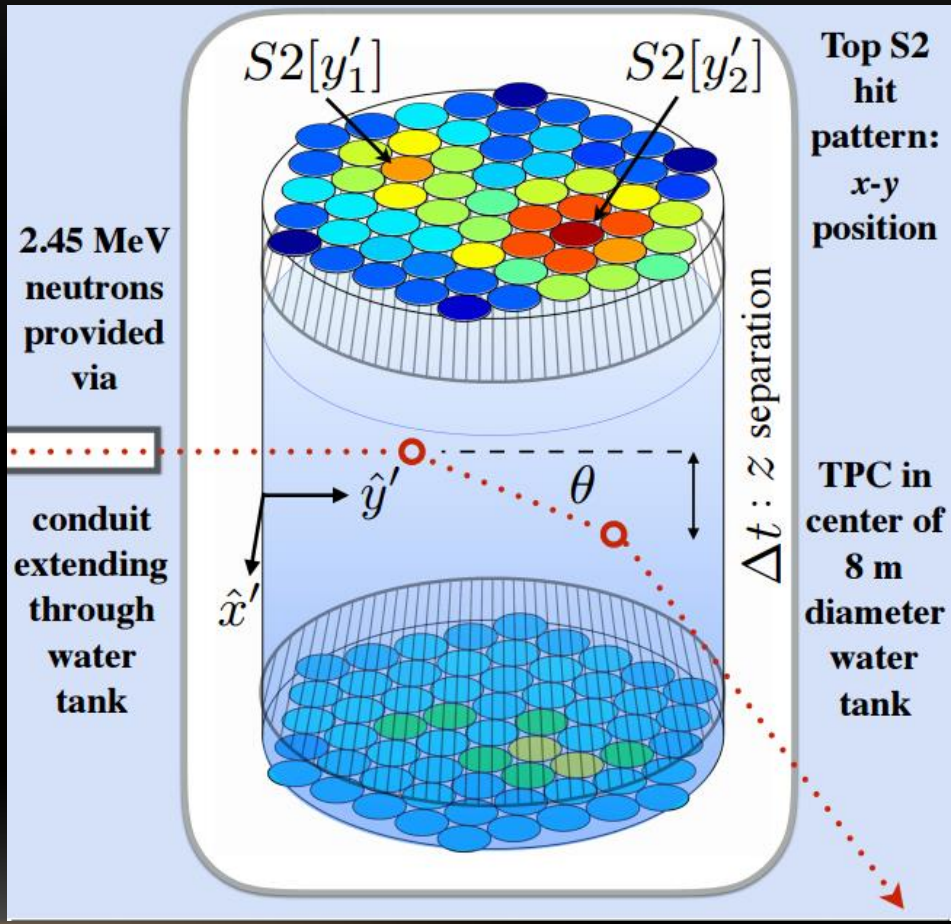

LUX CALIBRATION - THE Q_Y MEASUREMENT

- The S2 of an individual event can be written $S_2 = n_e g_2$ (Q_y is a distribution)
- Obtain $n_e = \frac{S_2}{g_2}$ for each event
- Bin (in energy) and fit to a model

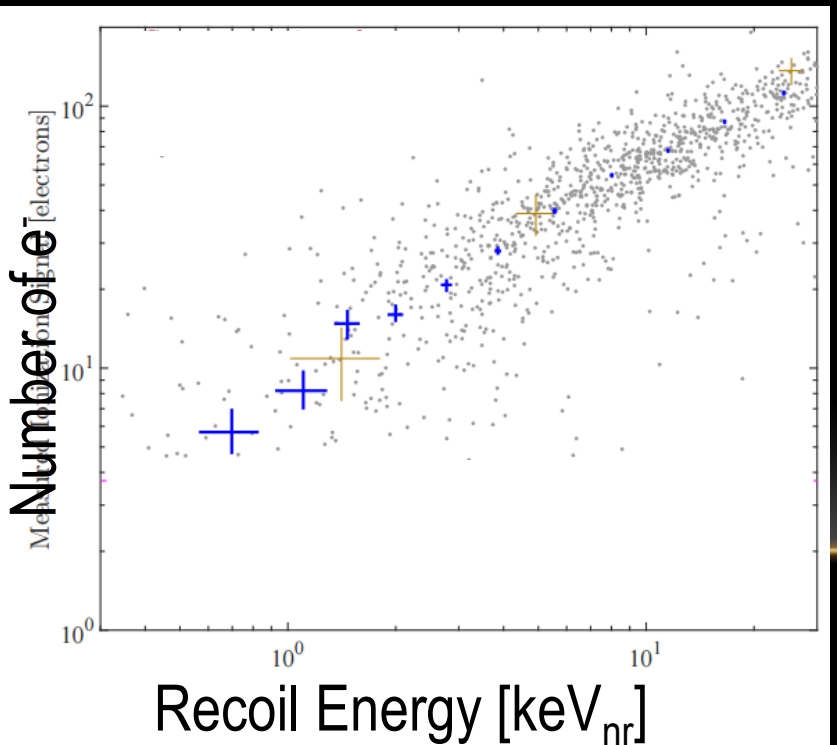

Left: Grey: individual events, Blue: best fits from bins on the right, Gold: representative uncertainties for individual events
Right: Red: best fit model, Blue: data

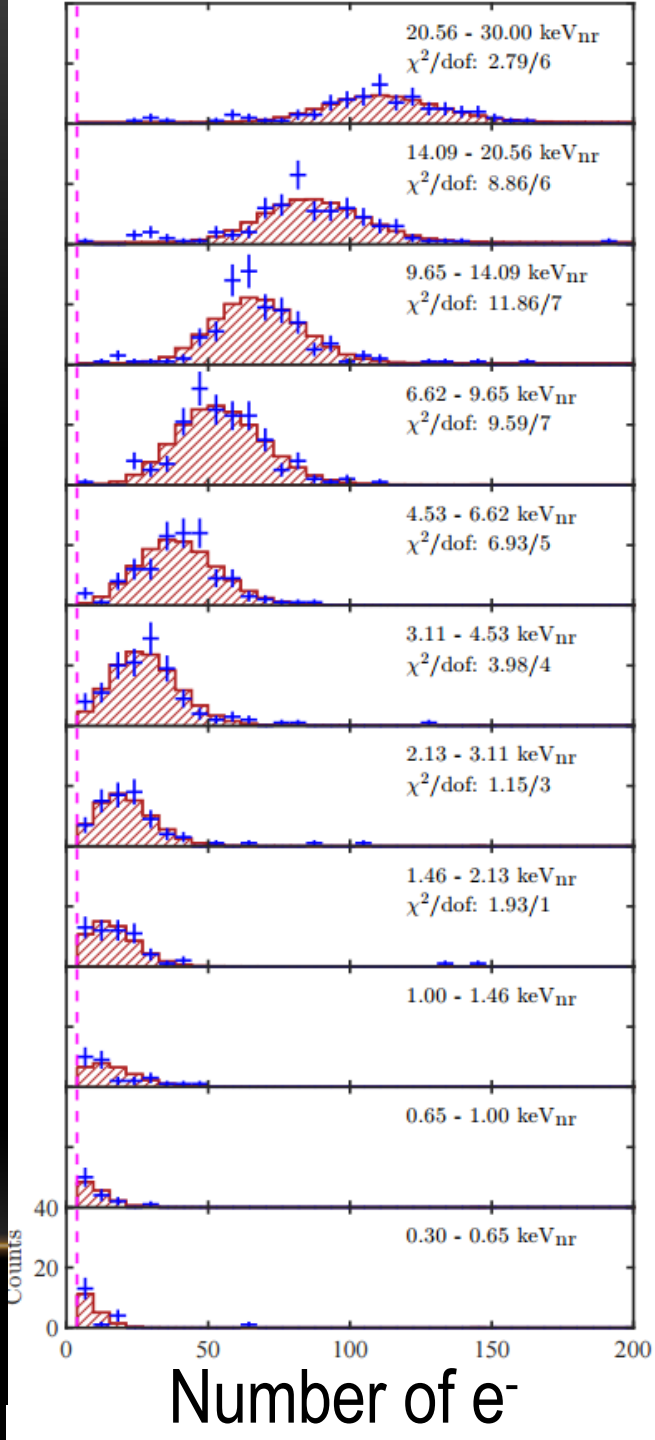

LUX CALIBRATION – THE L_Y MEASUREMENT

- Similar to the Q_y measurement, but using single scatter events instead, and the now calibrated S2 as a proxy for energy
- The S1 of an individual event can be written $S_1 = n_\gamma g_1$ (L_y is really a distribution)
- Obtain $n_\gamma = \frac{S_1}{g_1}$ for each event
- Bin (in S2) and fit to model

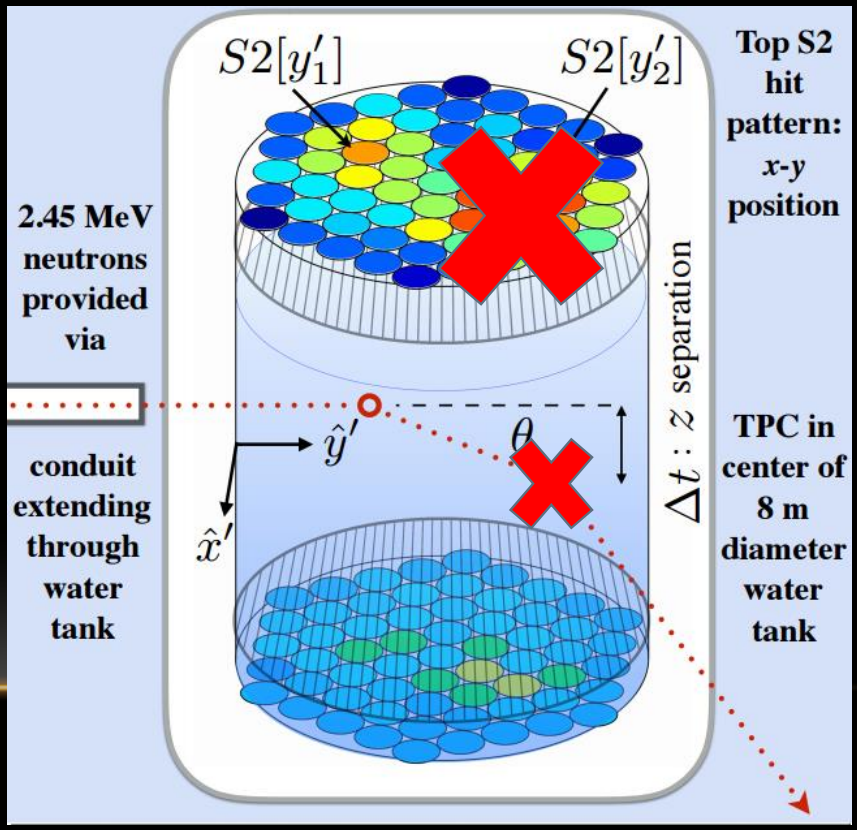

LUX CALIBRATION - THE ENDPOINT MEASUREMENTS

- The maximum allowed energy deposition is 74 keV
- L_y and Q_y can be determined at this energy by modeling the endpoints of the S1 and S2 (single scatter) spectra.

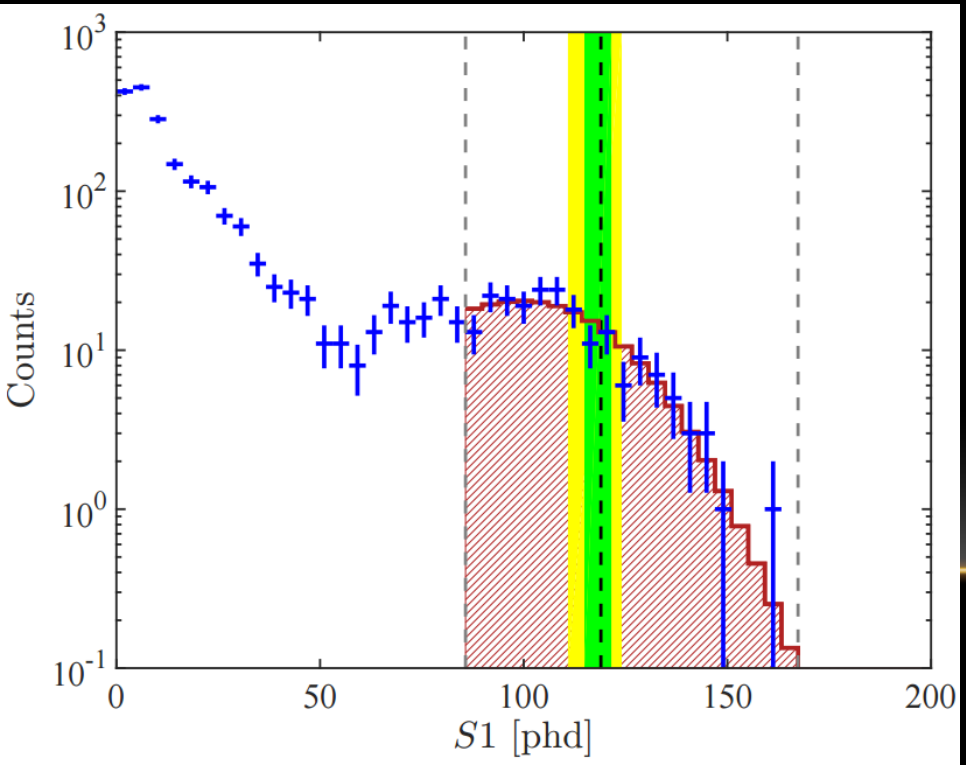

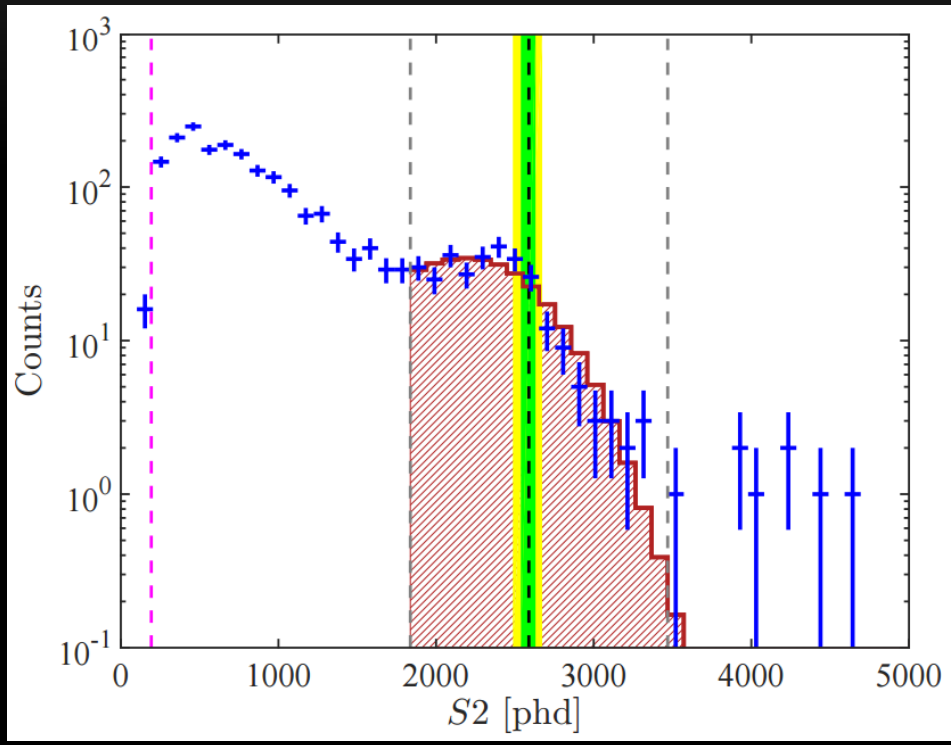

Red: best fit endpoint model, Blue: data, Black vertical dashed line: best fit for mean value of L_y (left) or Q_y (above)

LUX CALIBRATION - L_Y AND Q_Y

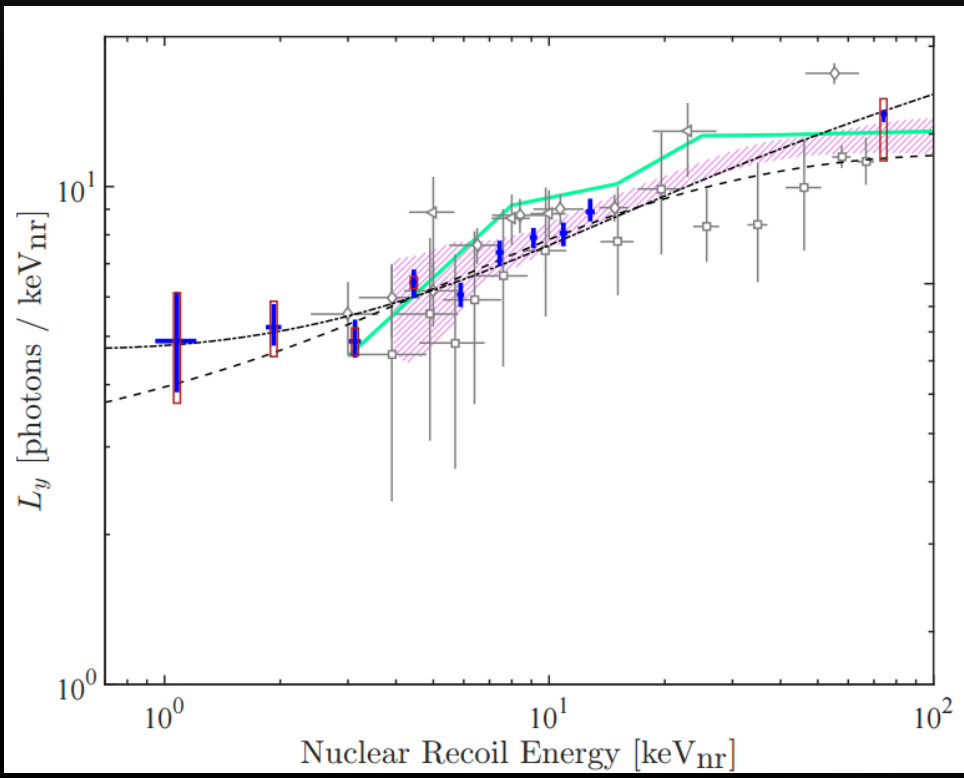

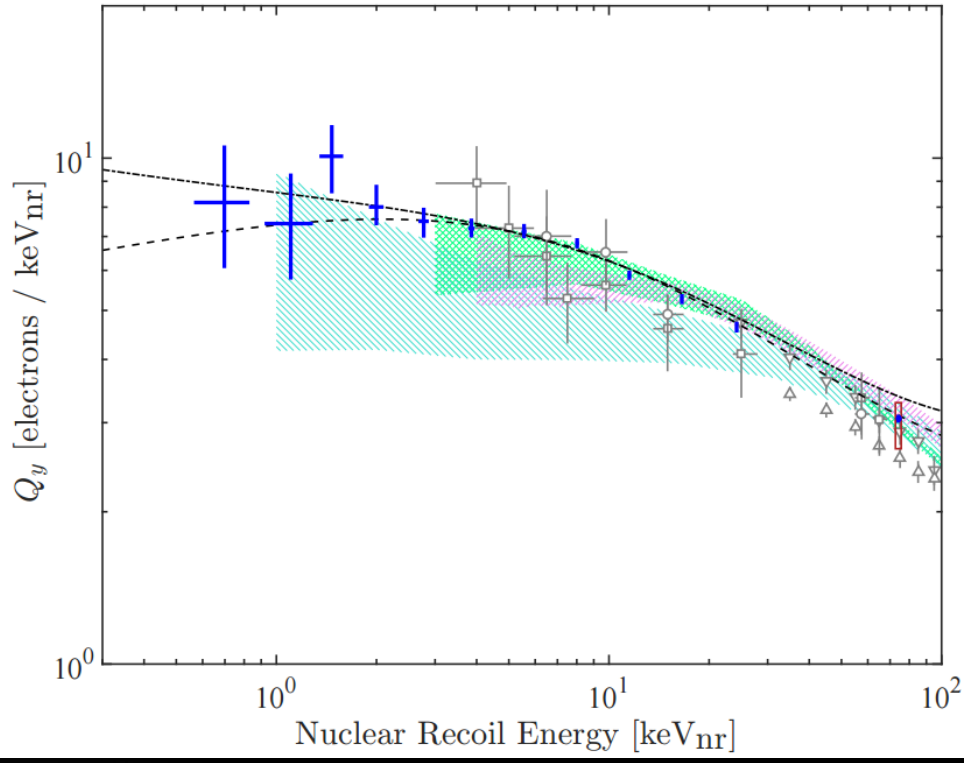

Blue: measurements of the mean from the first analysis, Red box on right: measurement of the mean from endpoint analysis, Dashed line: Lindhard-based model, Dot-dashed line: Bezrukov-based model

BUT THAT'S NOT THE WHOLE STORY…

- The ER and NR responses also depend on electric field…
- LUX Run04 had position and time dependent electric field
- Need to measure field dependence of L_y and Q_y

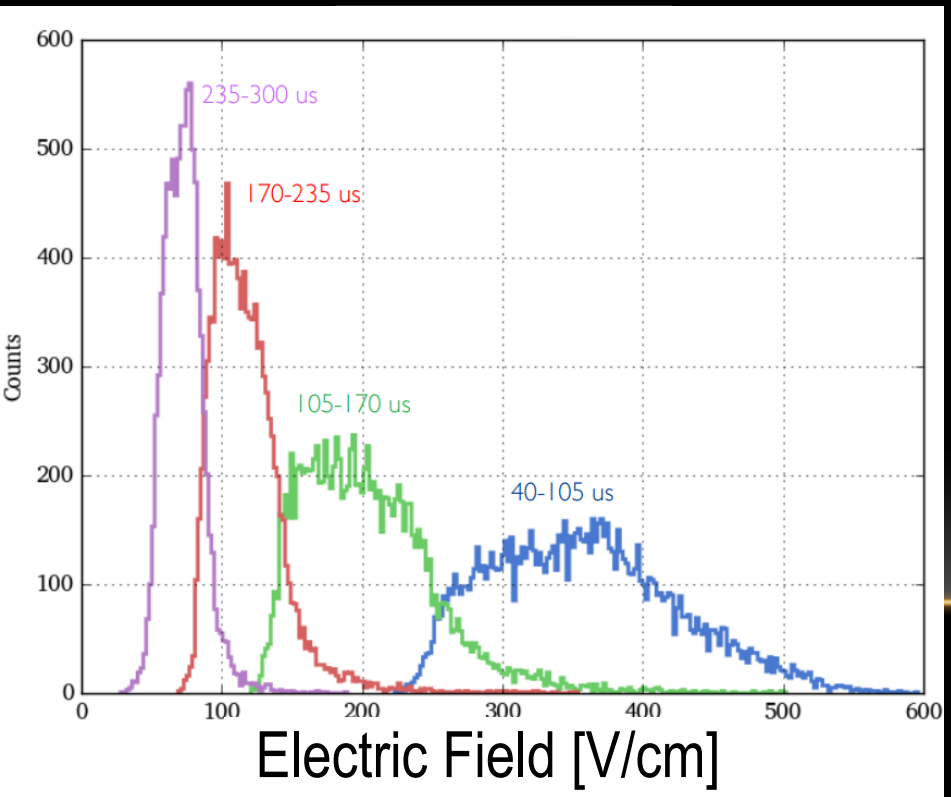

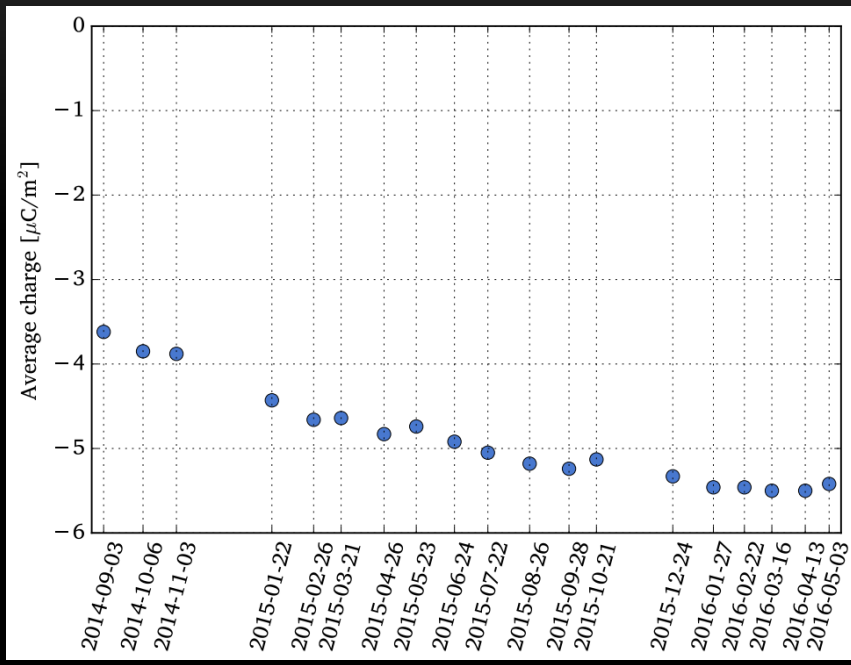

Electric field variations throughout run04 can be well modeled by a buildup of charge on the TPC walls.

Left: The different colors represent different depths in the detector. A sampling of points from those regions illustrate the field magnitude at different depths.

LUX WIMP SEARCH - ADAPTING TO FIELD VARIATIONS

- ER simulation model updated to include dependence on varying electric field
- NR model will be similarly updated
- Initial analysis split detector into bins with similar field and modeled each bin separately

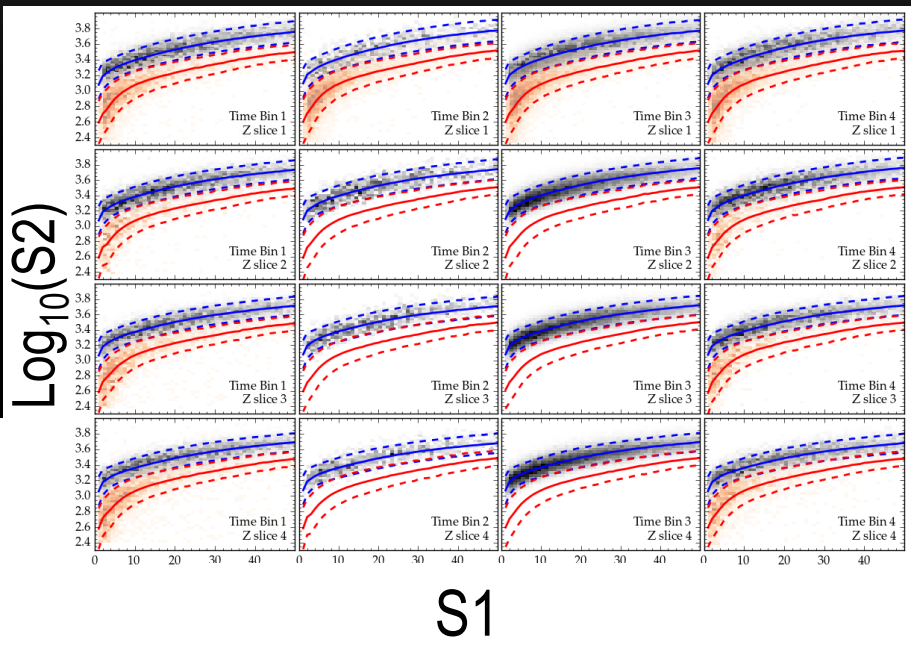

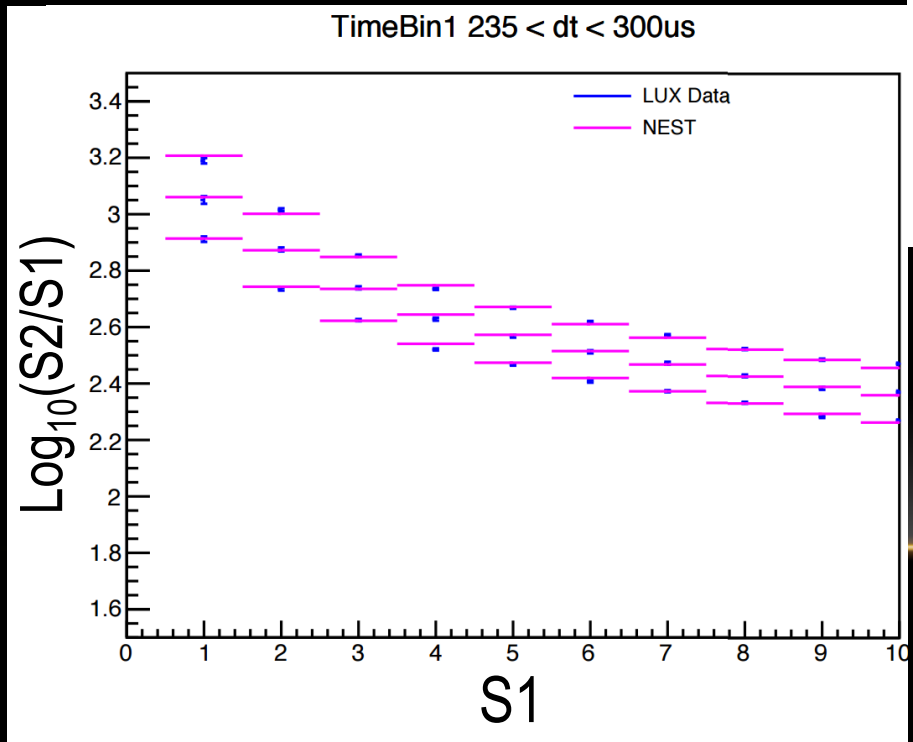

Above: Models for the 16 bins with similar field. Split into 4 "time bins" and 4 "Z slices." Blue=Electron Recoil, Red=Nuclear Recoil.
Left: A Unique NEST (simulation) model of the ER band for a specific bin

LUX WIMP SEARCH - THE DATA

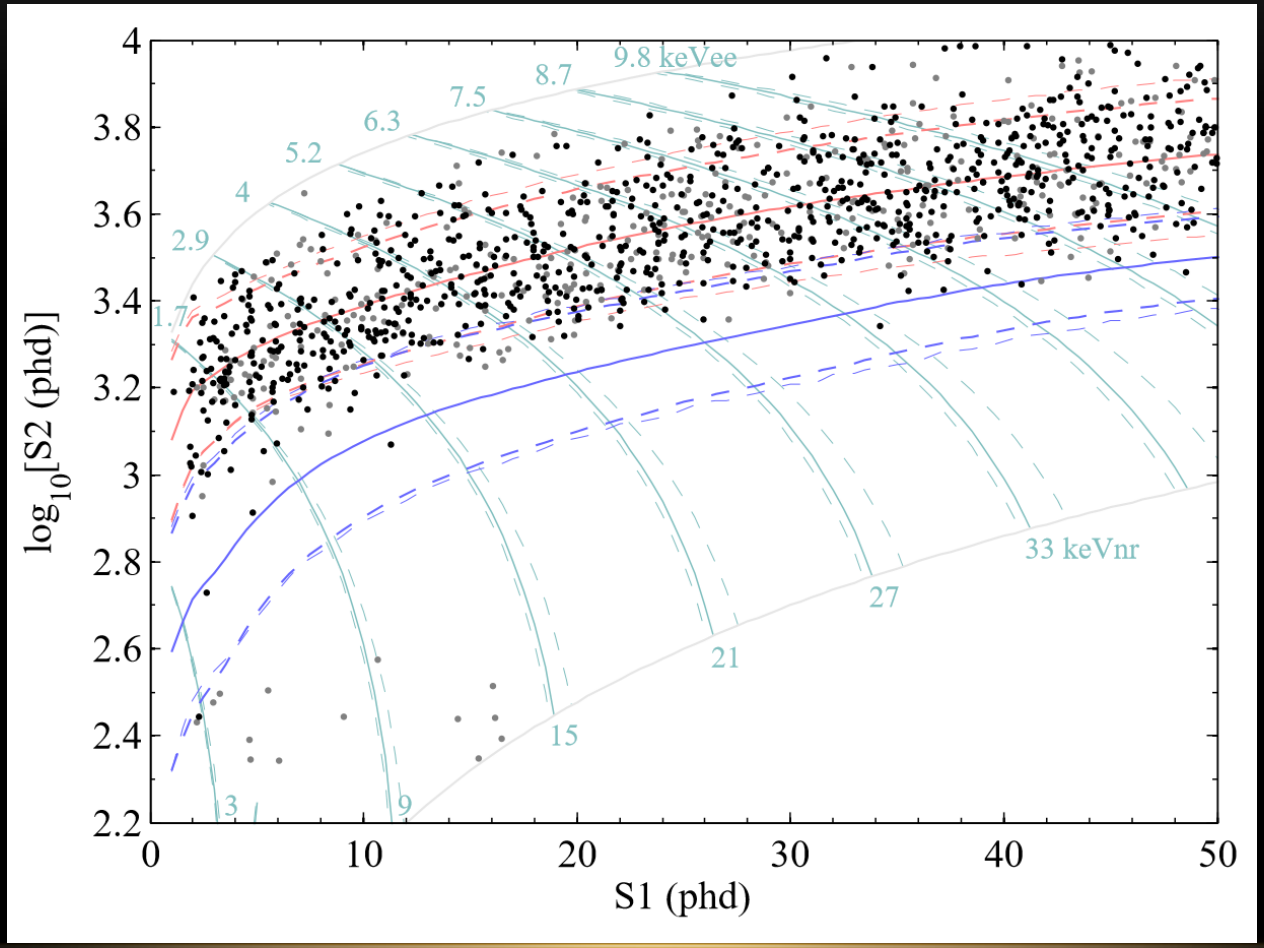

Data from the LUX Run04 result (not combined with previous run). Black and grey are data, Blue is the NR band, Red is the ER. Actual data, but recall the result was obtained by modelling many bins with similar E-field separately.

LUX WIMP SEARCH – COMPUTING THE LIMIT

- Combine background model with various strength signal models
- Assess how well each matches the data

Right: Example of a signal model.

Expected signal distribution for a 33 GeV WIMP

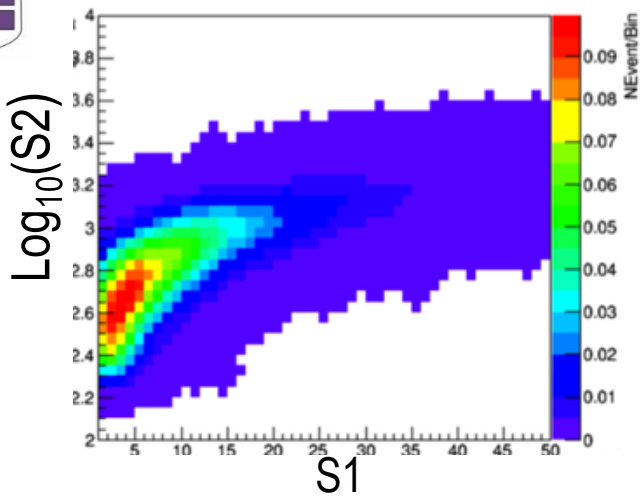

Background model PDFs

Signal model PDF

Data comparison

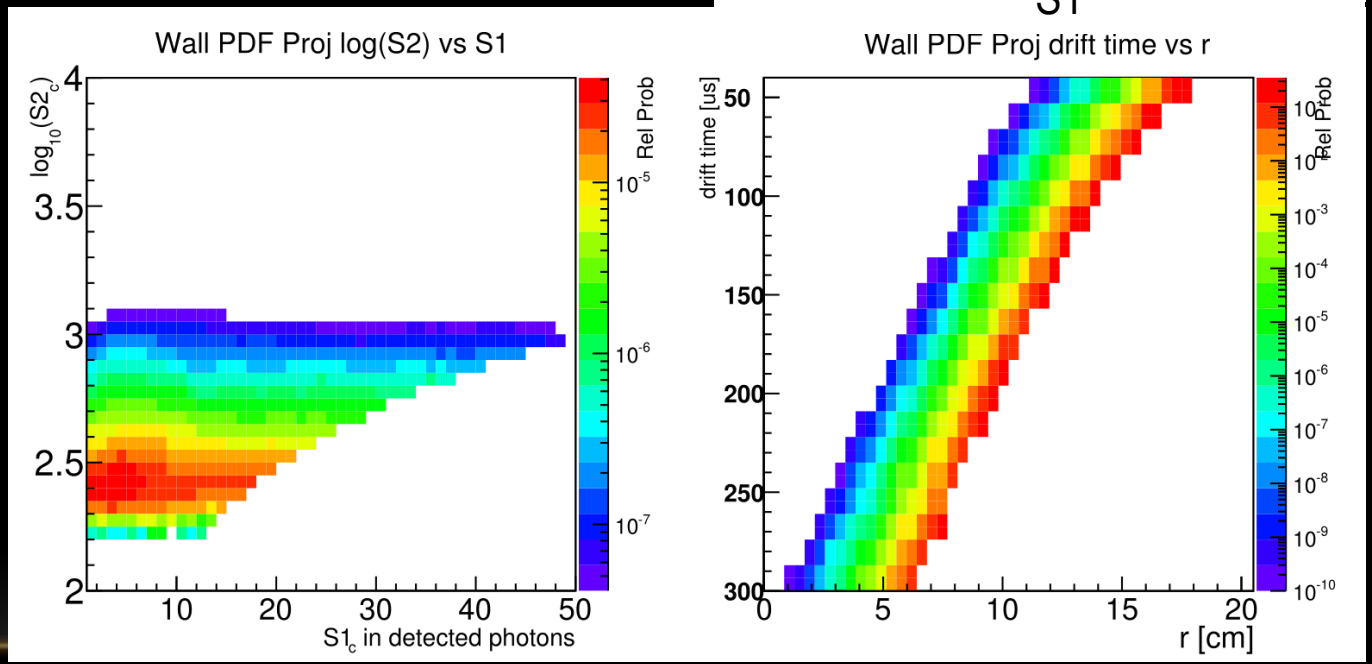

Above: Example of a background model component, the wall model. Distributions of data that match this (and other) background models are do not contribute to a WIMP signal.

LUX WIMP SEARCH – THE LIMIT

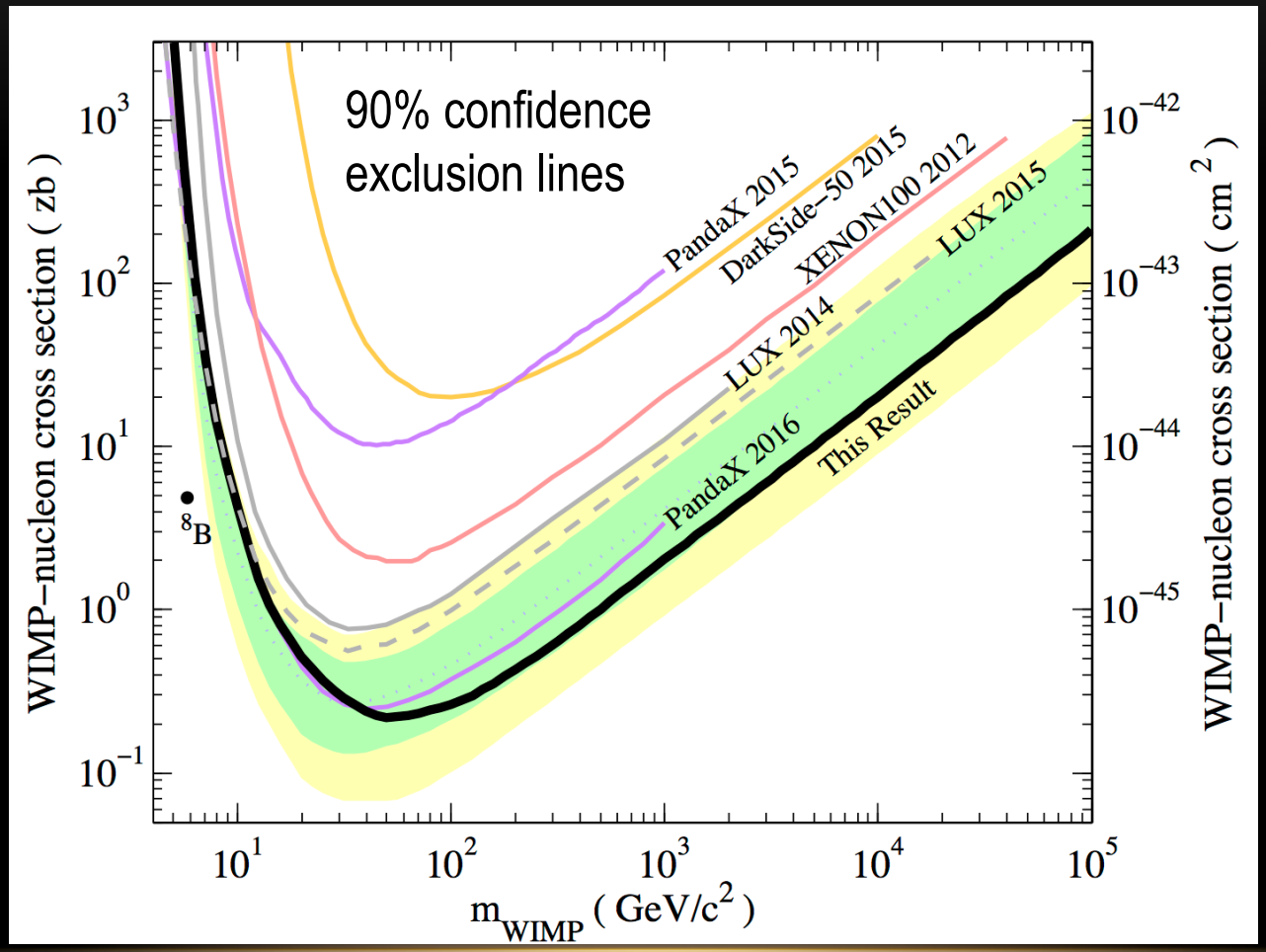

Identical to LUX 2015 result at low masses, factor of 4 better at high masses

Spin-independent result only!

FUTURE WORK

- Design and construct gas system components for System Test Phase II
  - Heat exchange elements
  - Flow control panel
- Update NR simulation model to include field variations
- Analyze electric field dependence of L_y and Q_y
- Analyze WIMP interaction models beyond the spin independent only case


LUX

BACKUP

DARK MATTER – EVIDENCE: THE COMA CLUSTER

- Fritz Zwicky measured the doppler shifts of ~1000 galaxies in the Coma Cluster.
- Mass of the cluster can be determined via the virial theorem
- Not consistent with the mass determined via luminosity measurements.
- There's something we're not seeing…

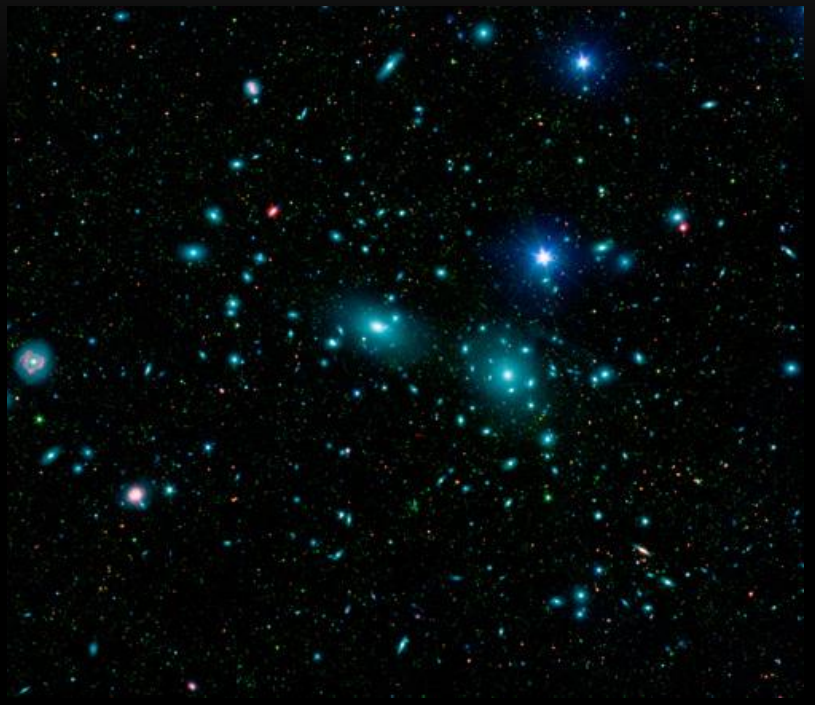

The Coma Cluster.

DARK MATTER – EVIDENCE: BULLET CLUSTER

Composite Credit: X-ray: NASA/CXC/CfA/ M.Markevitch et al.;
Lensing Map: NASA/STScI; ESO WFI; Magellan/U.Arizona/ D.Clowe et al.
Optical: NASA/STScI; Magellan/U.Arizona/D.Clowe et al.;
From http://apod.nasa.gov/apod/ap060824.html

The Bullet cluster

- Red is gas
- Blue is mass concentration located via gravitational lensing.
- Gas slowed via electromagnetic interactions
- Most mass separated from gas
  - Most mass experienced no electromagnetic interactions

DARK MATTER – EVIDENCE: CMB

- The Cosmic Microwave Background can be written in terms of the spherical harmonics.
- The sum over all m_ls for each l gives the power spectrum.

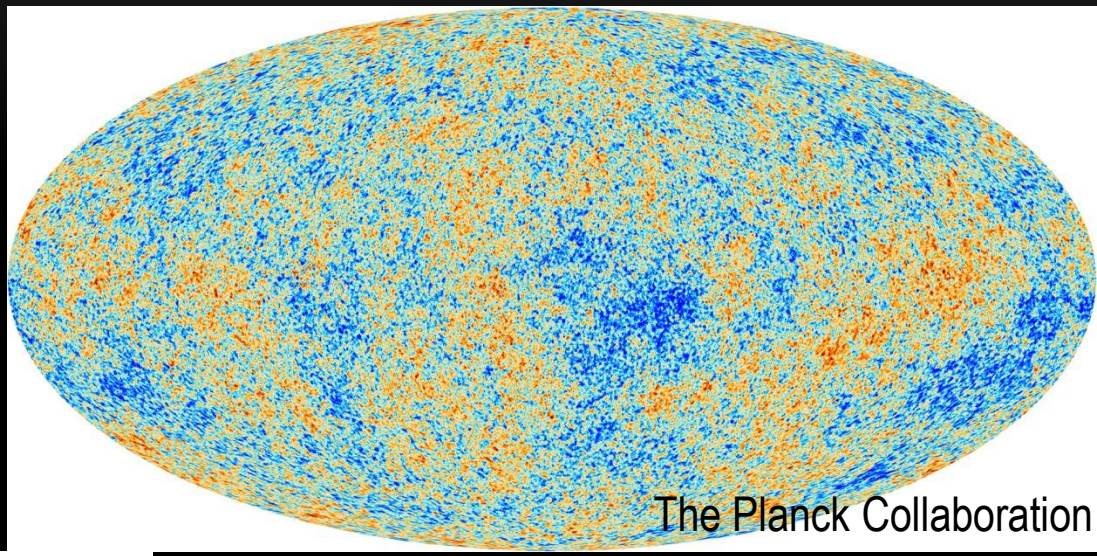

The Planck Collaboration

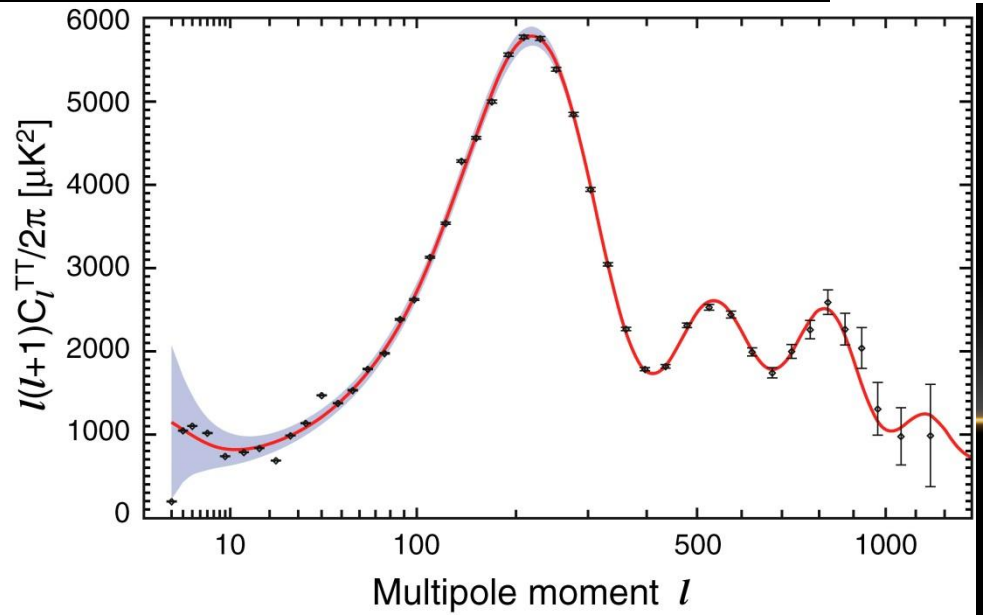

- The ratio of cold dark matter determines the shape
- Consistent with ~84% of matter being cold dark mater
- Only consistent if DM has no electromagnetic interactions

DARK MATTER - WIMPS

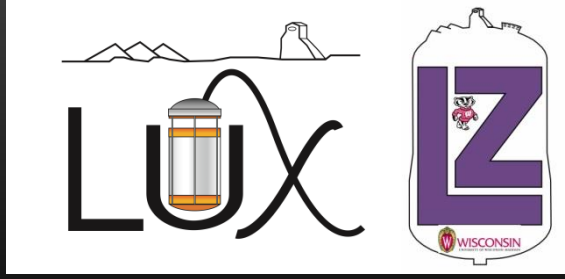

- Weakly Interacting Massive Particle
  - Particle:
    - MACHOs (Massive Compact Halo Objects) have been mostly ruled out by gravitational lensing
    - Bullet cluster casts doubt on modified gravity
  - Massive:
    - Dominant source of gravity, **heavy**
  - Weakly Interacting:
    - Freeze out gives self-annihilation cross section of ~ 3×10^{-26} cm^3 s^{-1}, the weak scale
    - No electromagnetic interactions

WHY XENON?

- Easy to make large target mass out of liquids
- Easy to purify
- Good self-shielding
- Transparent to its scintillation
- Higher interaction rate than other noble elements

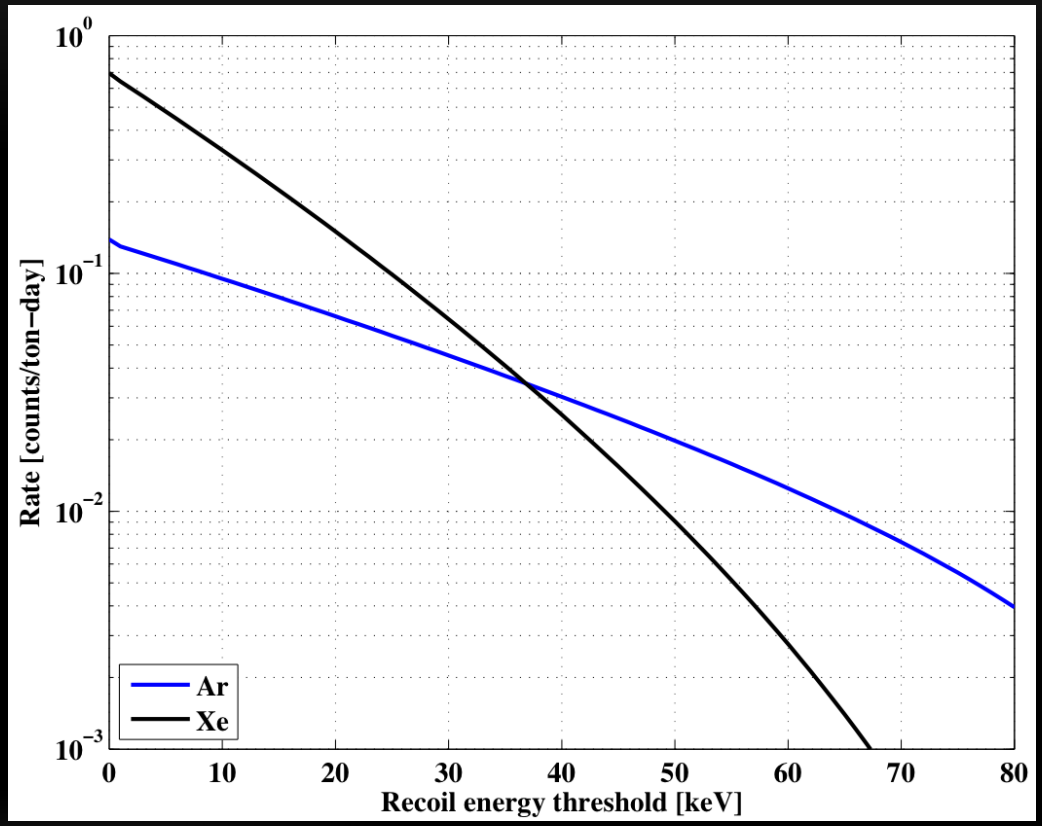

Waveform Example in LUX

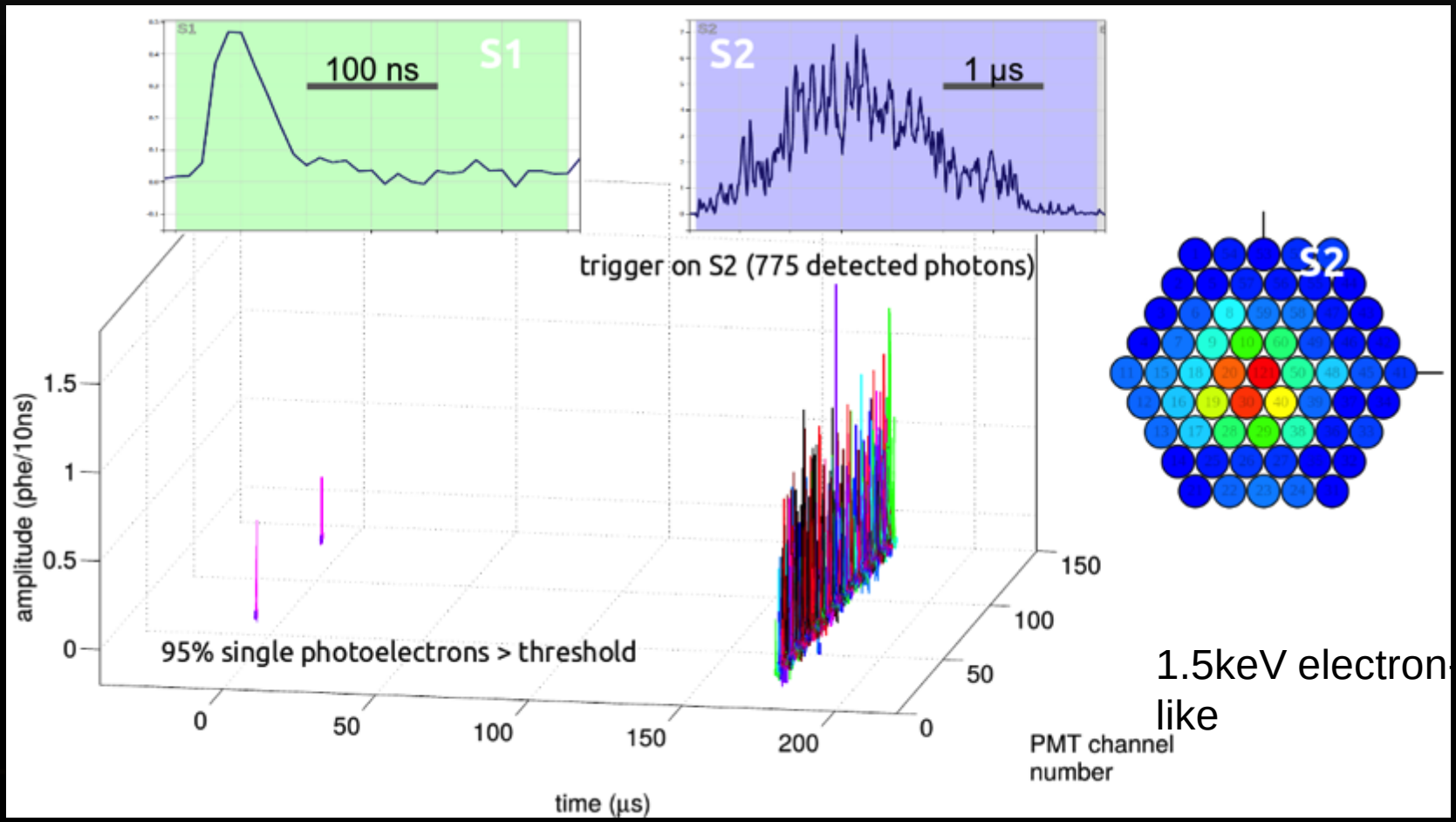

BACKGROUNDS

Table 1: The estimated backgrounds from all significant sources in the LZ 1000 day WIMP search exposure. Mass-weighted average activities are shown for composite materials. Solar ^{8}B neutrinos are expected contribute 7±3 NRs but only at very low energies and are excluded from the table. This is a simple latex version maintained by Alex Lindote (last updated February 24 2016 using git revision 5ddccd67)

	Mass	$^{238}U_e$	$^{238}U_l$	$^{232}Th_e$	$^{232}Th_l$	^{60}Co	^{40}K	n/yr	ER	NR
	(kg)	mBq/kg							(cts)	(cts)
Upper PMT Structure	40.2	3.86	0.23	0.48	0.38	0.00	1.45	2.51	0.06	0.000
Lower PMT Structure	69.9	2.40	0.13	0.30	0.24	0.00	0.91	6.06	0.07	0.001
R11410 3" PMTs	90.8	49.8	2.88	2.85	2.63	2.83	14.1	73.1	1.50	0.009
R11410 PMT Bases	2.6	546	76.2	31.7	30.5	2.33	82.6	44.3	0.39	0.003
R8520 Skin 1" PMTs	4.2	60.5	5.19	4.75	4.75	24.2	333	8.91	0.12	0.001
R8520 Skin PMT Bases	0.6	766	79.1	38.1	34.6	3.40	128	13.3	0.04	0.001
PMT Cabling	85.5	29.8	1.47	3.31	3.15	0.65	33.1	2.19	1.02	0.000
TPC PTFE	275	0.02	0.02	0.03	0.03	0.00	0.12	33.7	0.08	0.010
Grid Wires	0.8	1.20	0.27	0.33	0.49	1.60	0.40	0.02	0.00	0.000
Grid Holders	62.2	1.20	0.27	0.33	0.49	1.60	0.40	6.33	0.25	0.002
Field Shaping Rings	91.6	4.79	0.86	0.80	0.75	0.00	1.21	38.8	1.03	0.011
TPC Sensors	0.90	21.1	13.5	22.9	14.2	0.50	26.3	24.8	0.01	0.002
TPC Thermometers	0.06	336	90.5	38.5	25.0	7.26	3360	1.49	0.05	0.000
Xe Recirculation Tubing	15.1	0.79	0.18	0.23	0.33	1.05	0.30	0.64	0.01	0.000
HV Conduits and Cables	138	1.80	2.00	0.50	0.60	1.40	1.20	7.20	0.71	0.001
HX and PMT Conduits	200	1.25	0.40	2.59	0.66	1.24	1.47	5.33	0.21	0.001
Cryostat Vessel	2410	1.59	0.11	0.29	0.25	0.07	0.56	124	0.57	0.010
Cryostat Seals	37.1	25.7	12.5	4.53	5.68	0.32	3.61	84.6	0.25	0.003
Cryostat Insulation	23.8	18.9	18.9	3.45	3.45	1.97	51.7	69.8	0.34	0.006
Cryostat Teflon Liner	70.7	0.02	0.02	0.03	0.03	0.00	0.12	8.65	0.00	0.001
Outer Detector Tanks	4010	0.15	0.37	0.02	0.06	0.04	4.32	91.9	2.29	0.008
Liquid Scintillator	20800	0.01	0.01	0.01	0.01	0.00	0.00	16.8	0.15	0.001
Outer Detector PMTs	122	1510	1510	1070	1070	0.00	3900	14500	0.00	0.000
OD PMT Supports	770	1.20	0.27	0.33	0.49	1.60	0.40	14.3	0.00	0.000
^{222}Rn (2.0 μBq/kg)									783	-
^{220}Rn (0.2 μBq/kg)									129	-
^{nat}Kr (0.015 ppt)									24.5	-
^{nat}Ar (0.45 ppb)									2.47	-
Laboratory and Cosmogenics									7.80	0.12
Fixed Surface Contamination									0.19	0.37
Subtotal (Non-n counts)									956	0.56
^{136}Xe $2n\beta\beta$									67	0.00
Astrophysical n counts (pp+^{7}Be+^{14}N)									255	0.00
Astrophysical n counts (^{8}B)									0.00	0.00
Astrophysical n counts (hep)									0.00	0.21
Astrophysical n counts (diffuse supernova)									0.00	0.05
Astrophysical n counts (atmospheric)									0.00	0.46
Subtotal (Physics backgrounds)									322	0.72
Total									1,280	1.28
Total (with 99.5 % ER discrimination, 50 % NR efficiency)									6.39	0.64
Sum of ER and NR in LZ for 1000 days, 5.6 tonne FV, with all analysis cuts									**7.03**	

U238 DECAY CHAIN

Most Common Radon

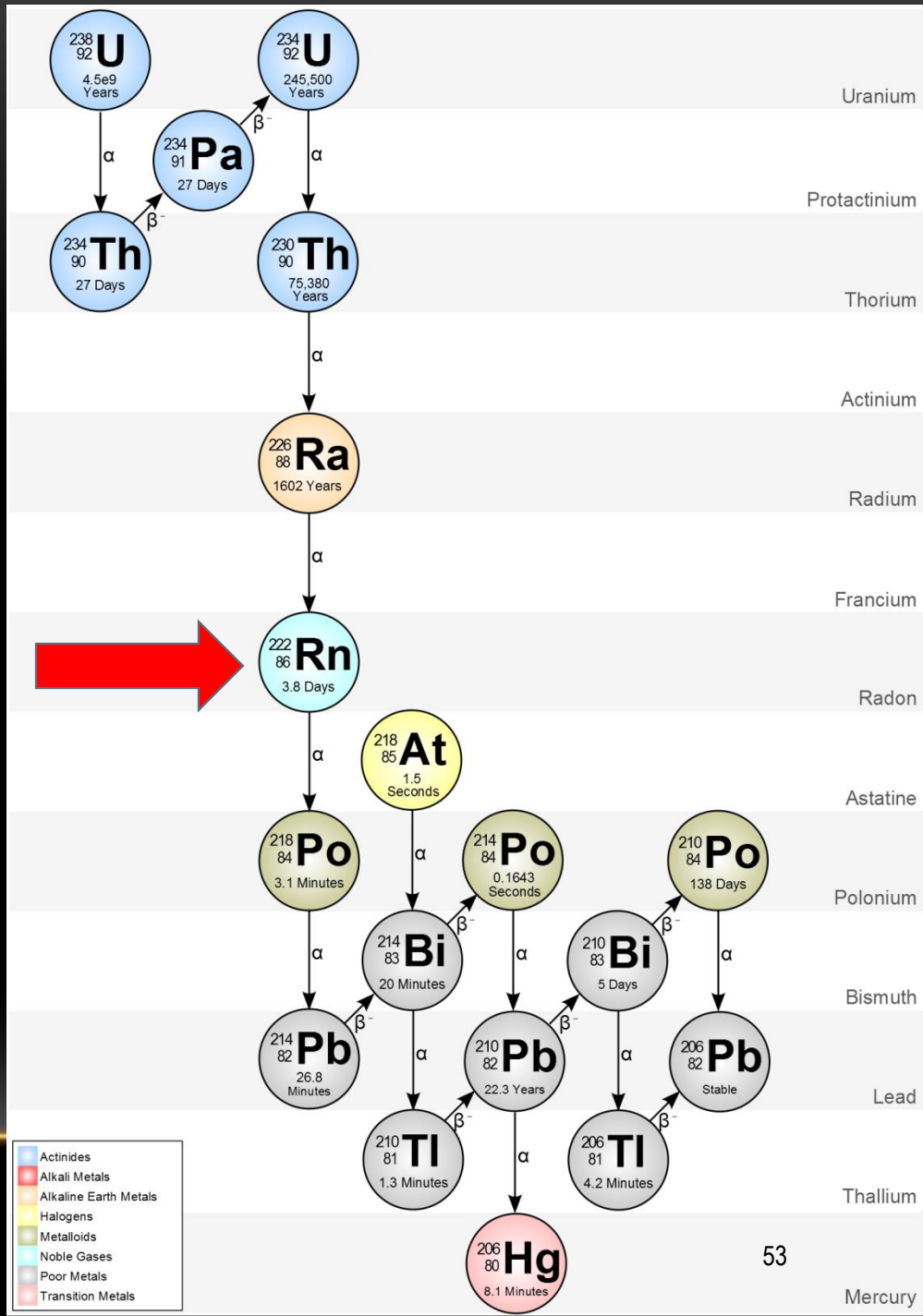

TH232 DECAY CHAIN

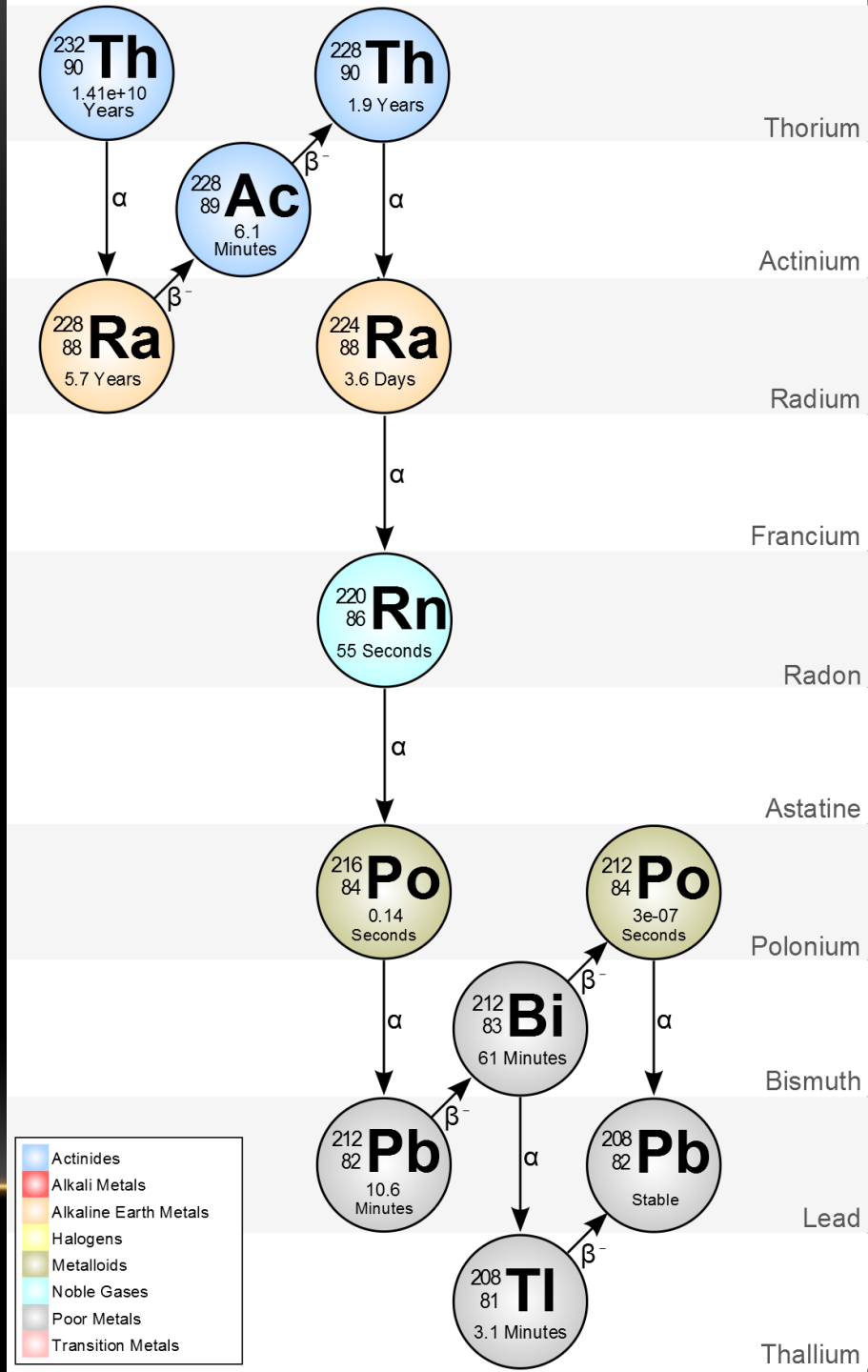

Purification via Getter

- SAES Monotorr commercial getter.
  - Previous experiment experience
  - Requires Gas flow not liquid
- How it works:
  - non-noble impurities bind to surface of highly reactive zirconium pellets
  - pellets are heated (~450° C) to allow diffusion into bulk

Circulation - Compressor

- Fluitron A2-10-CS Diaphragm compressor
  - All-metal diaphragms and seals.
  - Far larger than the LUX pumps (200 slpm vs 20 slpm)
  - Noise and vibration isolation needed
    - Located in separate structure
- System test trying smallest model for practice with technology

Circulation - Weir

- Xe level maintained between two grids
- 3 precision level sensors monitor stability and uniformity of surface.
- Flow from bottom to top minimizes dead zones.

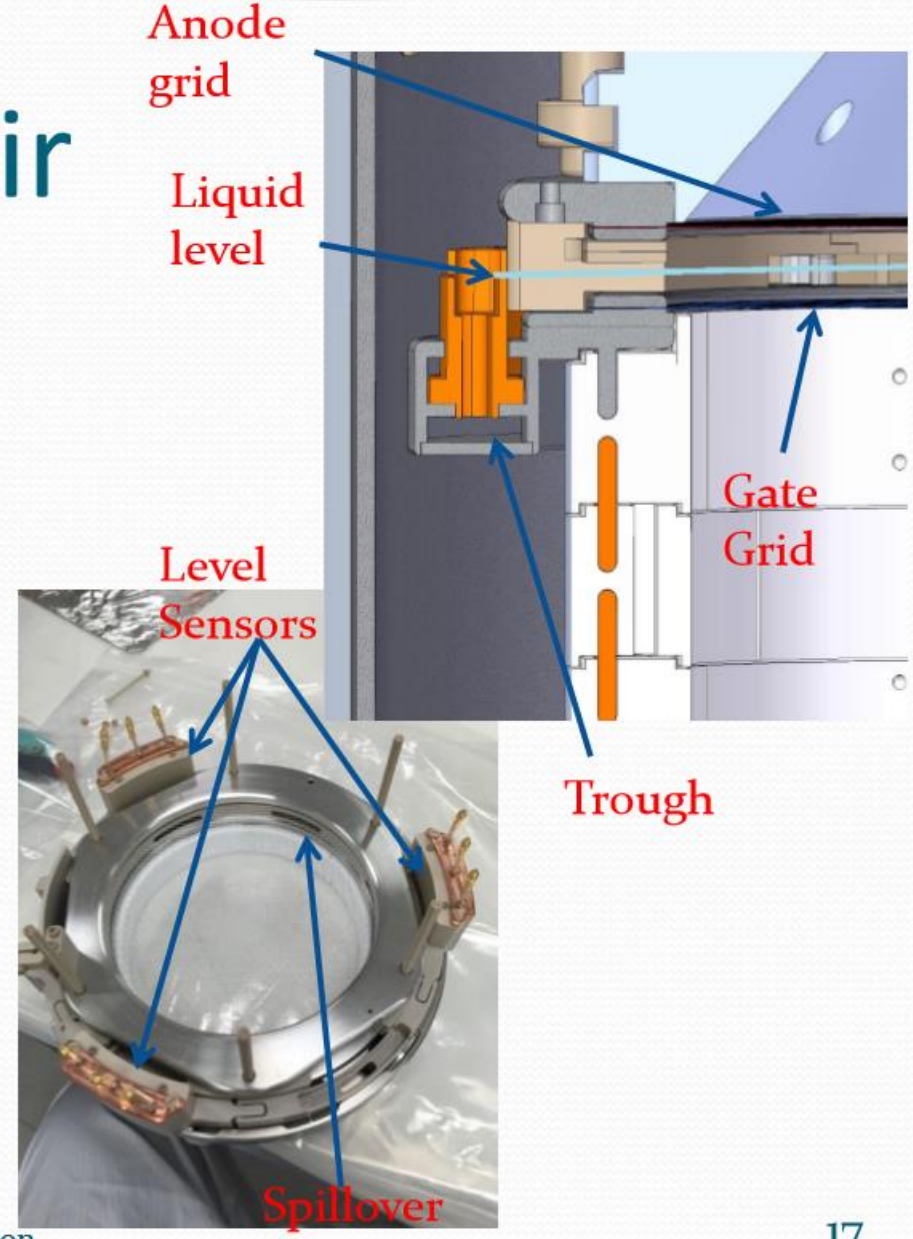

SIGNAL EVENTS

- Nuclear Recoils
- Lower charge-to-light ratio

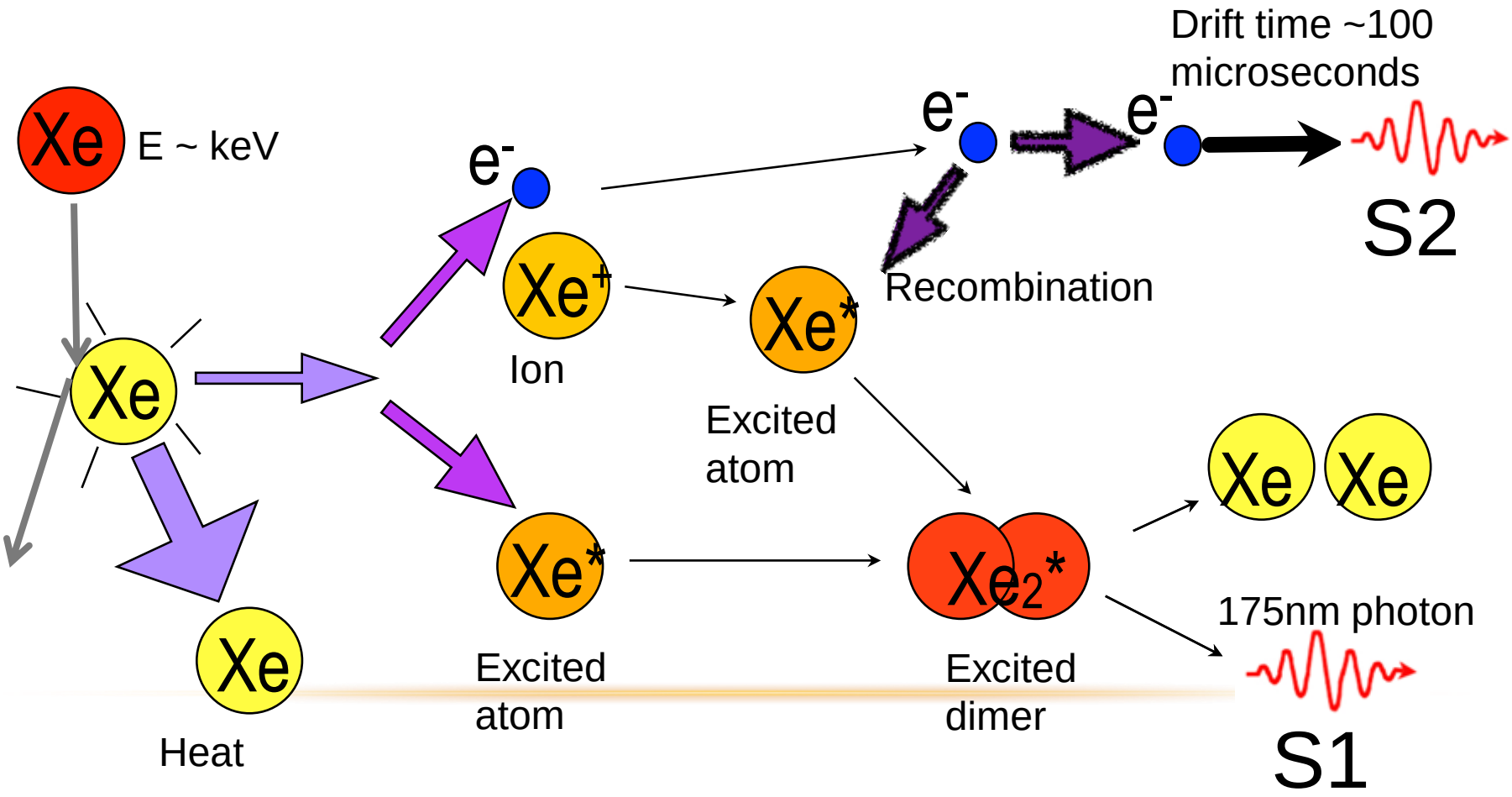

Figure: Gibson/Shutt

BACKGROUND EVENTS

- Electron Recoils
- Higher charge-to-light ratio

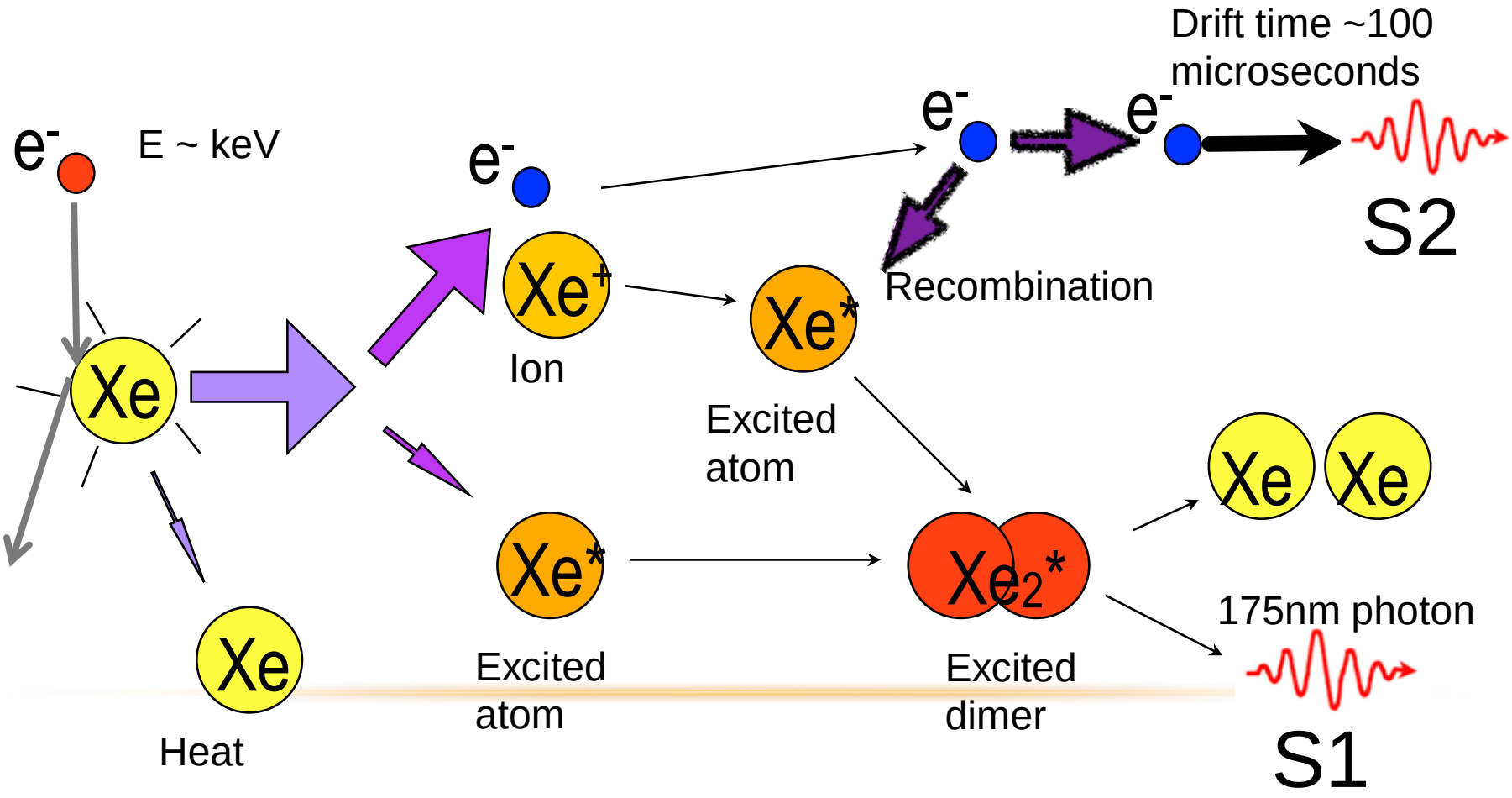

Figure: Gibson/Shutt

CHARGE VS LIGHT BRANCHING RATIOS

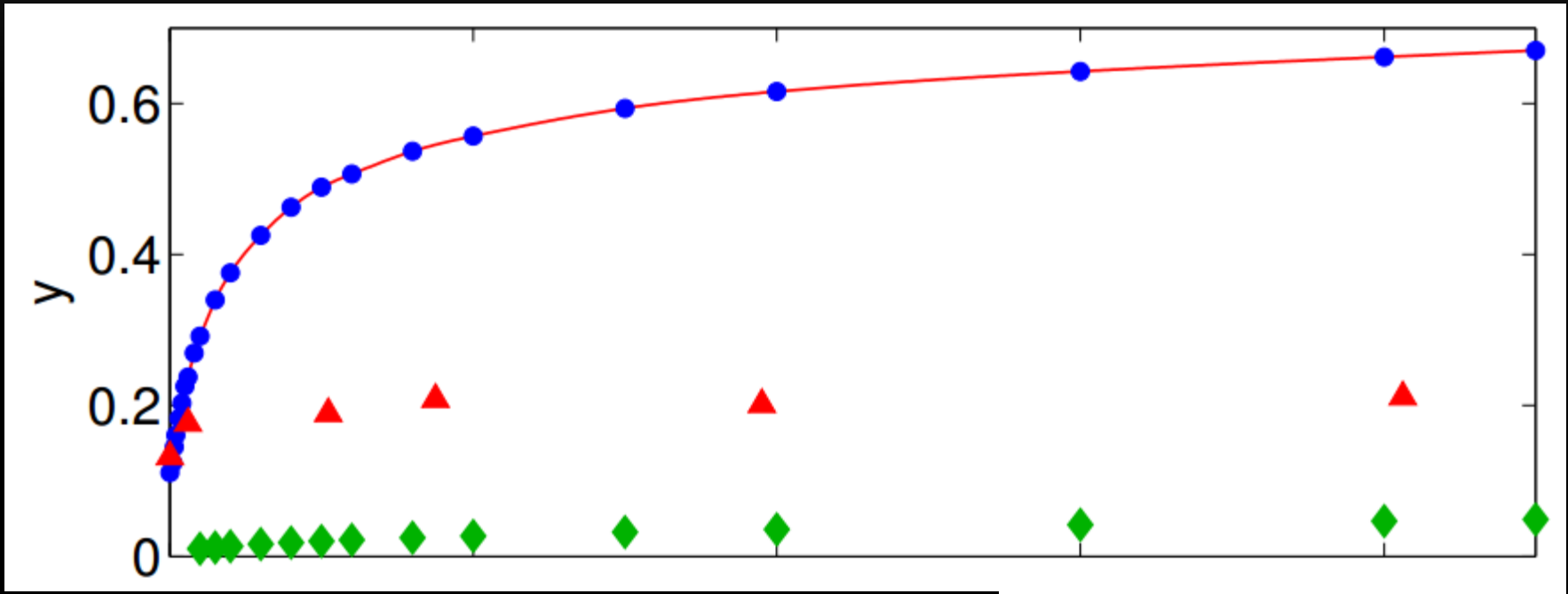

y is $\frac{n_e}{n_e+n_\gamma}$ the fraction of detectable signal in charge

CALIBRATIONS IN LUX - ER

- Several external γ sources
- Xe radioactivity
- Two injected sources
  - CH_3T - β source at < 18.6 keV (mean e^- energy of 5.7 keV)
  - ^{83m}Kr - Emits two γs at 41.6 keV and 9.4 keV.

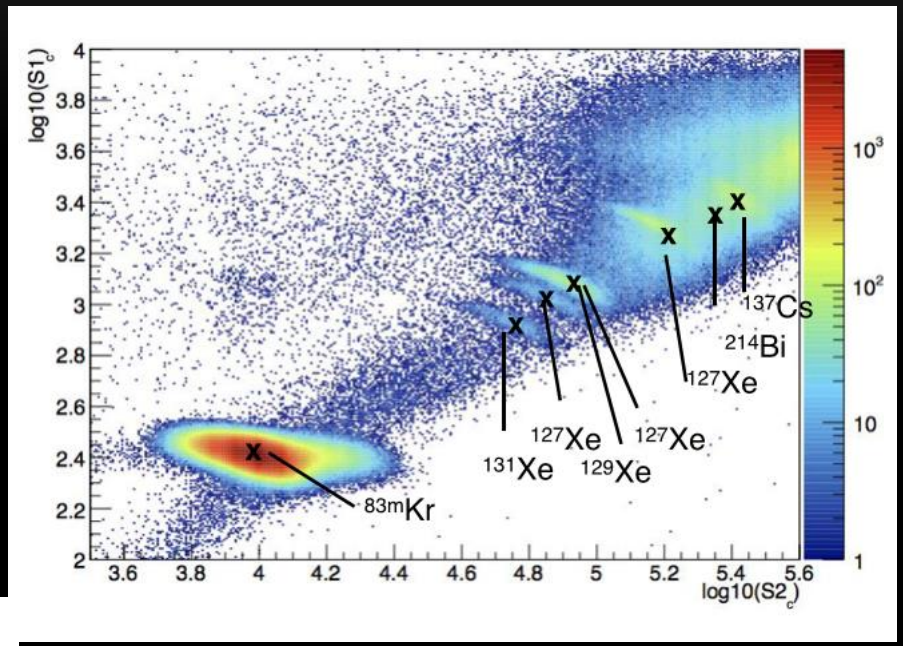

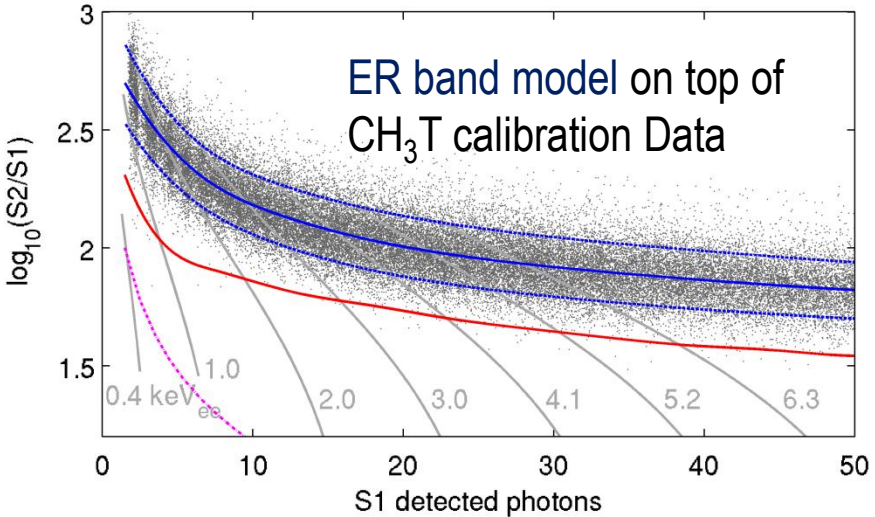

- CH_3T used to model ER band
- Other sources used to probe detector response

CALIBRATIONS IN LUX – ER: G1, G2

- Energy deposited in ER given by $E = W(n_\gamma + n_e)$
  - $W = 13.7\ ^{ev}/_{particle}$
  - Can write this $E = W\left(\frac{S_1}{g_1} + \frac{S_2}{g_2}\right)$
    - g_1, g_2 are the number of photons detected per scintillation photon or ionized electron.
  - Or $\frac{S_1}{E} = \frac{g_1}{W} - \frac{g_1}{g_2}\left(\frac{S_2}{E}\right)$
- Signals in the detector normalized to center

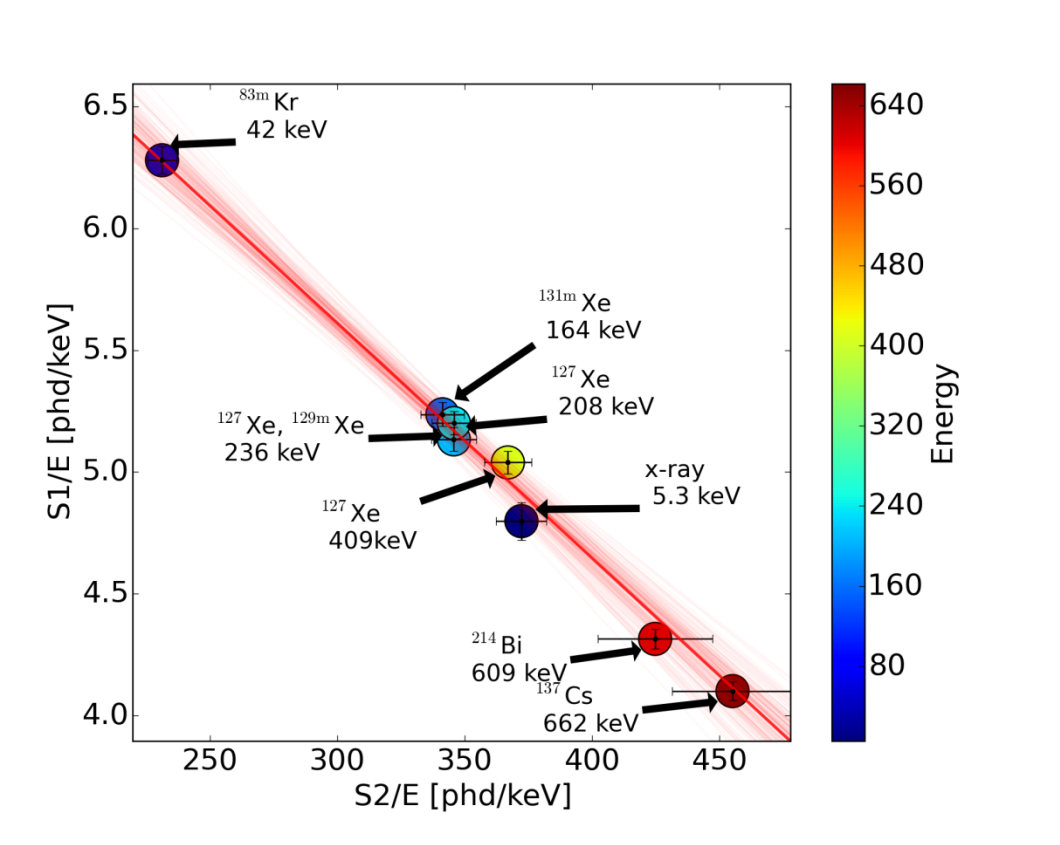

Doke plot: used to extract detector parameters g_1 and g_2 as well as verify $E = W(n_\gamma + n_e)$

THE DEUTERIUM

- Deuterium gas fed into plasma chamber
- Constant bleeding from the D_2 bottle, constant pumping from the chamber
- D_2 ionized via microwaves from magnetron + optical cavity
- Magnetron pulsed to ionize in bursts

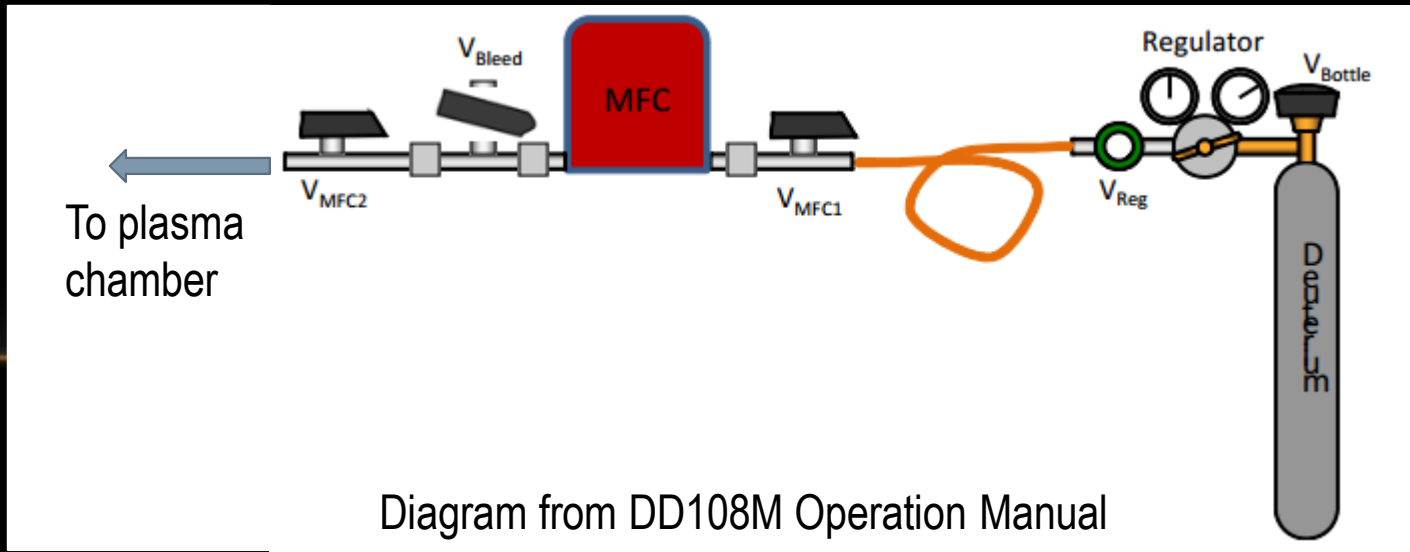

Diagram from DD108M Operation Manual

BINDING ENERGY

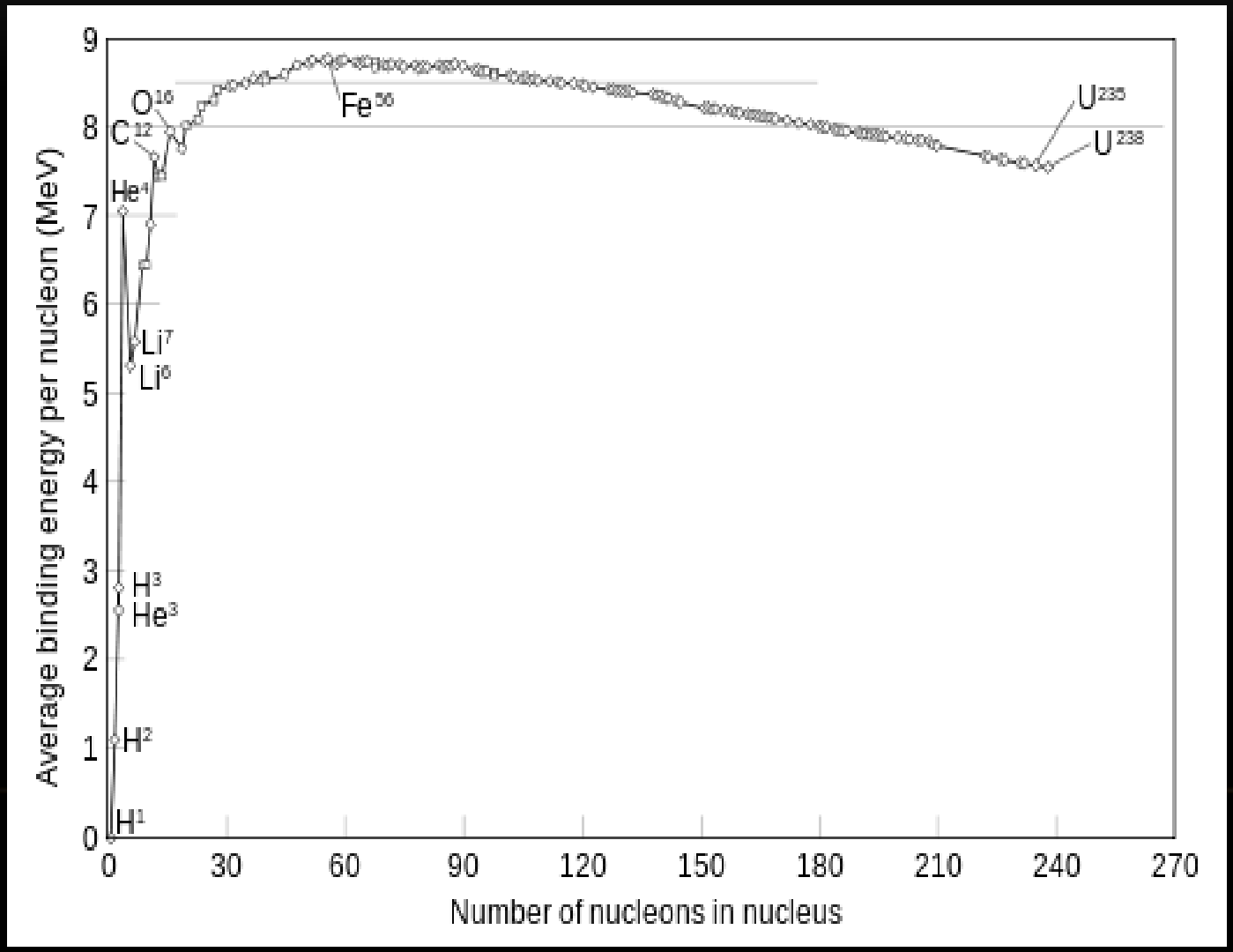

DD Q_Y EVENT SELECTION

- One S1 followed by two S2 pulses.
- Upper limit on S2 pulse RMS < 775 ns (cuts double scatters close in z)
- First scatter is >15 cm inward from the wall and within radius of the tube.
- Only one scatter within radius of the tube

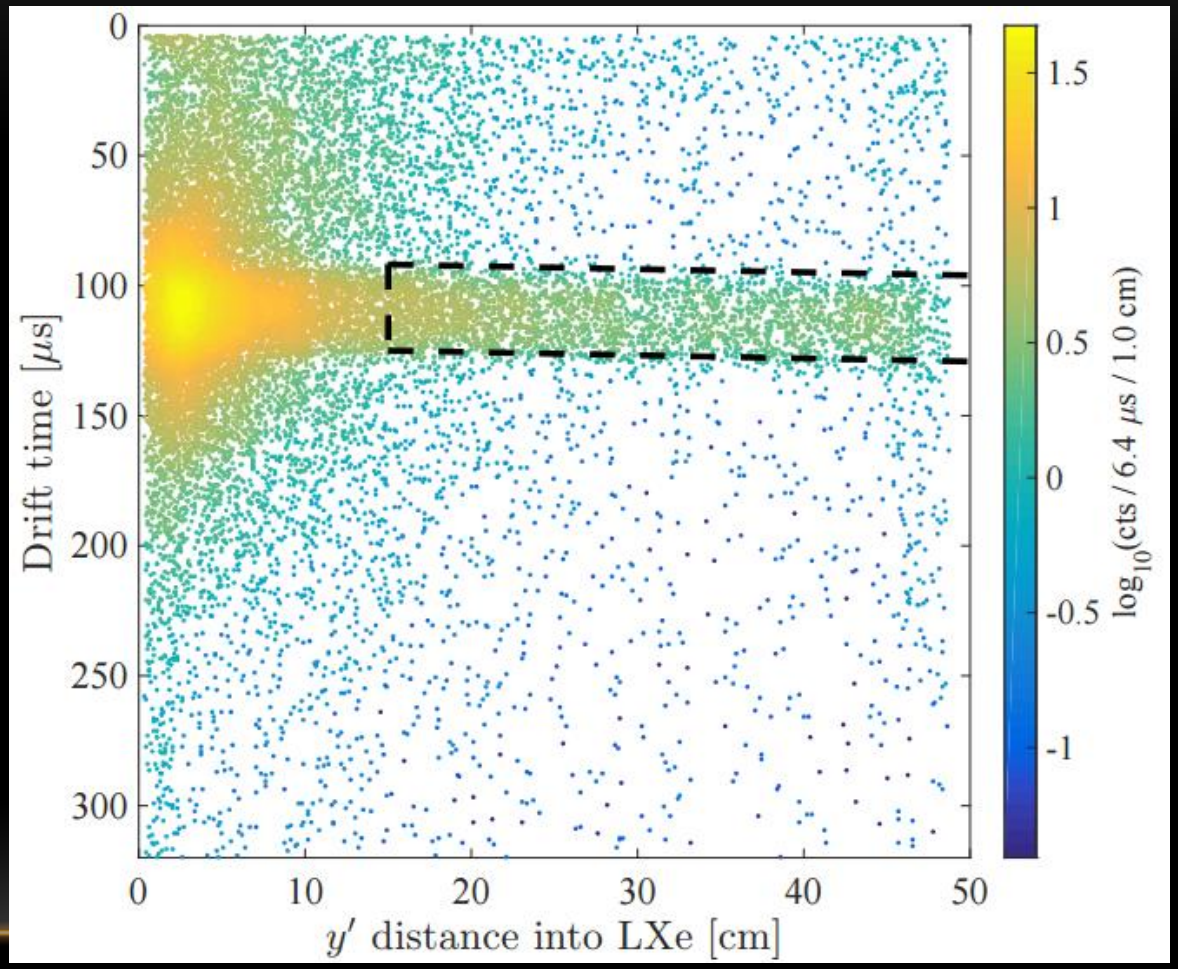

PLR (PROFILE LIKELIHOOD RATIO) METHOD

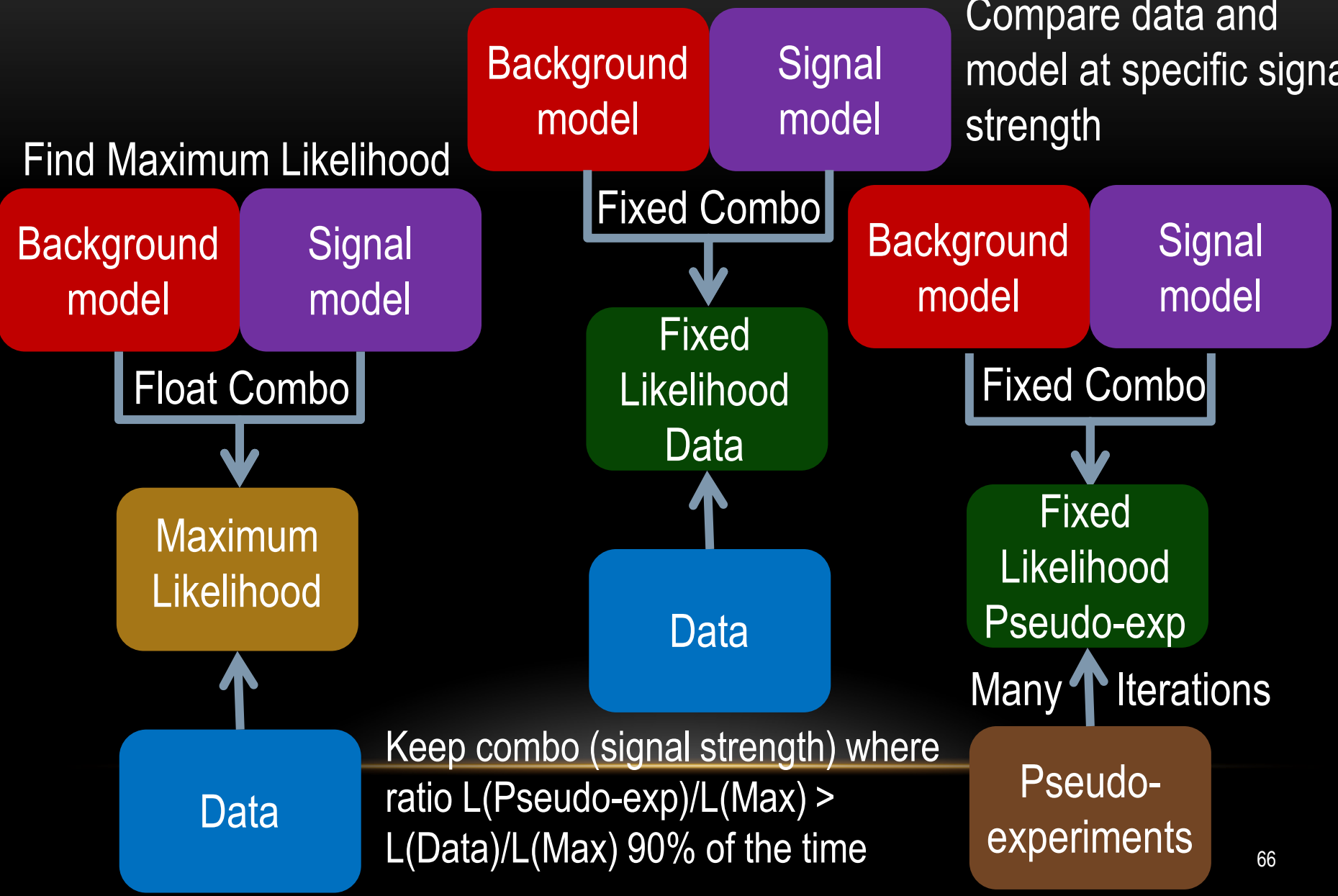

ALL LIMITS – FROM SNOWMASS

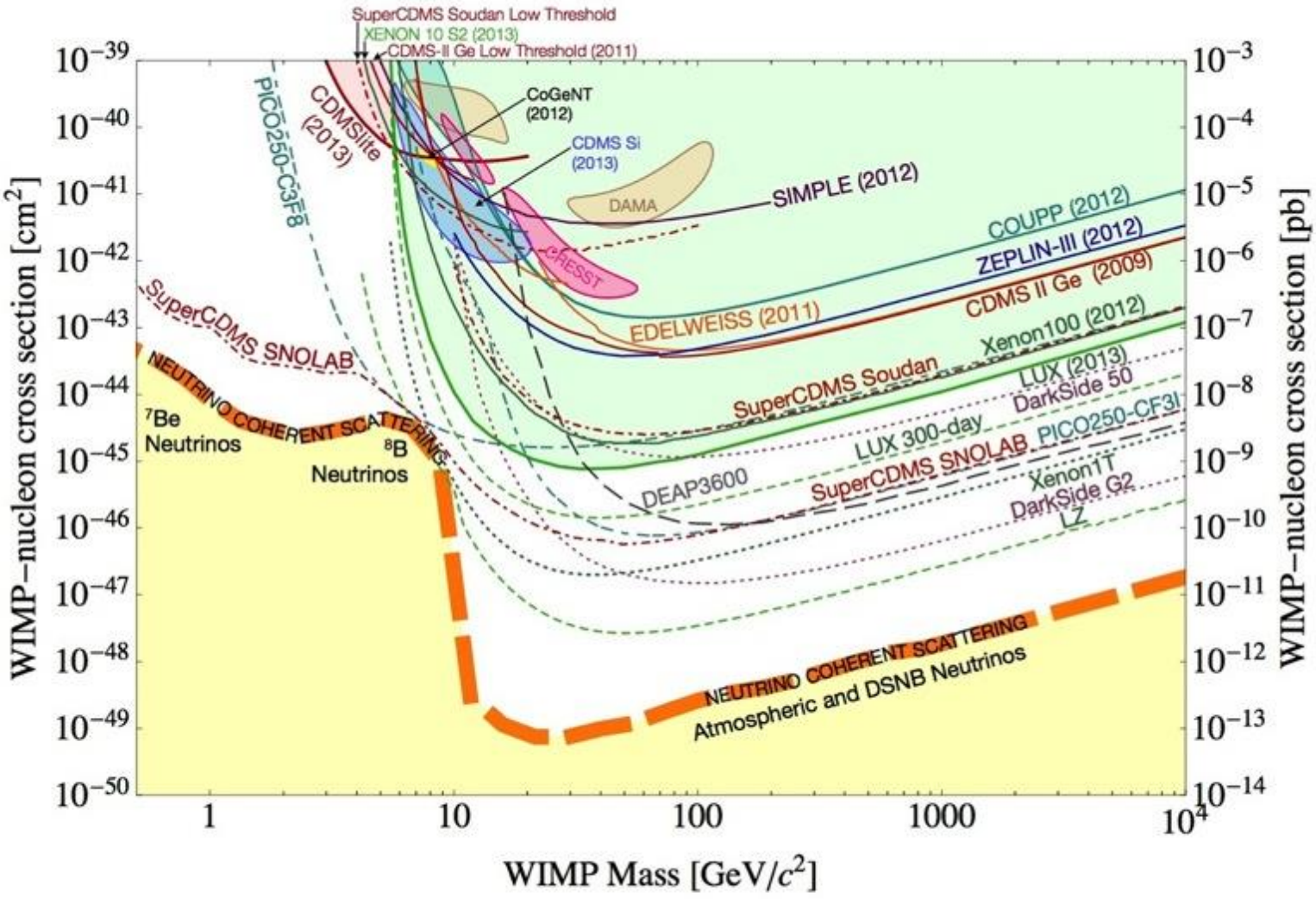

EFT

- Many more interactions possible than simple spin independent and spin dependent.
- Any combination of Galilean and Hermitian invariant quantities $i\vec{q}, \vec{v}^{\perp} = \vec{v} + \frac{\vec{q}}{2\mu_N}, \vec{S}_X, \vec{S}_N$

$$
\begin{aligned}
\mathcal{O}_1 &= 1 & \mathcal{O}_9 &= i\vec{S}_\chi \cdot (\vec{S}_N \times \vec{q}) \\
\mathcal{O}_2 &= (v^\perp)^2 & \mathcal{O}_{10} &= i\vec{S}_N \cdot \vec{q} \\
\mathcal{O}_3 &= i\vec{S}_N \cdot (\vec{q} \times \vec{v}^\perp) & \mathcal{O}_{11} &= i\vec{S}_\chi \cdot \vec{q} \\
\mathcal{O}_4 &= \vec{S}_\chi \cdot \vec{S}_N & \mathcal{O}_{12} &= \vec{S}_\chi \cdot (\vec{S}_N \times \vec{v}^\perp) \\
\mathcal{O}_5 &= i\vec{S}_\chi \cdot (\vec{q} \times \vec{v}^\perp) & \mathcal{O}_{13} &= i(\vec{S}_\chi \cdot \vec{v}^\perp)(\vec{S}_N \cdot \vec{q}) \\
\mathcal{O}_6 &= (\vec{S}_\chi \cdot \vec{q})(\vec{S}_N \cdot \vec{q}) & \mathcal{O}_{14} &= i(\vec{S}_\chi \cdot \vec{q})(\vec{S}_N \cdot \vec{v}^\perp) \\
\mathcal{O}_7 &= \vec{S}_N \cdot \vec{v}^\perp & \mathcal{O}_{15} &= -(\vec{S}_\chi \cdot \vec{q})((\vec{S}_N \times \vec{v}^\perp) \cdot \vec{q}) \\
\mathcal{O}_8 &= \vec{S}_\chi \cdot \vec{v}^\perp & \mathcal{O}_{16} &= -((\vec{S}_\chi \times \vec{v}^\perp) \cdot \vec{q})(\vec{S}_N \cdot \vec{q})
\end{aligned}
$$

EFT (CONT.)

- Interaction rate given by

$$\frac{dR}{dE_R} = \frac{\rho_0}{32\pi m_X^3 m_N^2} \int_{v>v_{min}} \frac{f(\vec{v})}{v} \sum_{i,j} \sum_{N,N'=n,p} c_i^N c_j^{N'} F_{i,j}^{(N,N')}$$

  where *i*, *j* correspond to the operators

- Each $F_{i,j}^{(N,N')}$ can be written as a linear combination of six nuclear responses

$$F_{i,j}^{(N,N')} = \sum_{k=M,\Sigma'',\Sigma',\Delta,\Phi'',\tilde{\Phi}'} a_{ijk} F_{i,j}^{(N,N')}$$

  which are known

EFT XENON COMPARISON M, Σ'

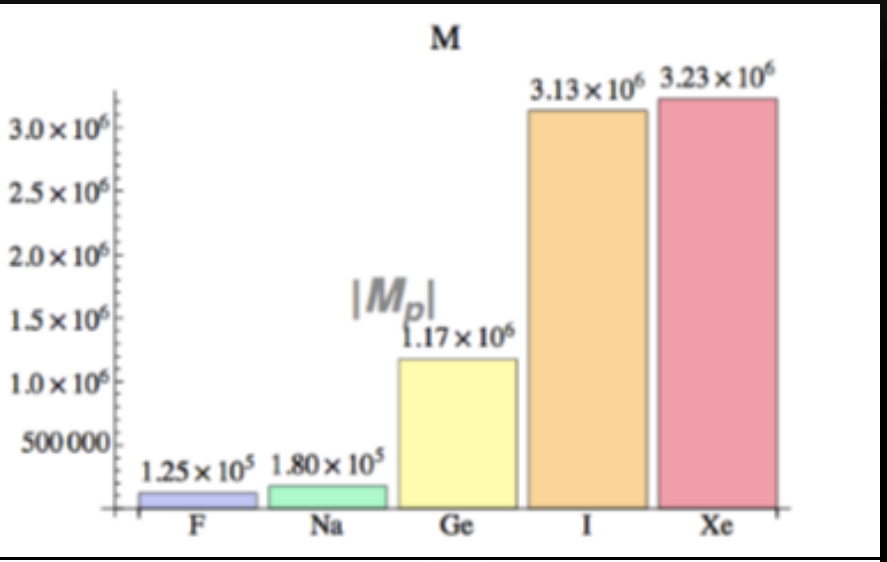

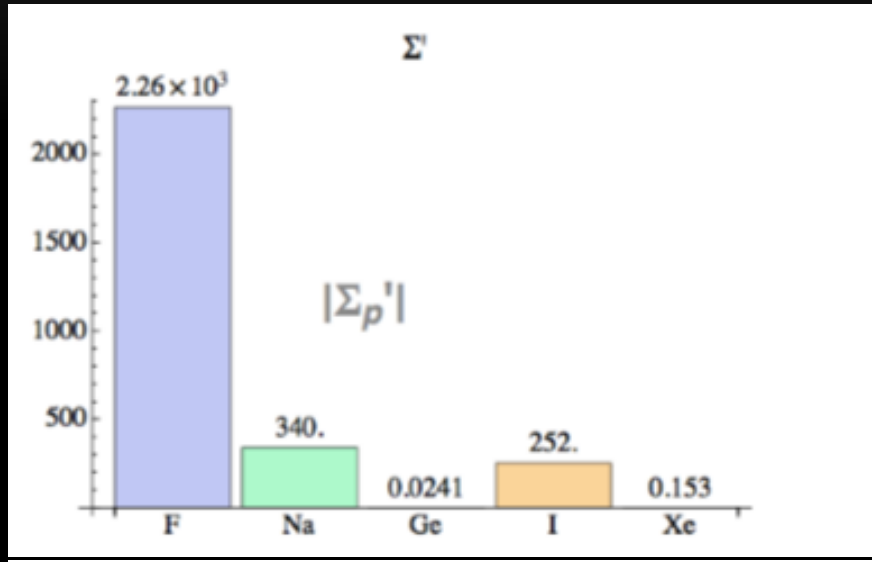

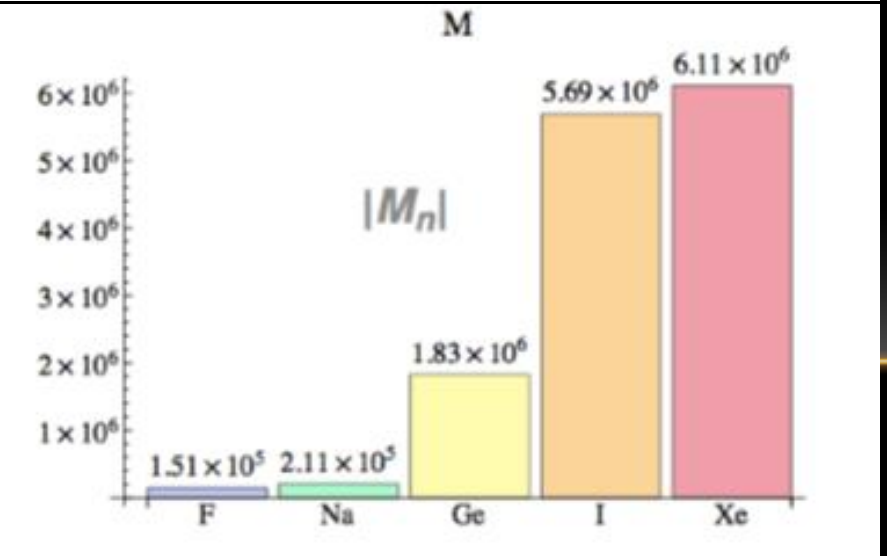

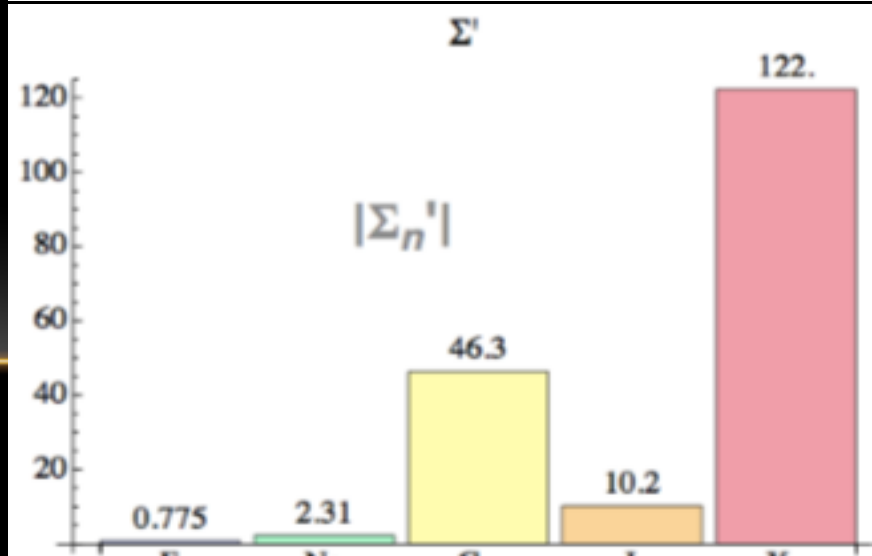

EFT XENON COMPARISON Σ", Δ

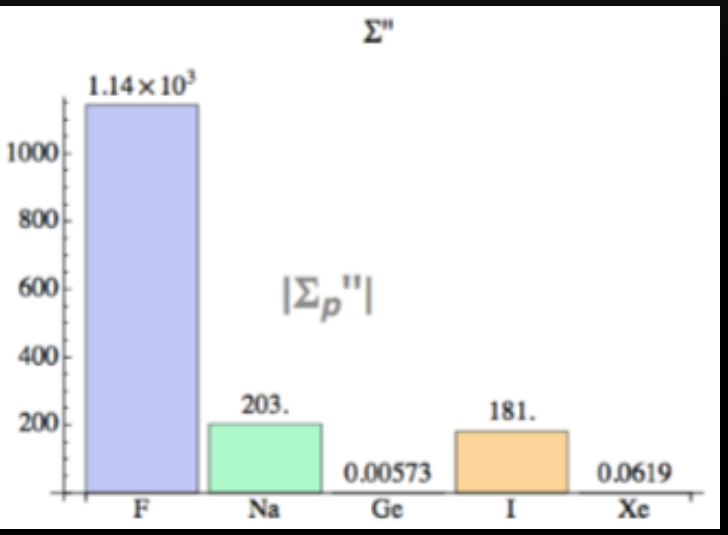

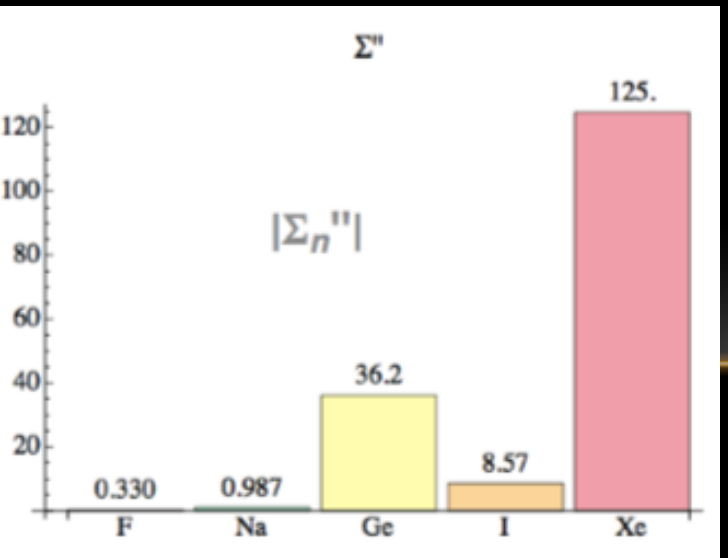

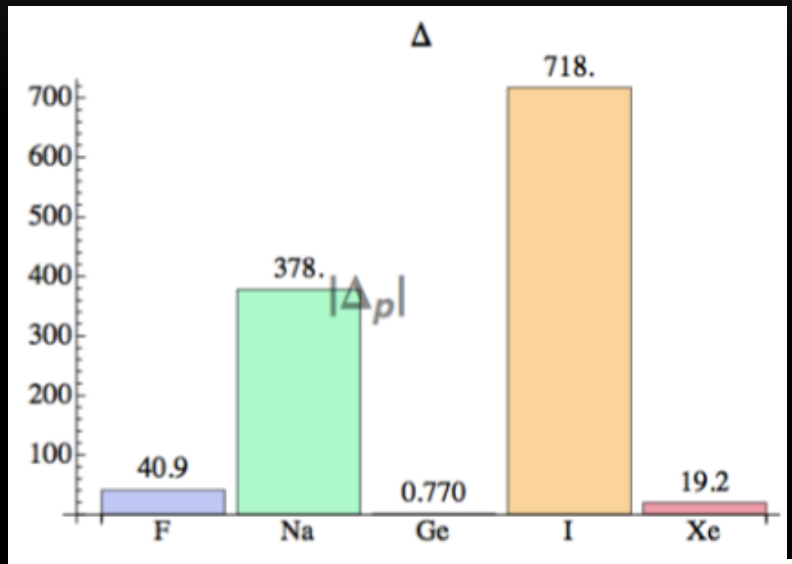

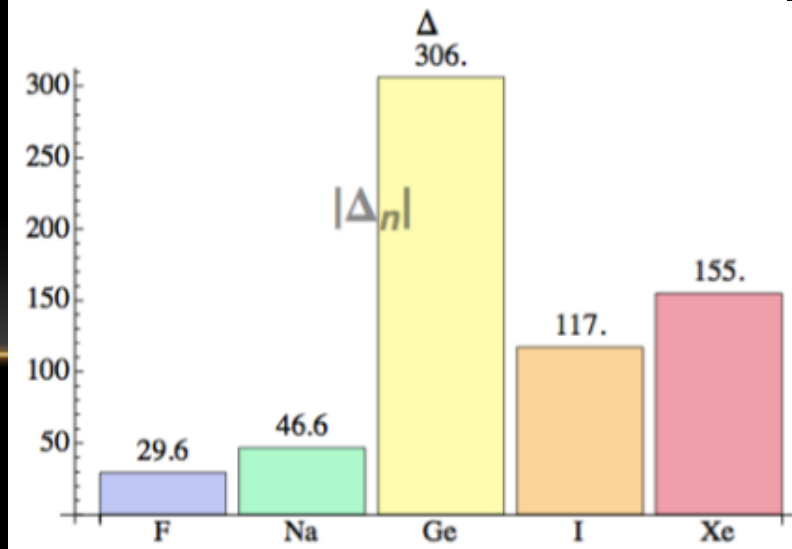

EFT XENON COMPARISON Φ"

Xenon has the highest response for 4 out of 10 options